MACH REFLECTION

A thesis submitted to the University of Manchester
for the degree of Master of Philosophy
in the Faculty of Engineering and Physical Sciences

2008

Mat Hunt

School of Mathematics

Contents

Word count xxxxx

List of Figures

The University of Manchester

Mat Hunt
Master of Philosophy
Mach Reflection
September 15, 2008

Since 1943 oblique shock reflection has become an increasingly important topic of study. The overall plan of this thesis is to begin with the Euler equations build up the knowledge and techniques to tackle the calculation of the shape of the Mach stem near the triple point and the shape of the contact discontinuity downstream of the triple point.

The thesis is essentially split into two parts, the first part introduces the basic theory of supersonic flow for an perfect gas incorporating 2D characteristics for steady flow, the Rankine-Hugoniot equations for an oblique shock for both perfect gas and solids obeying the shock equation of state $U_S = a + bu_p$, Shock polars for both equations of state, Mach reflection which includes direct and indirect Mach reflection at the criteria for the transition from regular reflection to Mach reflection, the numerical method used to solve the Euler equations and an examination of the results.

The second part is split up into two chapters, the first calculates the shape of the downstream asymptote of the contact discontinuity using von Mises variables and the last chapter derives an equation for the pressure in the subsonic region. A numerical solution to this equation shows that there is a singularity in the pressure at the triple point and so a polar co-ordinate system is set up here and an analytical expression for the stem shape is calculated in a region of the origin. For a perfect gas, the shape of the stem near the triple point is:

$$f(y) = -\frac{2p_4}{\pi\sqrt{1-M_4^2}}\left[\frac{2\gamma}{\gamma+1} + \frac{2}{(\gamma+1)M_4^2}\right]^{-1}(y\log y - y). \tag{1}$$

Declaration

No portion of the work referred to in this thesis has been submitted in support of an application for another degree or qualification of this or any other university or other institute of learning.

Copyright Statement

i. The author of this thesis (including any appendices and/or schedules to this thesis) owns any copyright in it (the "Copyright") and s/he has given The University of Manchester the right to use such Copyright for any administrative, promotional, educational and/or teaching purposes.

ii. Copies of this thesis, either in full or in extracts, may be made **only** in accordance with the regulations of the John Rylands University Library of Manchester. Details of these regulations may be obtained from the Librarian. This page must form part of any such copies made.

iii. The ownership of any patents, designs, trade marks and any and all other intellectual property rights except for the Copyright (the "Intellectual Property Rights") and any reproductions of copyright works, for example graphs and tables ("Reproductions"), which may be described in this thesis, may not be owned by the author and may be owned by third parties. Such Intellectual Property Rights and Reproductions cannot and must not be made available for use without the prior written permission of the owner(s) of the relevant Intellectual Property Rights and/or Reproductions.

iv. Further information on the conditions under which disclosure, publication and exploitation of this thesis, the Copyright and any Intellectual Property Rights and/or Reproductions described in it may take place is available from the Head of the School of Mathematics.

Acknowledgements

I would first like to thank Dr Ron Winter at the Atomic Weapons Establishment and by Prof Anatoly Ruban at the University of Manchester for coming up with the idea of this project and allowing me to study it full time at Manchester. I would also like to thank AWE for all funding which went into this MPhil specifically Pete Taylor, Toni Lilly, Sian Butler and Lee Markland for organising all the paperwork from their end. I would also like to thank Chris Paul for allowing me to ask lots of questions about computing and linux and for having a seemingly infinite amount of patience with me and Prof John Dold for illuminating discussions. To my office mates Phil, Kwan and Dmitri for being a good laugh throughout the day and Bren for being a good mate whilst up in Manchester. To my girlfriend Rachel for giving me support when writing up and understanding when I said I had to work, it's all over now!!! Last but not least I would like to give a heartfelt thanks to Prof Ruban for putting up with my endless questions and interruptions and having endless patience with me.

Chapter 1

Supersonic Flow

The defining property of supersonic flow is that the flow speed is greater than the local speed of sound. The *Mach number* defined by:

$$M = \frac{V}{a}, \tag{1.1}$$

where a is the local speed of sound. The condition for a flow to be supersonic in terms of the Mach number is $M > 1$

In subsonic flow at low Mach number the viscosity and heat conduction are normally important effects as the timescale is relatively long; a supersonic flow however, the timescales are much shorter and these effects are usually ignored. Also in subsonic flow $M << 1$, density effectively remains constant, this is not so in supersonic flows as can be seen in experiment. In 2D supersonic flow there is another important quantity called the *Mach angle* defined next.

1.1 Mach's Construction

Consider a point source moving in a fluid at a supersonic speed V which is emitting sound waves at a speed a at regular intervals. Suppose at time $t = 0$ the point source emits a sound wave and at a time t later the point source will have moved a distance Vt whilst the sound wave will have travelled a distance at. In this time the point source will have emitted other sound waves, which are represented by smaller

circles than the original sound wave. The key point to note is that the point source is *constantly* outside the region of disturbance caused by the sound waves. A straight line can be drawn from the point source which is tangent to the family of circles; this line is called a *Mach line*. The angle this makes with the direction of motion of the point source is called the *Mach angle* ϑ. The Mach angle can be easily calculated,

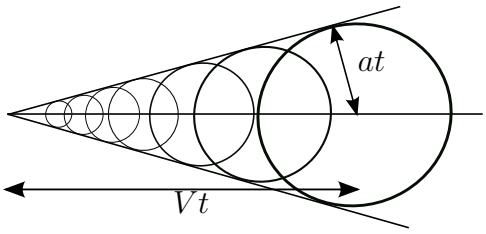

Figure 1.1: Mach's Construction

$$\sin\vartheta = \frac{at}{Vt} = \frac{a}{V} = \frac{1}{M}.$$

So

$$\vartheta = \sin^{-1}\frac{1}{M}.$$

Signals can only be propagated within this cone.

1.2 Equation's of Motion for Supersonic Flow

As was mentioned at the start of the chapter, the timescale is relatively small for viscosity and heat conduction to develop and the terms in the Navier-Stokes equations corresponding to these phenomena can be ignored. The resulting set of equations are called the *Euler equations*. In two dimensions they are written as:

$$\frac{\partial\rho}{\partial t} + \frac{\partial}{\partial x}(\rho u) + \frac{\partial}{\partial y}(\rho v) = 0 \tag{1.2}$$

$$\frac{\partial u}{\partial t} + u\frac{\partial u}{\partial x} + v\frac{\partial u}{\partial y} = -\frac{1}{\rho}\frac{\partial p}{\partial x} \tag{1.3}$$

$$\frac{\partial v}{\partial t} + u\frac{\partial v}{\partial x} + v\frac{\partial v}{\partial y} = -\frac{1}{\rho}\frac{\partial p}{\partial y}. \tag{1.4}$$

The Euler equations are a set of quasi-linear partial differential equations in ρ, u, v and p. There are only three equations for four unknowns, the final equation comes from the condition of constant entropy and will be discussed in the next section.

1.3 Thermodynamics of a Perfect Gas

1.3.1 Derivation of the Entropy Conservation Law

The ideal gas law states that:

$$p = \rho RT, \tag{1.5}$$

where p is pressure, R is called the gas constant, ρ is the density and T is the temperature. The first law of thermodynamics states that:

$$de = TdS - pd\nu, \tag{1.6}$$

where e is internal energy per unit mass, S is the entropy and ν is specific volume. Equation (1.6) represents the change in internal energy, the term $-pd\nu$ is the work done by the system and the term TdS is the change in heat for a reversible system. So (1.6) represents the interplay of work and heat of a system. The gas consant R is the difference of the heat capacity at constant pressure, c_p and the heat capacity at constant volume, c_v. The relationship between the internal energy per unit mass and the temperature is given by $e = c_v T$. Inserting these expressions in the ideal gas law results in:

$$e = \frac{1}{\gamma - 1}\frac{p}{\rho}, \tag{1.7}$$

where γ is c_p/c_v. Inserting (1.5) and (1.7) into (1.6) S is found for a perfect gas:

$$\frac{dp}{p} = \frac{dS}{c_v} + \gamma\frac{d\rho}{\rho}. \tag{1.8}$$

Integrating (1.8) and re-arranging for S gives:

$$\frac{S}{c_v} = \log\left(\frac{p}{\rho^\gamma}\right) + \text{constant}. \tag{1.9}$$

1.3.2 Speed of Sound

The speed of sound, a is defined to be:

$$a^2 = \left.\frac{\partial p}{d\rho}\right|_{S=\text{constant}}. \tag{1.10}$$

If $S =$ constant, then it follows from (1.9) the pressure is a function of density only via:

$$p = k\rho^{\gamma}, \tag{1.11}$$

with k being a constant. Using (1.11) in (1.10) gives:

$$a^2 = \frac{\gamma p}{\rho}. \tag{1.12}$$

In regions where shocks are not present the entropy is a constant. This applies for any equation of state, so:

$$\frac{DS}{Dt} = 0. \tag{1.13}$$

There is another form of (1.13) which is useful:

$$\frac{Dp}{Dt} = a^2 \frac{D\rho}{Dt}. \tag{1.14}$$

This is particularly interesting result as it states that linear perturbations for solids and gases are the same. Equation (1.14) completes the set of equations for all the variables. The problem studied is a problem in two dimensional *steady* flow and so (1.2)-(1.4) and (1.14) become:

$$\frac{\partial}{\partial x}(\rho u) + \frac{\partial}{\partial y}(\rho v) = 0 \tag{1.15}$$

$$u\frac{\partial u}{\partial x} + v\frac{\partial u}{\partial y} = -\frac{1}{\rho}\frac{\partial p}{\partial x} \tag{1.16}$$

$$u\frac{\partial v}{\partial x} + v\frac{\partial v}{\partial y} = -\frac{1}{\rho}\frac{\partial p}{\partial y} \tag{1.17}$$

$$u\frac{\partial p}{\partial x} + v\frac{\partial p}{\partial y} = \frac{\gamma p}{\rho}\left(u\frac{\partial \rho}{\partial x} + v\frac{\partial \rho}{\partial y}\right) \tag{1.18}$$

1.3.3 A Different Form of the Energy Equation

Working directly with the first law of thermodynamics (1.6) and setting $dS = 0$ shows that:

$$de = -pd\nu, \tag{1.19}$$

which in turn gives:

$$\frac{De}{Dt} = \frac{p}{\rho^2}\frac{D\rho}{Dt} \tag{1.20}$$

The case most of interest is that of steady flow, where (1.20) reduces to:

$$\mathbf{u} \cdot \nabla e = \frac{p}{\rho^2} \mathbf{u} \cdot \nabla \rho, \tag{1.21}$$

here $\mathbf{u} = (u, v)$ is the velocity vector. Using (1.7) in (1.21) and re-arranging yields:

$$u\frac{\partial p}{\partial x} + v\frac{\partial p}{\partial y} + \gamma p\left(\frac{\partial u}{\partial x} + \frac{\partial v}{\partial y}\right) = 0 \tag{1.22}$$

This form of the energy equation is most suited when solving the Euler equations with the method of characteristics which is discussed in the next section.

1.4 Method of Characteristics

The idea of this section is to develop a method of solving the following set of first order quasi-linear partial differential equations:

$$\mathbf{A}(x, y, \mathbf{u})\frac{\partial \mathbf{u}}{\partial x} + \mathbf{B}(x, y, \mathbf{u})\frac{\partial \mathbf{u}}{\partial y} = \mathbf{c}(x, y, \mathbf{u}), \tag{1.23}$$

where $\mathbf{A}$ and $\mathbf{B}$ are $n \times n$ matrices and $\mathbf{c}$ is a column vector of length n. The geometrical interpretion is to find n surfaces $u_i(x, y)$

1.4.1 Cauchy Data

Suppose that Γ is a curve in the (x, y) plane parameterized by $s \in [s_1, s_2]$; *Cauchy data* is the prescription of $\mathbf{u}$ on Γ. So geometrically, the surfaces $u_i(x, y)$ all have to pass through these lines. Such boundary conditions can be written in the form:

$$\mathbf{u} = \mathbf{u}_0(s), \quad x = x_0(s), \quad y = y_0(s). \tag{1.24}$$

1.4.2 Characteristics

Differentiating $\mathbf{u}_0(s)$ along Γ gives:

$$\mathbf{u}_0' = x_0'\frac{\partial \mathbf{u}}{\partial x} + y_0'\frac{\partial \mathbf{u}}{\partial y}. \tag{1.25}$$

Combining (1.25) and (1.23) the partial derivatives $(\partial_x \mathbf{u}, \partial_y \mathbf{u})$ are then uniquely defined if:

$$\begin{vmatrix} \mathbf{A} & \mathbf{B} \\ x_0' \mathbf{I} & y_0' \mathbf{I} \end{vmatrix} \neq 0 \quad s \in [s_1, s_2]. \tag{1.26}$$

With $y_0' = \lambda x_0'$, (1.26) reduces to:

$$\det(\mathbf{B} - \lambda \mathbf{A}) \neq 0. \tag{1.27}$$

In the case where $\mathbf{A}$ and $\mathbf{B}$ are scalar functions of x and y the condition (1.27) is sufficient to ensure well-posedness of the problem. Define a *characteristic* to be a curve where the partial derivatives are not uniquely defined. With this definition, the characteristic of:

$$\mathbf{A}(x, y, \mathbf{u}) \frac{\partial \mathbf{u}}{\partial x} + \mathbf{B}(x, y, \mathbf{u}) \frac{\partial \mathbf{u}}{\partial y} = \mathbf{c}(x, y, \mathbf{u}) \tag{1.28}$$

is a curve (x(t),y(t)) such that the left-hand sides of (1.28) and

$$\dot{x} \frac{\partial \mathbf{u}}{\partial x} + \dot{y} \frac{\partial \mathbf{u}}{\partial y} = \dot{\mathbf{u}} \tag{1.29}$$

are linearly dependant. So a curve in the (x, y) plane is a characteristic if:

$$\det(\dot{x}\mathbf{B} - \dot{y}\mathbf{A}) = 0, \tag{1.30}$$

where $dy/dx = \dot{y}/\dot{x} = \lambda$. In general (1.29) will be a polynomial of degree n. A *hyperbolic* system is where all the solutions λ are non-zero real numbers.

1.4.3 Riemann Invariants

There is more information which can be extracted from (1.28). Suppose the ℓ^T is a left eigenvalue corresponding to the root λ, so that $\ell^T(\mathbf{A}^{-1}\mathbf{B} - \lambda \mathbf{I}) = \mathbf{0}^T$. Multiplying (1.28) by $\dot{x}$ and using (1.29) gives:

$$\dot{\mathbf{u}} + \dot{x}(\mathbf{A}^{-1}\mathbf{B} - \lambda \mathbf{I}) \frac{\partial \mathbf{u}}{\partial y} = \dot{x} \mathbf{A}^{-1} \mathbf{c}. \tag{1.31}$$

Multiplying both sides of this equation by ℓ^T on the left gives:

$$\ell^T \dot{\mathbf{u}} = \ell^T \dot{x} \mathbf{A}^{-1} \mathbf{c}. \tag{1.32}$$

The integral of (1.32) yield functions which are *constant* along the corresponding characteristic, such functions are called *Riemann invariants*.

1.4.4 2D Gas Flow

As an example of how this theory works, the characteristics of the steady two-dimensional Euler equations will be calculated. The first task is to write the Euler equations in the form of (1.28), the relevent matrices and column vectors are:

$$\mathbf{A} = \begin{pmatrix} u & \rho & 0 & 0 \\ 0 & u & 0 & 1/\rho \\ 0 & 0 & u & 0 \\ 0 & \gamma p & 0 & u \end{pmatrix}, \quad \mathbf{B} = \begin{pmatrix} v & 0 & \rho & 0 \\ 0 & v & 0 & 0 \\ 0 & 0 & v & 1/\rho \\ 0 & 0 & \gamma p & v \end{pmatrix}. \tag{1.33}$$

Calculating $\det(\mathbf{B} - \lambda\mathbf{A}) = 0$ yields:

$$(v - \lambda u)^2(((u^2 - a^2)\lambda^2 - 2uv\lambda + v^2 - a^2) = 0. \tag{1.34}$$

Which gives the eigenvalues to be:

$$\lambda_{1,2} = \frac{v}{u}, \quad \lambda_{3,4} = \frac{-uv \pm a\sqrt{u^2 + v^2 - a^2}}{a^2 - u^2}. \tag{1.35}$$

It follows from (1.35) that the first two characteristics (corresponding to $\lambda_{1,2}$) coincide with the streamlines. In order to have a clear understanding the geometrical meaning of the third and fourth characteristics it is convenient to use the Euclidian norm of the velocity vector V and directional angle θ . Write $u = V\cos\theta$, $v = V\sin\theta$ and $a = V\sin\vartheta$, the characteristics become:

$$\begin{aligned} \lambda_{3,4} &= \frac{-V^2\sin\theta\cos\theta \pm V^2\sin\vartheta\sin\vartheta}{V^2\sin^2\vartheta - V^2\cos^2\theta} = \frac{\sin\theta\cos\theta \mp \sin\vartheta\cos\vartheta}{\cos^2\theta - \sin^2\vartheta} \\ &= \frac{\sin 2\theta \mp \sin 2\vartheta}{\cos 2\theta + \cos 2\vartheta} = \frac{\sin(\theta \mp \vartheta)\cos(\theta \pm \vartheta)}{\cos(\theta + \vartheta)\cos(\theta - \vartheta)} = \tan(\theta \mp \vartheta) \end{aligned} \tag{1.36}$$

This shows that the projection of the characteristic onto the (x, y) plane coincides with the corresponding Mach line. The next task is to calculate the left eigenvectors of $\mathbf{A}^{-1}\mathbf{B}$; The matrix of $\mathbf{A}^{-1}\mathbf{B}$ is given by:

$$\mathbf{A}^{-1}\mathbf{B} = \begin{pmatrix} \frac{v}{u} & \frac{\rho v}{a^2-u^2} & -\frac{\rho u}{a^2-u^2} & -\frac{v}{u(a^2-u^2)} \\ 0 & -\frac{uv}{a^2-u^2} & \frac{a^2}{a^2-u^2} & \frac{v}{\rho(a^2-u^2)} \\ 0 & 0 & \frac{v}{u} & \frac{1}{\rho u} \\ 0 & \frac{\rho a^2 v}{a^2-u^2} & -\frac{\rho u a^2}{a^2-u^2} & -\frac{uv}{a^2-u^2} \end{pmatrix}. \tag{1.37}$$

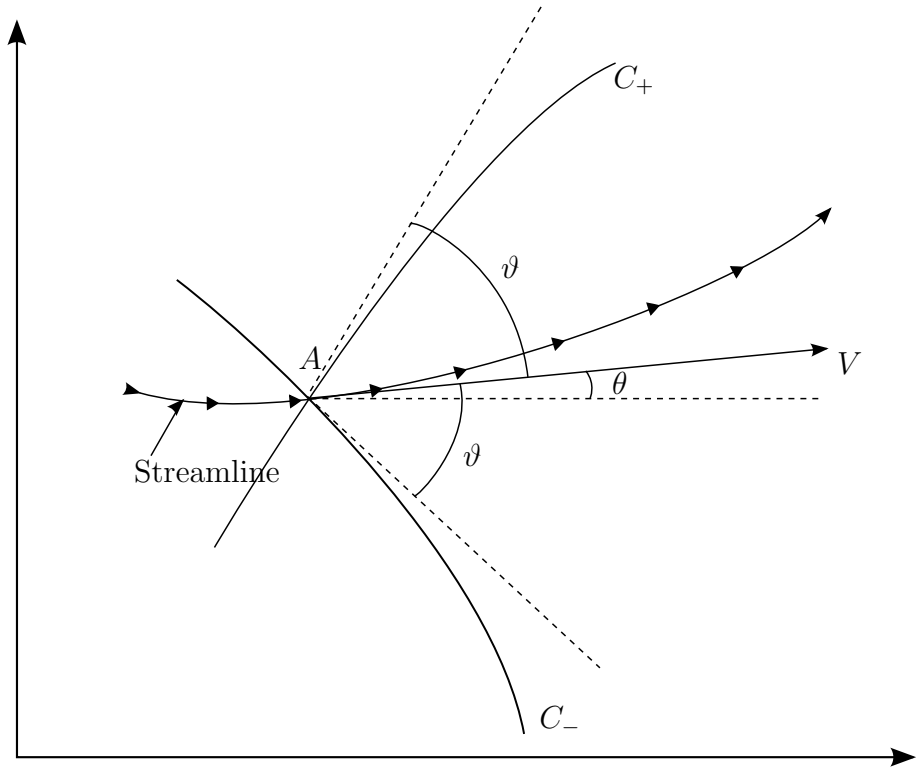

Figure 1.2: Illustration of Left and Right Running Characteristics

Writing the left eigenvector as (l_1, l_2, l_3, l_4), the four equations are:

$$l_1 v - u\lambda l_1 = 0 \tag{1.38}$$

$$\rho v l_1 - (uv + \lambda(a^2 - u^2))l_2 + a^2 \rho v l_4 = 0 \tag{1.39}$$

$$-\rho u l_1 + a^2 l_2 + (a^2 - u^2)(\frac{v}{u} - \lambda)l_3 - \rho u a^2 l_4 = 0 \tag{1.40}$$

$$-\frac{v}{u}l_1 + \frac{v}{\rho}l_2 + \frac{a^2 - u^2}{\rho u}l_3 - (uv + \lambda(a^2 - u^2))l_4 = 0. \tag{1.41}$$

Examining the eigenvalue $\lambda = v/u$ first of all as the Riemann invariants from these characteristics will be valid on the streamlines gives two different Riemann invariants. For the first invariant take $l_2 = l_3 = 0$ and to see that:

$$l_1 = -a^2 l_4. \tag{1.42}$$

Choosing $l_1 = 1$ which in turn gives $l_4 = -a^{-2}$. Inserting this into (1.32) gives:

$$\dot{\rho} - \frac{\rho}{\gamma p}\dot{p} = 0. \tag{1.43}$$

Integrating this up gives the Riemann invariant for the characteristic (which in this case on the steamlines). In this case the Riemann invariant is given by:

$$R_1 = \log\left(\frac{p}{\rho^\gamma}\right). \tag{1.44}$$

Which is just the entropy up to a multiplicative factor. To calculate the other Riemann invariant, set $l_1 = 0$ and this immediately gives:

$$l_2 = \rho u l_4. \tag{1.45}$$

Taking $l_2 = u$, this gives $l_4 = 1/\rho$. Inserting these into any other of the linear equations shows that $l_3 = v$. Inserting these into (1.32) gives:

$$u\dot{u} + v\dot{v} + \frac{\dot{p}}{\rho} = 0 \tag{1.46}$$

Integrating this equation leads to the second Riemann invariant:

$$R_2 = \frac{u^2 + v^2}{2} + \int \frac{dp}{\rho}, \tag{1.47}$$

which is just the Bernoulli equation for a compressible medium. The other characteristics are given by:

$$\lambda = \frac{-uv \pm a\sqrt{u^2 + v^2 - a^2}}{a^2 - u^2}. \tag{1.48}$$

Immediately, it can be seen that $l_1 = 0$ for both of these characteristics. Likewise a simple relation can be derived relating l_2 and l_4 which is:

$$\mp\sqrt{u^2 + v^2 - a^2} l_2 + \rho a v l_4 = 0. \tag{1.49}$$

Taking:

$$l_4 = \frac{1}{\rho v a}, \tag{1.50}$$

gives l_2 and l_3 to be:

$$l_2 = \pm\frac{1}{\sqrt{u^2 + v^2 - a^2}} \tag{1.51}$$

$$l_3 = \mp\frac{u/v}{\sqrt{u^2 + v^2 - a^2}}. \tag{1.52}$$

Inserting these into (1.32) results in:

$$\pm\frac{\dot{u}}{\sqrt{u^2+v^2-a^2}} \mp \frac{u/v}{\sqrt{u^2+v^2-a^2}}\dot{v} + \frac{\dot{p}}{\rho a v} = 0. \tag{1.53}$$

As the Bernoulli equation (1.47) can be applied throughout the flow region, it can be used to reduce (1.53) to an equation in $\dot{u}$ and $\dot{v}$ only. Doing this yields:

$$(\pm av - u\sqrt{u^2+v^2-a^2})\dot{u} + (\mp au - v\sqrt{u^2+v^2-a^2})\dot{v} = 0. \tag{1.54}$$

The equation can be re-arranged as follows:

$$\frac{dv}{du} = \frac{\pm av - u\sqrt{u^2+v^2-a^2}}{\pm au + v\sqrt{u^2+v^2-a^2}}. \tag{1.55}$$

Multiplying the numerator and denominator on the RHS of (1.55) by $\pm au + v\sqrt{u^2-v^2-a^2}$ gives:

$$\frac{dv}{du} = \frac{uv \pm \sqrt{u^2+v^2-a^2}}{a^2-v^2}. \tag{1.56}$$

Again write $u = V\cos\theta$ and $v = V\sin\theta$, then:

$$du = -V\sin\theta d\theta + \cos\theta dV, \quad dv = V\cos\theta d\theta + \sin\theta dV. \tag{1.57}$$

Inserting these into (1.56) and re-arranging gives:

$$(a\cos\theta \pm \sqrt{V^2-a^2}\sin\theta)(aVd\theta \mp \sqrt{V^2-a^2}dV) = 0. \tag{1.58}$$

The first multiplier is zero if and only if:

$$\tan\theta = \pm\frac{1}{\sqrt{M^2-1}}, \tag{1.59}$$

which corresponds to the Mach angle. By rotation of the co-ordinate system this can be avoided. Therefore:

$$aVd\theta \mp \sqrt{V^2-a^2}dV. \tag{1.60}$$

In order to integrate (1.60), the Bernoulli equation is used. For a perfect gas it has the form:

$$\frac{1}{\gamma-1}a^2 + \frac{1}{2}V^2 = \frac{1}{\gamma-1}a_\infty^2 + \frac{1}{2}V_\infty^2, \tag{1.61}$$

where the subscript ∞ denotes the free stream value. Taking out a factor of $V^2/2$ from the LHS gives:

$$\frac{V^2}{2}\left[1 + \frac{2}{(\gamma-1)M^2}\right] = \frac{1}{\gamma-1}a_\infty^2 + \frac{1}{2}V_\infty^2. \tag{1.62}$$

Taking the log of both sides and differentiating gives:

$$\frac{dV}{V} = \frac{1}{1+\frac{\gamma-1}{2}M^2}\frac{dM}{M}. \tag{1.63}$$

Combining (1.63) with (1.60) yields:

$$d\theta \mp \frac{\sqrt{M^2-1}}{1+\frac{\gamma-1}{2}M^2}\frac{dM}{M} = 0. \tag{1.64}$$

It remains to perform the integration which yields to a conclusion that along the third and fourth characteristics

$$R_{3,4} = \theta \mp \nu(M), \tag{1.65}$$

where

$$\nu(M) = \sqrt{\frac{\gamma+1}{\gamma-1}}\tan^{-1}\left[\sqrt{\frac{\gamma-1}{\gamma+1}(M^2-1)}\right] - \tan^{-1}\sqrt{M^2-1} \tag{1.66}$$

is referred to as the *Prandtl-Meyer function*. In general the Riemann invariant will be different for different characteristics. So 2D steady supersonic flow in characteristic form is written as:

$$\begin{aligned}
p\rho^{-\gamma} &= \text{const.} \quad \text{on} \quad \frac{dy}{dx} = \frac{v}{u} \\
(u^2+v^2)/2 + \int \rho^{-1}dp &= \text{const.} \quad \text{on} \quad \frac{dy}{dx} = \frac{v}{u} \\
\theta + \nu(M) &= \text{const.} \quad \text{on} \quad \frac{dy}{dx} = \tan(\theta - \vartheta) \\
\theta - \nu(M) &= \text{const.} \quad \text{on} \quad \frac{dy}{dx} = \tan(\theta + \vartheta)
\end{aligned}$$

The crossing of the two Riemann invariants in figure (1.3) indicates a point in the 2D gas flow.

1.5 Prandtl-Meyer Flow

1.5.1 Basic Set-up

Prandtl-Meyer flow deals with supersonic flow around a smooth bend of a rigid body contour.

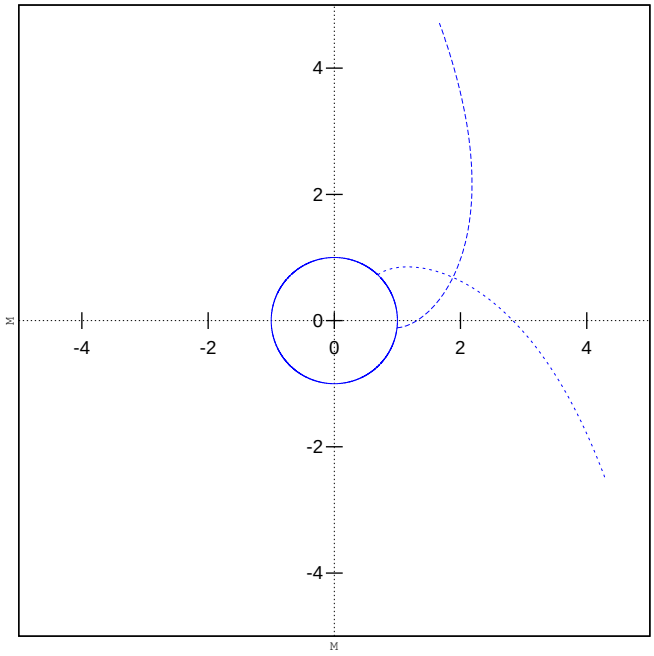

Figure 1.3: Polar Plot in (M, θ) plane of Riemann Invariants for 2D Gas Flow

The method of characteristics is applied to this scenario, the characteristic equations are given by:

$$\theta + \nu(M) = \xi \quad \text{on} \quad dy/dx = \tan(\theta + \vartheta) \tag{1.67}$$

$$\theta - \nu(M) = \eta \quad \text{on} \quad dy/dx = \tan(\theta - \vartheta). \tag{1.68}$$

Characteristics which satisfy (1.67) will be called *positive characteristics* and characteristics which satisfy (1.68) will be called *negative characteristics*.

The flow is unperturbed everywhere upstream of the characteristic AA' on the first characteristic originating from point A where the wall begins to bend, this is a positive characteristic as the gradient will be always positive. Consider an arbitrary point B on the curved bend, and consider a positive characteristic originating from it. There will be a negative characteristic which connects the two regions as shown in (1.4). The parameter ξ can be easily calculated by noting that for the undisturbed flow $\theta = 0$ and $\nu(M) = \nu(M_\infty)$ and so:

$$\theta + \nu(M) = \nu(M_\infty) \quad \text{on} \quad dy/dx = \tan\vartheta = \frac{1}{\sqrt{M^2 - 1}} \tag{1.69}$$

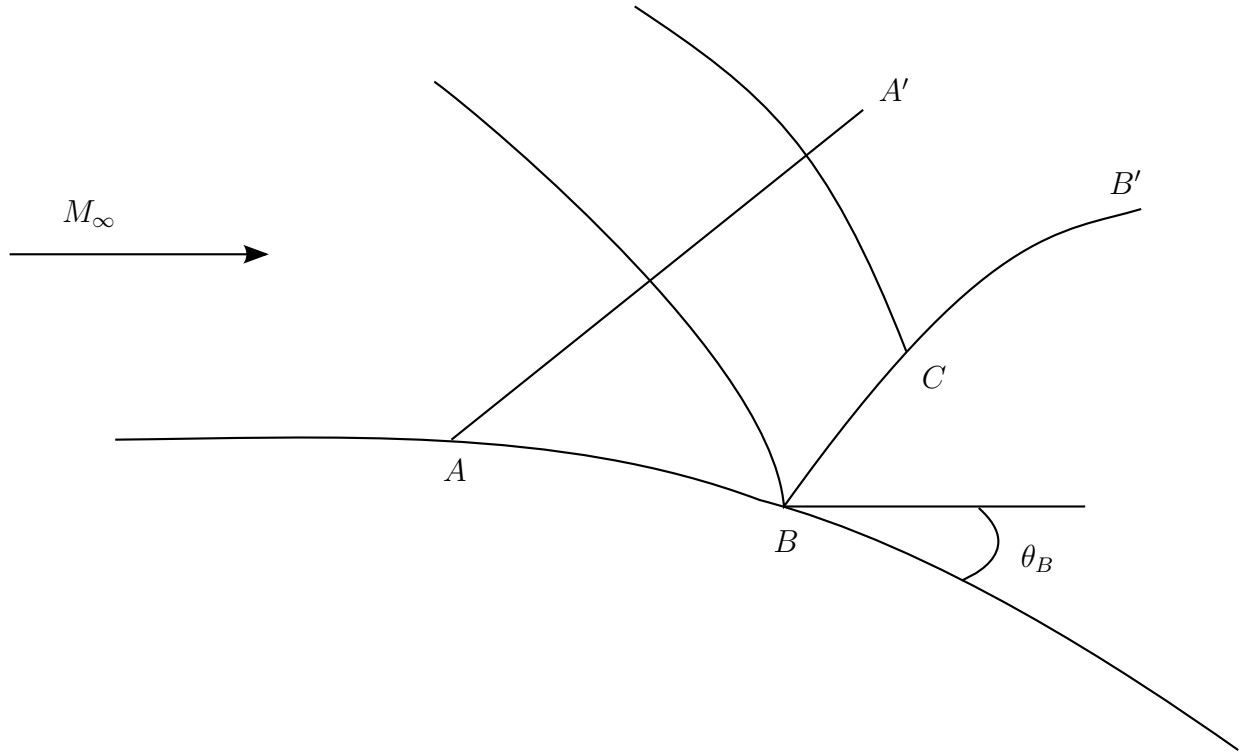

Figure 1.4: Flow Around a Bend

The velocity vector at B makes an angle $-\theta_B$ with the tangent of the bend at B and the x-axis, so the Mach number may be found from:

$$-\theta_B + \nu(M_B) = \nu(M_\infty). \tag{1.70}$$

In order to analyse the flow, consider a positive characteristic BB' shown in (figure 1.4), along this characteristic:

$$\theta - \nu(M) = \xi. \tag{1.71}$$

Solving (1.69) and (1.71) together gives at point C:

$$\theta = \frac{1}{2}(\nu(M_\infty) + \xi), \quad \nu(M) = \frac{1}{2}(\nu(M_\infty) - \xi). \tag{1.72}$$

As the quantity ξ does not change as the point C moves along BB', then the Mach number and angle does remain constant along BB' and coincide with their values along the boundary. As M is constant this also shows that the that the dimensional velocity is also constant along BB' (via the Bernoulli equation with one of the states taken to be the free stream flow). Then using the Bernoulli equation and the conservation of entropy, shows that both ρ and p are also constant along BB'.

The shape of the physical characteristics are governed by:

$$\frac{dy}{dx} = \tan(\theta + \vartheta). \tag{1.73}$$

Consider the characteristics BB' again, as the Mach number M is constant then the Mach Angle:

$$\vartheta = \sin^{-1}\left(\frac{1}{M}\right), \tag{1.74}$$

will also be constant along BB', the velocity direction is also constant on BB' and so this shows that the characteristic will be a straight line.

1.5.2 Small Angle Approximations

If the slope angle of the corner is small then it is possible to obtain analytical expressions for the pressure and the modulus of the velocity in the following way. Consider the Riemann invariant:

$$d\theta + \sqrt{M^2 - 1}\frac{dV}{V} = 0. \tag{1.75}$$

Then writing $d\theta = \theta$ and $dV = V - V_\infty$, (1.75) becomes:

$$\theta + \sqrt{M_\infty^2 - 1}\frac{V - V_\infty}{V_\infty} = 0. \tag{1.76}$$

Re-arranging this gives:

$$V = V_\infty - \frac{V_\infty}{\sqrt{M_\infty^2 - 1}}\theta. \tag{1.77}$$

From the Bernoulli equation

$$\frac{\gamma}{\gamma - 1}\frac{p}{\rho} + \frac{1}{2}V^2 = \frac{\gamma}{\gamma - 1}\frac{p_\infty}{\rho_\infty} + \frac{1}{2}V_\infty^2. \tag{1.78}$$

Writing $p = p_\infty + \triangle p$, $\rho = \rho_\infty + \triangle\rho$ and $V = V_\infty + \triangle V$ (1.78) reduces to:

$$\frac{\gamma}{\gamma - 1}\left(-\frac{p_\infty}{\rho_\infty^2}\triangle\rho + \frac{\triangle p}{\rho_\infty}\right) + V_\infty\triangle V = 0. \tag{1.79}$$

Using the previous notation, the entropy conservation law:

$$p\rho^{-\gamma} = p_\infty\rho_\infty^{-\gamma} \tag{1.80}$$

reduces to:

$$\triangle p = \frac{\gamma p_\infty}{\rho_\infty}\triangle\rho. \tag{1.81}$$

Substituting for $\triangle\rho$ from (1.81) into (1.79) gives:

$$\frac{\triangle p}{\rho_\infty} + V_\infty \triangle V = 0. \tag{1.82}$$

Substituting for $\triangle V$ in (1.82) using (1.78) gives:

$$p = p_\infty + \rho_\infty V_\infty^2 \frac{\theta}{\sqrt{M_\infty^2 - 1}} \tag{1.83}$$

1.6 Weak Solutions and Shocks

Consider a set of equations in the form:

$$\frac{\partial P}{\partial x} + \frac{\partial Q}{\partial y} = c. \tag{1.84}$$

Suppose there is a discontinuity in the fluid dynamic quantities somewhere in the flow field, such discontinuities are called *shock waves*. In order to study them consider a small box around the shock (fig 1.5): Multiply (1.84) by a smooth test function ψ

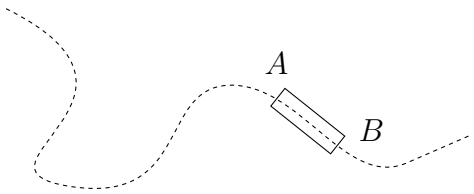

Figure 1.5: Weak Solutions

and integrate over the box shown, this gives:

$$\iint_{\text{box}} P\frac{\partial \psi}{\partial x} + Q\frac{\partial \psi}{\partial x} - c\psi = \oint_c \psi(Q dx - P dy). \tag{1.85}$$

As the box is shrunk to the shock the sides of the box are shrunk to zero length, so only the integrals from A to B matter. Denote the values of P and Q on either side of the shock by $\pm$. Then:

$$\int_A^B Q_+ dx - P_+ dy + \int_B^A Q_- dx - P_- dy = \int_A^B [Q]_-^+ dx - [P]_-^+ dy = 0. \tag{1.86}$$

Which gives:

$$\frac{dy}{dx} = \frac{[Q]_-^+}{[P]_-^+}. \tag{1.87}$$

This is in general called a *Rankine-Hugoniot* equation and is valid across the shock front. Discontinuities can occur across characteristics, in general however the discontinuities occur along curves called *shocks*, which are *not* characteristics.

However, the solutions need not be unique. There are however ways to obtain unique solutions from weak solutions by adding extra information. There are a number of ways to do this, one way is via the entropy. Across a shock the entropy *must* increase. Entropy increase will normally give a unique solution to the conservation equations.

Chapter 2

Oblique Shock Waves

The equations of fluid mechanics admit both continuous and discontinuous solutions; shock waves represent discontinuities in solutions of the general fluid flow equations. The shock wave is (mathematically) a surface across where the field variables are discontinuous.

The fluid variables like density, pressure, internal energy, and entropy may be discontinuous across a shock but certain *functions* of these variables are *not* discontinuous. These functions are:

- Mass flux
- Momentum flux
- Energy flux

So this will give a starting point for the investigation of shock waves.

2.1 Rankine-Hugoniot Relations

This section will explore in more depth the conservation of the mass flow, momentum flow and energy to derive the *Rankine-Hugoniot Equations* which are the basic set of equations used in shock physics.

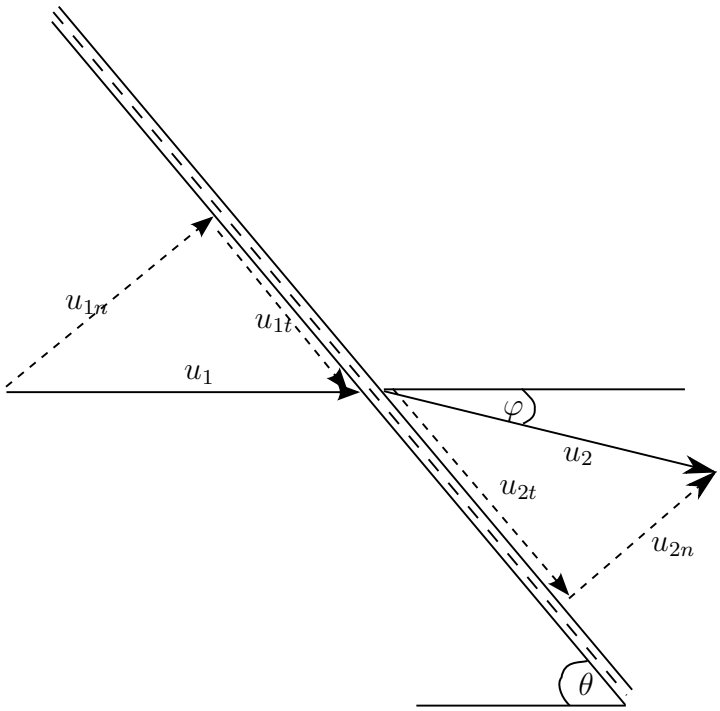

Figure 2.1: Oblique Shock Wave

2.1.1 Conservation of Mass

Consider the mass flow *across* an area A of the shock wave. The mass flow rate, $\dot{M}$ is given by:

$$\dot{M} = \rho u_n A. \tag{2.1}$$

The mass flow is the same on both sides of the shock, hence: $\rho_1 u_{1n} A = \rho_2 u_{2n} A$ which gives the first equation:

$$\rho_1 u_{1n} = \rho_2 u_{2n}. \tag{2.2}$$

The convention is to use the index $'1'$ for quantities in advance of the shock and the index $'2'$ for quantities in rear of the shock (see figure 2.1).

2.1.2 Conservation of Momentum

For a mass M of fluid passing through a shock in a time δt, Newton's second law states:

$$\frac{\mathbf{P}_2 - \mathbf{P}_1}{\delta t} = \mathbf{F}_2 - \mathbf{F}_1.$$

The momentum, $\mathbf{P}$ is the product of mass and velocity. The velocity is a vector, given by

$$\mathbf{u} = u_n\hat{\mathbf{n}} + u_t\hat{\mathbf{t}}, \tag{2.3}$$

where $\hat{\mathbf{n}}$ and $\hat{\mathbf{t}}$ denote the unit normal and tangent vectors respectively. The mass is given by

$$M = \rho u_n A \delta t. \tag{2.4}$$

The forces are due to pressure, which acts normal to the shock, accounting for direction the forces are:

$$\mathbf{F}_1 = p_1 A\hat{\mathbf{n}} \quad \mathbf{F}_2 = -p_2 A\hat{\mathbf{n}}. \tag{2.5}$$

Inserting these into Newton's second law then yields:

$$\rho_2 u_{2n}^2\hat{\mathbf{n}} + \rho_2 u_{2n}u_{2t}\hat{\mathbf{t}} - \rho_1 u_{1n}^2\hat{\mathbf{n}} + \rho_1 u_{1n}u_{1t}\hat{\mathbf{t}} = p_1\hat{\mathbf{n}} - p_2\hat{\mathbf{n}}. \tag{2.6}$$

The normal component of this equation reads:

$$\rho_2 u_{2n}^2 - \rho_1 u_{1n}^2 = p_1 - p_2. \tag{2.7}$$

Or, equivalently

$$p_1 + \rho_1 u_{1n}^2 = p_2 + \rho_2 u_{2n}^2. \tag{2.8}$$

The tangential component of (2.6) gives:

$$u_{1t} = u_{2t}. \tag{2.9}$$

So the tangential velocity is conserved across a shock.

2.1.3 Conservation of Energy

Neglecting the heat transfer effects, the first law of thermodynamics states that a change in the energy W of a mass equates to the work done by external forces Applying this across the shock gives:

$$\frac{W_2 - W_1}{\delta t} = \mathbf{F}_1 \cdot \mathbf{u}_1 + \mathbf{F}_2 \cdot \mathbf{u}_2. \tag{2.10}$$

The energy is made up from a mixture of internal energy per unit mass (denoted by e) and kinetic energy. This is given by:

$$W = \rho u_n A \delta t \left(e + \frac{u_n^2 + u_t^2}{2} \right). \tag{2.11}$$

Since $F_1 = p_1 \hat{\mathbf{n}}$ and $F_2 = -p_2 \hat{\mathbf{n}}$, then:

$$\mathbf{F}_1 \cdot \mathbf{u}_1 + \mathbf{F}_2 \cdot \mathbf{u}_2 = p_1 A u_{1n} - p_2 A u_{2n}. \tag{2.12}$$

Substituting (2.11) and (2.12) into (2.6) yields

$$\rho_2 u_{2n} \left(e_2 + \frac{1}{2}(u_{2n}^2 + u_{2t}^2) \right) - \rho_1 u_{1n} \left(e_1 + \frac{1}{2}(u_{1n}^2 + u_{1t}^2) \right) = p_1 u_{1n} - p_2 u_{2n}; \tag{2.13}$$

which in view of (2.2):

$$e_1 + \frac{p_1}{\rho_1} + \frac{1}{2} u_{1n}^2 = e_2 + \frac{p_2}{\rho_2} + \frac{1}{2} u_{2n}^2. \tag{2.14}$$

Combining (2.2), (2.8), (2.9) and (2.14) leads to the *Rankine-Hugoniot relations*:

$$u_{1t} = u_{2t} \tag{2.15}$$

$$\rho_1 u_{1n} = \rho_2 u_{2n} \tag{2.16}$$

$$p_1 + \rho_1 u_{1n}^2 = p_2 + \rho_2 u_{2n}^2 \tag{2.17}$$

$$e_1 + \frac{p_1}{\rho_1} + \frac{1}{2} u_{1n}^2 = e_2 + \frac{p_2}{\rho_2} + \frac{1}{2} u_{2n}^2. \tag{2.18}$$

It should be noted that the derivation given here is for a completely arbitrary equation of state. In order to derive the Rankine-Hugoniot equations for solids, the conservation of energy will be replaced by an experimental equation of state.

2.1.4 Solving the Rankine-Hugoniot Equations

For a perfect gas, the solution of the Rankine-Hugoniot equations are well known, this section will go over their solution. The ideal gas law states that;

$$p = \rho R T. \tag{2.19}$$

The gas constant $R = c_p - c_v$, where c_v is heat capacity at constant volume and c_p is the heat capacity at constant pressure. The internal energy per unit mass is related

to the temperature by $e = c_v T$, and if $\gamma = c_p/c_v$, then inserting these relations in the ideal gas law yields:

$$e = \frac{1}{\gamma - 1}\frac{p}{\rho}. \tag{2.20}$$

So the conservation of energy becomes;

$$\frac{\gamma}{\gamma - 1}\frac{p_1}{\rho_1} + \frac{1}{2}u_{1n}^2 = \frac{\gamma}{\gamma - 1}\frac{p_2}{\rho_2} + \frac{1}{2}u_{2n}^2. \tag{2.21}$$

Rearranging (2.16) gives:

$$u_{2n} = \frac{\rho_1 u_{1n}}{\rho_2}. \tag{2.22}$$

Inserting (2.22) into (2.17) and solving the resulting equation for p_2 gives:

$$p_2 = p_1 + \rho_1 u_{1n}^2\left(1 - \frac{\rho_1}{\rho_2}\right). \tag{2.23}$$

Inserting this into (2.21) gives a quadratic in ρ_2^{-1}:

$$\frac{\gamma + 1}{2(\gamma - 1)}\frac{\rho_1^2 u_{1n}^2}{\rho_2^2} - \frac{\gamma}{\gamma - 1}(p_1 + \rho_1 u_{1n}^2)\frac{1}{\rho_2} + \frac{\gamma}{\gamma - 1}\frac{p_1}{\rho_1} + \frac{1}{2}u_{1n}^2. \tag{2.24}$$

One solution of (2.24) is $\rho_2 = \rho_1$, which is the acoustic solution. Therefore by using the expression for the product of the roots of a general quadratic equation, the following holds:

$$\frac{1}{\rho_2\rho_1} = \frac{\frac{2\gamma p_1}{\rho_1} + (\gamma - 1)u_{1n}^2}{(\gamma + 1)\rho_1^2 u_{1n}^2}. \tag{2.25}$$

The speed of sound in an ideal gas is given by $a^2 = \gamma p/\rho$; the ratio of the speed to the speed of sound is called the *Mach number*, denoted by M. This reduces the product of the roots to be:

$$\frac{1}{\rho_2\rho_1} = \frac{2 + (\gamma - 1)M_{1n}^2}{\rho_1^2 M_{1n}^2}. \tag{2.26}$$

Which gives the ratio of densities to be

$$\frac{\rho_2}{\rho_1} = \frac{(\gamma + 1)M_{1n}^2}{2 + (\gamma - 1)M_{1n}^2}. \tag{2.27}$$

Pressure behind the shock can be written in terms of the ratio of densities:

$$p_2 = p_1 + \rho_1 u_{1n}^2\left(1 - \frac{\rho_1}{\rho_2}\right) \tag{2.28}$$

Inserting (2.27) into (2.28) and rearranging yields:

$$\frac{p_2}{p_1} = 1 + \frac{2\gamma}{\gamma+1}(M_1^2 \sin^2 - 1) \tag{2.29}$$

In order to calculate the Mach number behind the shock, use the notation:

$$[\phi] = \phi_2 - \phi_1. \tag{2.30}$$

Then the Rankine-Hugoniot equations can be written as:

$$[\rho M a] = 0 \tag{2.31}$$

$$\left[(1+\gamma M^2)\rho a^2\right] = 0 \tag{2.32}$$

$$\left[\left(1 + \frac{\gamma-1}{2}M^2\right)a^2\right] = 0 \tag{2.33}$$

Examining the quotient $(2.32)^2/((2.31)^2(2.33)$, the Mach number is given to be:

$$\left[\frac{(1+\gamma M_n^2)^2}{M_n^2(1+\frac{\gamma-1}{2}M_n^2)}\right] = 0 \tag{2.34}$$

Expanding (2.34) results:

$$\frac{(1+\gamma M_{1n}^2)^2}{M_{1n}^2(1+\frac{\gamma-1}{2}M_{1n}^2)} = \frac{(1+\gamma M_{2n}^2)^2}{M_{2n}^2(1+\frac{\gamma-1}{2}M_{2n}^2)} \tag{2.35}$$

Equation (2.35) can be re-arranged in a quadratic equation in M_{2n}^2, as before one of the solutions is $M_{2n}^2 = M_{1n}^2$, and using the product of roots argument shows that:

$$M_{2n}^2 = \frac{2+(\gamma-1)M_{1n}^2}{1-\gamma+2\gamma M_{1n}^2}. \tag{2.36}$$

2.2 Prandtl's Relation For An Oblique Shock

There is a very simple relationship between the values of the normal velocity of the flow before and after the shock and the tangential velocity. The speed of sound a is given by:

$$a^2 = \frac{\gamma p}{\rho}. \tag{2.37}$$

This renders the conservation of energy (2.18) in the form:

$$\frac{a^2}{\gamma-1} + \frac{1}{2}(u_n^2 + u_t^2) = \text{constant}. \tag{2.38}$$

It is possible to express (2.38) in terms of the fluid speed at a point where the flow is sonic, i.e. $v = a$. This speed is the termed the *critical velocity* $\hat{a}$. This gives:

$$\frac{a^2}{\gamma-1} + \frac{1}{2}|\mathbf{u}|^2 = \frac{\hat{a}^2}{\gamma-1} + \frac{1}{2}\hat{a}^2 = \frac{1}{2}\left(\frac{\gamma+1}{\gamma-1}\right)\hat{a}^2. \tag{2.39}$$

So across the shock:

$$\frac{a_1^2}{\gamma-1} + \frac{1}{2}(u_{1n}^2 + u_{1t}^2) = \frac{a_2^2}{\gamma-1} + \frac{1}{2}(u_{2n}^2 + u_{2t}^2) = \frac{1}{2}\left(\frac{\gamma+1}{\gamma-1}\right)\hat{a}^2. \tag{2.40}$$

Subtracting[1] $1/2u_t^2$ from (2.40) yields:

$$\frac{a_1^2}{\gamma-1} + \frac{1}{2}u_{1n}^2 = \frac{a_1^2}{\gamma-1} + \frac{1}{2}u_{2n}^2 = \frac{1}{2}\left(\frac{\gamma+1}{\gamma-1}\right)\hat{a}^2 - \frac{1}{2}u_t^2. \tag{2.41}$$

Divide (2.17) through by (2.16) to get:

$$\frac{p_1}{\gamma\rho_1 u_{1n}} + u_{1n} = \frac{p_2}{\gamma\rho_2 u_{2n}} + u_{2n}. \tag{2.42}$$

Using the critical velocity to get rid of the sound speed gives:

$$\frac{1}{\gamma u_{1n}}\left[\left(\frac{\gamma+1}{2}\right)\hat{a}^2 - \frac{\gamma-1}{2}(u_{1n}^2+u_t^2)\right] + u_{1n} = \frac{1}{\gamma u_{2n}}\left[\left(\frac{\gamma+1}{2}\right)\hat{a}^2 - \frac{\gamma-1}{2}(u_{2n}^2+u_t^2)\right] + u_{2n}. \tag{2.43}$$

Multiplying through by $\gamma u_{1n}u_{2n}$; (2.43) can be arranged into a quadratic in u_{2n}

$$\begin{aligned} 0 \;=\; & \left(\frac{\gamma+1}{2}\right)u_{1n}u_{2n}^2 - \\ & - \left[\left(\frac{\gamma+1}{2}\right)\hat{a}^2 - \left(\frac{\gamma-1}{2}\right)(u_{1n}^2+u_t^2) + \gamma u_{1n}^2\right]u_{2n} + \\ & + \left(\frac{\gamma+1}{2}\right)\hat{a}^2 u_{1n} - \left(\frac{\gamma-1}{2}\right)u_t^2 u_{1n}. \end{aligned}$$

One of the roots of this equation is known to be u_{1n} and so using the product of the roots arguments the solution is:

$$u_{2n}u_{1n} = \hat{a}^2 - \left(\frac{\gamma-1}{\gamma+1}\right)u_t^2. \tag{2.44}$$

[1] As $u_{1t} = u_{2t}$, the notation $u_{1t} = u_{2t} = u_t$ is used

2.2.1 Relationship Between Flow Deflection Angle and Shock Angle

An important part of oblique shock wave theory is to find the angle at which the flow is deflected by given the shock angle and vice versa. Dividing (2.16) by (2.15) gives (figure 2.1):

$$\frac{\tan\theta}{\tan(\theta-\varphi)} = \frac{\rho_2}{\rho_1}. \tag{2.45}$$

Using expression (2.27) for the ratio of the densities it is possible to obtain two important relationships between the flow deflection angle and the shock angle. To derive the flow deflection angle from the shock angle:

$$\tan\varphi = 2\cot\theta \frac{M^2\sin^2\theta - 1}{2 + M^2(\gamma + \cos 2\theta)}. \tag{2.46}$$

To get from the flow deflection angle to the shock angle use the equations:

$$\begin{aligned} 0 \;=\; & \left(1 + \frac{\gamma-1}{2}M^2\right)\tan\varphi\tan^3\theta - (M^2-1)\tan^2\theta + \\ & + \left(1 + \frac{\gamma+1}{2}M^2\right)\tan\varphi\tan\theta + 1. \end{aligned}$$

Plotting (2.46) for a given Mach number (figure 2.2) shows that for a given flow deflection angle, there are two shock angles. This means the solution is not unique. The same flow deflection angle can be obtained through two shocks which are termed "strong" and "weak". The flow speed after a strong shock is *subsonic* whereas the flow after a weak shock can still be supersonic. Note that from the Mach Construction given in chapter 1, the smallest possible angle for an oblique shock wave is the Mach angle and likewise the largest possible angle it can be is just the normal shock. So the range of shock angles is given by:

$$\sin^{-1}\frac{1}{M} \leq \theta \leq \frac{\pi}{2}. \tag{2.47}$$

Note that the maximum values of the shock angle corresponds to zero flow deflection angle.

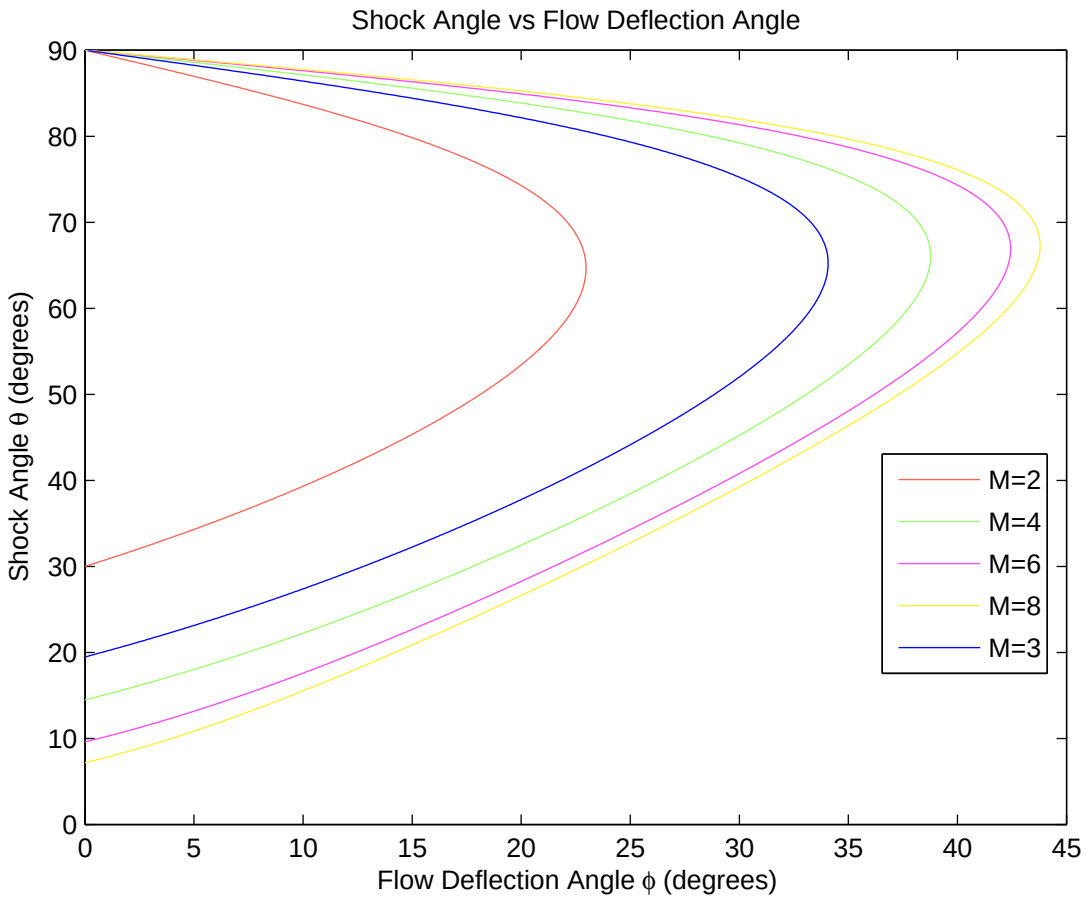

Figure 2.2: Flow Deflection Angle vs Shock Angle

2.2.2 Oblique Shocks in Solids

It is usual in the theory of shock in solids to have the shock moving into undisturbed material rather then having a stationary shock and have the fluid flow through the shock. The notation is usually given as the speed of the shock being U_S and the speed of the material in rear of the shock is given by u_p and is referred to as the *particle velocity*. The next task is to relate these variables to the stationary shock case. Assume that the shock is moving from right to left. Looking at the Rankine-Hugoniot equations for stationary shock waves the interpretations of the particle

velocities are the following:

$$\begin{aligned} u_1 &= \text{velocity of the flow in advance of the shock } \textit{relative} \text{ to the shock} \\ u_2 &= \text{velocity of the flow in rear of the shock } \textit{relative} \text{ to the shock} \end{aligned}$$

However, as the shock was stationary, the particle velocities were also relative to the laboratory. So if a moving shock wave moves into undisturbed air with speed U_S, then U_S must have the interpretation of particle velocity of the medium in advance of the shock. Likewise $U_S - u_p$ has the interpretation of particle velocity of the medium in rear of the shock relative to the shock.

So it is possible to make the following "substitutions"

$$\begin{aligned} u_1 &= U_S \\ u_2 &= U_S - u_p. \end{aligned}$$

As a result the Rankine-Hugoniot equations become

$$\begin{aligned} \rho_1 U_S &= \rho_2 (U_S - u_p) \\ p_1 + \rho_1 U_S^2 &= p_2 + \rho_2 (U_S - u_p)^2 \\ e_1 + \frac{p_1}{\rho_1} + \frac{1}{2} U_S^2 &= e_2 + \frac{p_2}{\rho_2} + \frac{1}{2} (U_S - u_p)^2. \end{aligned}$$

The theory of oblique shocks in gases is well known, however there has been little work examining the relevant equations for solids. The jump conditions for mass and momentum follow through exactly as before the only difference is the equation of state. It is well known experimentally that the shock speed U_S in a solid obeys the relationship:

$$U_S = a + b u_p, \tag{2.48}$$

where a is taken to be the bulk sound velocity and b is related to the second derivative of the bulk modulus. An experimental fact is that at high pressures (GPa) solids act as if they were fluids and so the hydrodynamic equations are appropriate for the analysis. For an oblique shock the equation of state is refined to:

$$U_{Sn} = a + b u_{pn}.$$

Rearranging for u_{pn} gives:

$$u_{pn} = \frac{U_{Sn} - a}{b}.$$

Inserting this into (2.16) makes the ratio of densities:

$$\frac{\rho_2}{\rho_1} = \frac{bU_{Sn}}{a + (b-1)U_{Sn}}.$$

However, $U_{Sn} = U_S \sin\theta$, and therefore:

$$\frac{\rho_2}{\rho_1} = \frac{bU_S \sin\theta}{a + (b-1)U_S \sin\theta}. \tag{2.49}$$

Inserting this into (2.45) gives:

$$\frac{\tan\theta}{\tan(\theta - \varphi)} = \frac{bU_S \sin\theta}{a + (b-1)U_S \sin\theta}. \tag{2.50}$$

Using the trigonometric identity:

$$\tan(\theta - \varphi) = \frac{\tan\theta - \tan\varphi}{1 + \tan\theta \tan\varphi}.$$

It is possible to deduce the following expression for the flow deflection angle:

$$\tan\varphi = \frac{U_S \sin\theta - a}{a\tan\theta + (b-1)U_S \sin\theta \tan\theta + bU_S \cos\theta}. \tag{2.51}$$

Getting values for a, b, U_S and plotting (2.51) shows that there are two shock angles for a given flow deflection angle, which correspond to the strong and weak solutions of the Rankine-Hugoniot equations (figure 2.3). The graph also shows that there is a maximum flow deflection angle which is also like the ideal gas case although (2.51) is very different in structure. It may also be noted that it is possible to divide the denominator and numerator by a which represents the sound speed in the material and get the equation in terms of the Mach number $M = U_S/a$.

2.2.3 Deriving θ from φ

In this section equation (2.50) is re-examined. The goal of this section is to derive an equation which enables the shock angle to be calculated from the flow deflection angle. The method taken mirrors the ideal gas case, so the idea is to turn $\sin\theta$ on the RHS of (2.50) to $\tan\theta$ via the equation:

$$\sin\theta = \frac{\tan\theta}{\sqrt{1 + \tan^2\theta}}.$$

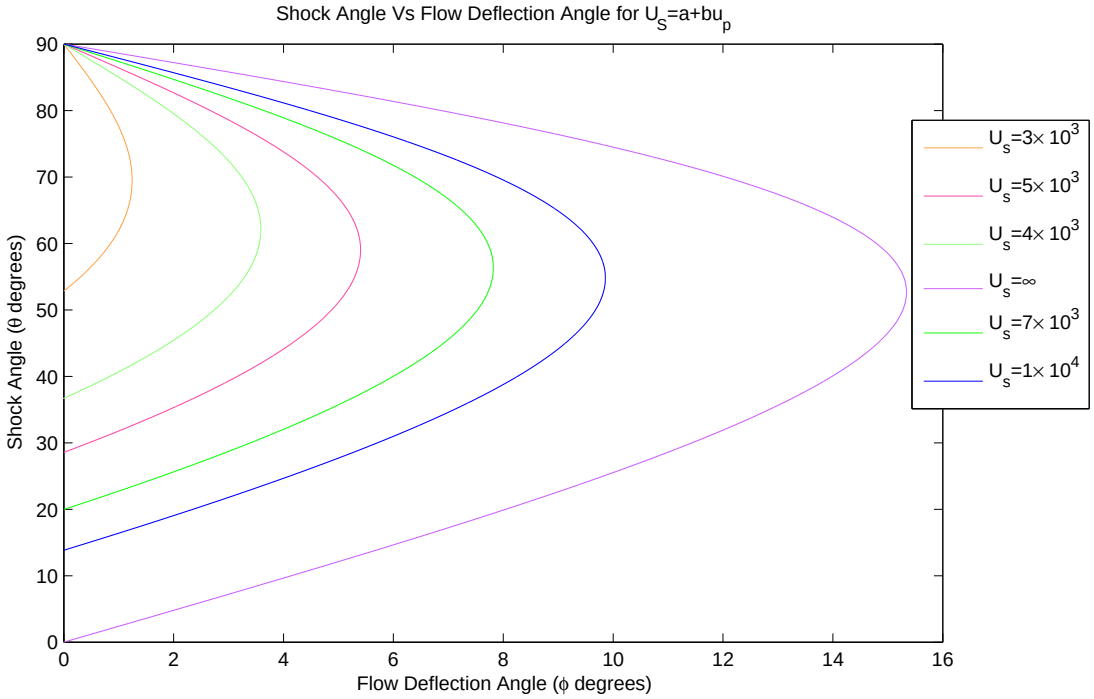

Figure 2.3: Shock Angle Vs Flow Deflection Angle

Inserting this into (2.50) gives after cancelling a $\tan\theta$:

$$\frac{1+\tan\theta\tan\varphi}{\tan\theta-\tan\varphi}=\frac{bU_S}{(b-1)U_S\tan\theta+a\sqrt{1+\tan^2\theta}}. \tag{2.52}$$

The idea now is to remove the square root by squaring, this gives:

$$a^2(1+\tan\theta\tan\varphi)^2(1+\tan^2\theta)=(U_S\tan\theta-bU_S\tan\varphi-(b-1)U_S\tan^2\theta\tan\varphi)^2.$$

This may now be arranged into a polynomial in $\tan\theta$:

$$A\tan^4\theta+B\tan^3\theta+C\tan^2\theta+D\tan\theta+E=0.$$

Where;

$$\begin{aligned}
A &= (a^2-(b-1)^2U_S^2)\tan^2\varphi\\
B &= 2(a^2+(b-1)U_S^2)\tan\varphi\\
C &= a^2-U_S^2+(a^2-2b(b-1)U_S^2)\tan^2\varphi\\
D &= 2(a^2+bU_S^2)\tan\varphi\\
E &= a^2-b^2U_S^2\tan^2\varphi
\end{aligned}$$

In general, there are four real solutions to the above quartic, the solutions can be ordered in terms of size as (a_1, a_2, a_3, a_4). The first two solutions a_1, a_2 are negative which is unphysical and can be ignored. This leaves the other two solutions a_3 and a_4 which are the physical solutions and correspond to the weak and strong shocks respectively.

2.2.4 Maximum Flow Deflection Angle

As with the ideal gas case equation (2.51) can be differentiated to give the shock angle corresponding to the maximum flow deflection angle. The equation is:

$$\begin{aligned} 0 &= a^2 \sec^2\theta - aU_S \sin\theta + U_S^2 \sin^2\theta + (b-2)aU_S \sec\theta \tan\theta \\ &\quad - (b-1)U_S^2 \tan^2\theta + U_S \cos\theta. \end{aligned} \tag{2.53}$$

Once this equation is solved, the value of θ would then be inserted into (2.51) to give the maximum flow deflection angle. This is easily done numerically in the following way. Choose a range of shock angles which satisfy:

$$\sin^{-1}\frac{a}{U_S} \leq \theta \leq \frac{\pi}{2}.$$

Compute $\tan\varphi$ by using (2.51) and find the maximum value in the array, this will correspond to the maximum flow deflection angle.

2.3 Solving the Rankine-Hugoniot Equations

It was found that the density ratio across a shock is given by (2.49), namely,

$$\frac{\rho_2}{\rho_1} = \frac{bU_S \sin\theta}{a + (b-1)U_S \sin\theta}. \tag{2.54}$$

Another important quantity to calculate is the pressure. Using the conservation of mass, the conservation of momentum can be written as:

$$p_2 = p_1 + \rho_1 U_{Sn}^2 \left(1 - \frac{\rho_1}{\rho_2}\right).$$

Using further the equation (2.54) gives:

$$p_2 = p_1 + \rho_1 U_S \sin\theta \left[\frac{U_S \sin\theta - a}{b} \right]. \tag{2.55}$$

It is usual in the theory of shocks in solids to assume $p_1 = 0$ as this tends to be atmospheric pressure. As the pressure in a shocked solid is of the order of GPa so the initial pressure is usually neglected. Note that for an ideal gas the density varies with the *square* of the Mach number whilst the expression for a solid only depends on the shock speed, not the square of the shock speed. The same observation can be applied to the pressure but there is also a quadratic term in the shock speed. This is most likely due to the linear nature of the equation of state used as it does not take into account that although the solid can be treated as a fluid under pressure, there is still resistance to flow. Typically in experiments the shock speed is of the order of $10^3 \mathrm{ms}^{-1}$

2.4 Oblique Shock Reflection

2.4.1 Full Theory

Consider air flow down a channel with a wedge on one side. A shock will form at the tip of the wedge to turn the flow parallel to the wedge surface. As the width of the channel is finite the flow must be deflected back parallel to the opposite wall, the physical mechanism for this is a second shock which starts at the point where the first shock reaches the wall (figure 2.4). Unlike light, the angle of reflection is not equal to the angle of incidence but for a weak shock, that is when the flow deflection angle φ is small. There are three regions to consider in the diagram of the reflected shock. Region 1 lies in front of the first shock, region 2 is the region in between the incident shock and reflected and region 3 behind the reflected shock. To examine this phenomenon, two sets of Rankine-Hugoniot equations are needed, one set for the incident shock and one set for the reflected shock. The set of equations which deal

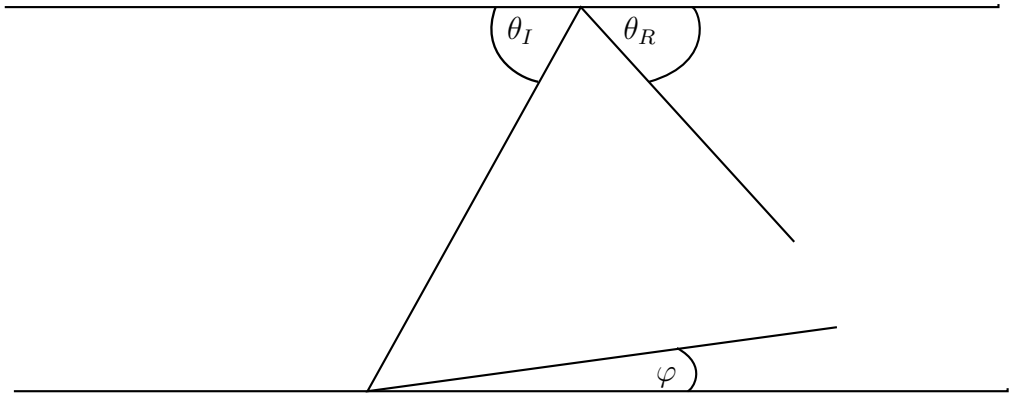

Figure 2.4: Oblique Shock Reflection

with the incident shock are:

$$\rho_1 u_1 \sin\theta_I = \rho_2 u_2 \sin(\theta_I - \varphi) \tag{2.56}$$

$$p_1 + \rho_1 u_1^2 \sin^2\theta_I = p_2 + \rho_2 u_2^2 \sin^2(\theta_I - \varphi) \tag{2.57}$$

$$\frac{\gamma}{\gamma-1}\frac{p_1}{\rho_1} + \frac{1}{2}u_1^2 \sin^2\theta_I = \frac{\gamma}{\gamma-1}\frac{p_2}{\rho_2} + \frac{1}{2}u_2^2 \sin^2(\theta_I - \varphi). \tag{2.58}$$

The set of equations which deal with the reflected shock are:

$$\rho_2 u_2 \sin\theta_R = \rho_3 u_3 \sin(\theta_R - \varphi) \tag{2.59}$$

$$p_2 + \rho_2 u_2^2 \sin^2\theta_R = p_3 + \rho_3 u_3^2 \sin^2(\theta_R - \varphi) \tag{2.60}$$

$$\frac{\gamma}{\gamma-1}\frac{p_2}{\rho_2} + \frac{1}{2}u_2^2 \sin^2\theta_R = \frac{\gamma}{\gamma-1}\frac{p_3}{\rho_3} + \frac{1}{2}u_3^2 \sin^2(\theta_R - \varphi). \tag{2.61}$$

The incident shock deflects the flow *toward* the boundary and the reflected shock deflects the flow parallel to the boundary again, which is the reason why the reflected shock exists. The equation which deals with the relationship between the flow deflection angle φ and the shock angle θ is also used:

$$\begin{aligned} 0 = &\left(1 + \frac{\gamma-1}{2}M^2\right)\tan\varphi\tan^3\theta - (M^2-1)\tan^2\theta + \\ &+ \left(1 + \frac{\gamma+1}{2}M^2\right)\tan\varphi\tan\theta + 1. \end{aligned} \tag{2.62}$$

To solve a shock reflection problem, equations (2.56) to (2.62) are analysed. It should be noted that in an oblique shock reflection problem, the weak shock solutions should be chosen and as such the flow will be supersonic throughout.

In general the solution of a typical shock reflection problem must be studied numerically. In the case of small flow deflection angle φ theoretical analysis can be carried out.

2.4.2 Weak Shock Reflection

For linearised supersonic flow, the equation for pressure is written as[2]:

$$(M^2-1)\frac{\partial^2 p}{\partial x^2}-\frac{\partial^2 p}{\partial y^2}=0. \tag{2.63}$$

The characteristics for the above equation are given by:

$$\frac{dy}{dx}=\pm\frac{1}{\sqrt{M^2-1}}=\pm\frac{1}{\beta}. \tag{2.64}$$

Integrating (2.64) gives the characteristics; $\beta y \pm x =$ constant, where $\beta=\sqrt{M^2-1}$. The angles of the shock wave relative to the wall are also given by (2.64), and therefore, for *weak* shock waves, the angle will always be the Mach angle. Define the characteristic co-ordindates by:

$$\begin{aligned}\xi &= \beta y + x\\ \eta &= \beta y - x.\end{aligned}$$

One of these characteristics deals with the incident shock and the other deals with the reflected shock; when describing the incident shock the portion of the solution which represents the reflected shock can be ignored as it has no effect on the incident wave . Writing (2.63) in terms of these new co-ordinates yields:

$$\frac{\partial^2 p}{\partial\xi\partial\eta}=0. \tag{2.65}$$

This can immediately be solved to get the general solution,

$$p(\xi,\eta)=f(\xi)+g(\eta). \tag{2.66}$$

Consider air flow down a channel of width h with a wedge which decreases the width of the channel and let this wedge be small enough so that if φ denotes the angle of

[2]The full derivation of this equation and other equations associated with linearised supersonic inviscid flow will be carried out fully in chapter 7

the wedge then $\tan\varphi \approx \varphi$. Also from the linearised theory of inviscid compressible flows:

$$\beta^2 \frac{\partial p}{\partial x} = -\rho_0 u_0 \frac{\partial v}{\partial y}. \tag{2.67}$$

The boundary conditions for this problem are:

$$\partial_y p(x,0) = 0 \tag{2.68}$$

$$\partial_y p(x,h) = 0 \tag{2.69}$$

$$\partial_x v(x,0) = \varphi\delta(x). \tag{2.70}$$

where $\delta(x)$ is the Dirac delta function. Also from linear theory:

$$u_0 \frac{\partial v}{\partial x} = -\frac{1}{\rho_0}\frac{\partial p}{\partial y}. \tag{2.71}$$

Hence, at $y = 0$,

$$u_0 \left.\frac{\partial v}{\partial y}\right|_{y=0} = -\frac{1}{\rho_0}\left.\frac{\partial p}{\partial y}\right|_{y=0} = -\beta f'(x). \tag{2.72}$$

Combining this with (2.70) shows:

$$u_0 \delta(x)\varphi = \frac{\beta}{\rho_0} f'(x). \tag{2.73}$$

Integrating the delta function gives the Heaviside function, so:

$$f(x,y) = -\frac{u_0}{\beta}\varphi(\beta y - x). \tag{2.74}$$

Now the other part of the solution is brought in, write,

$$p(x,y) = -\frac{u_0}{\beta}\varphi(\beta y - x) + g(\beta y + x). \tag{2.75}$$

Where g represents the reflected shock Using (2.69) shows that:

$$\left.\frac{\partial p}{\partial y}\right|_{y=h} = -u_0\varphi'(\beta h - x) + \beta g(\beta h + x) = 0. \tag{2.76}$$

Integrating (2.76) with respect to x gives:

$$g(\beta h + x) = -\frac{u_0}{\beta}\varphi(\beta h - x). \tag{2.77}$$

Re-labeling the argument shows that:

$$g(\eta) = -\frac{u_0}{\beta}\varphi(2\beta h - \eta), \tag{2.78}$$

and with this the full solution becomes:

$$p(x,y) = -\frac{u_0}{\beta}(\varphi(2\beta h + x - \beta y) + \varphi(\beta y - x)). \tag{2.79}$$

Chapter 3

Shock Polars and Pressure Deflection Diagrams

The shock polar/pressure deflection diagram[1] is the locus of all shocked states possible. The shock polar and pressure deflection diagram both do this in different ways. It is usual in the literature for the pressure deflection diagram to be used for solids instead of shock polars.

3.1 Shock Polars

From the conservation of energy:

$$\frac{1}{\gamma-1}a^2+\frac{1}{2}|\mathbf{V}|^2=\text{constant}. \tag{3.1}$$

Define the *critical velocity*, $\hat{a}$ to be the speed of the fluid at the flow location where the local flow is sonic, so the conservation of energy (2.39) becomes

$$\frac{1}{\gamma-1}a^2+\frac{1}{2}|\mathbf{V}|^2=\frac{1}{2}\left(\frac{\gamma+1}{\gamma-1}\right)\hat{a}^2. \tag{3.2}$$

Define the *normalised velocity* as:

$$\xi=\frac{|\mathbf{V}|}{\hat{a}}. \tag{3.3}$$

[1] Also called a shock polar

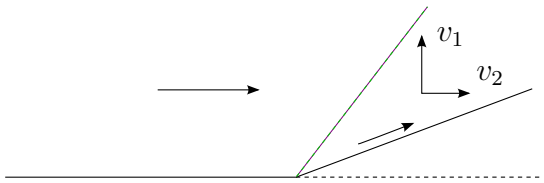

Figure 3.1: The new co-ordinates

Equation (3.2) can be written as:

$$\begin{aligned} |\mathbf{V}|^2\left[\frac{1}{(\gamma-1)M^2}+\frac{1}{2}\right] &= \frac{1}{2}\left(\frac{\gamma+1}{\gamma-1}\right)\hat{a}^2 \\ \text{or} \quad \xi^2\left[\frac{2}{(\gamma-1)M^2}+1\right] &= \left(\frac{\gamma+1}{\gamma-1}\right) \\ \text{which gives} \quad \xi^2 &= \frac{(\gamma+1)M^2}{2+(\gamma-1)M^2}. \end{aligned} \tag{3.4}$$

It is useful to write (3.4) in the form:

$$\frac{1}{M^2} = \frac{\gamma+1}{2}\frac{1}{\xi^2} - \frac{\gamma-1}{2}. \tag{3.5}$$

Now the ratio of densities across an oblique shock is given by equation (2.27):

$$\frac{\rho_2}{\rho_1} = \frac{(\gamma+1)M^2\sin^2\theta}{2+(\gamma-1)M^2\sin^2\theta}. \tag{3.6}$$

From the conservation of mass across a shock (2.2):

$$\rho_1 u_{1n} = \rho_2 u_{2n}. \tag{3.7}$$

So the ratio of normal velocities across a shock is given by:

$$\frac{u_{2n}}{u_{1n}} = \frac{\rho_1}{\rho_2} = \frac{\gamma-1}{\gamma+1} + \frac{2}{(\gamma-1)M^2\sin^2\theta}. \tag{3.8}$$

Define new variables by: If φ is the flow deflection angle and u_2 is the modulus of the velocity behind the shock then:

$$\begin{aligned} v_1 &= u_2\cos\varphi \\ v_2 &= u_2\sin\varphi. \end{aligned}$$

where v_1 is the velocity component in the direction parallel to the velocity before shock and v_2 is the normal direction (figure 3.1).

The idea is to shift the emphasis from a spacial Cartesian co-ordinates to a set of co-ordinates based upon *velocity*, this is called a *hodograph transformation*. So:

$$\begin{aligned} u_{2n} &= u_2 \sin(\theta - \varphi) \\ &= u_2(\sin\theta\cos\varphi - \sin\varphi\cos\theta) \\ &= v_1 \sin\theta - v_2\cos\theta \\ u_{1n} &= u_1 \sin\theta, \end{aligned}$$

where θ denotes the shock angle corresponding to the flow deflection angle. Taking this into account, equation (3.8) may be written as:

$$\frac{v_1}{u_1} - \frac{v_2}{\tan\theta} = \frac{\gamma-1}{\gamma+1} + \frac{2}{(\gamma-1)M^2\sin^2\theta}. \tag{3.9}$$

In order to remove θ from (3.9), note that the tangential part of the velocity is conserved across a shock, so:

$$\begin{aligned} u_1\cos\theta &= u_2\cos(\theta-\varphi) \\ &= v_1\cos\theta + v_2\sin\theta. \end{aligned} \tag{3.10}$$

This gives:

$$\tan\theta = \frac{u_1 - v_1}{v_2}, \quad \sin^2\theta = \frac{(u_1-v_1)^2}{v_2^2 + (u_1-v_1)^2} \tag{3.11}$$

Inserting these into (3.9) results in:

$$\frac{v_1}{u_1} - \frac{v_2^2}{u_1(u_1-v_1)} = \frac{\gamma-1}{\gamma+1} + \frac{2}{\gamma+1}\frac{v_2^2+(u_1-v_1)^2}{(u_1-v_1)^2}\frac{1}{M^2} \tag{3.12}$$

Using (3.5), equation (3.12) can be written as:

$$v_2^2 = \frac{(u_1v_1 - \hat{a}^2)(u_1-v_1)^2}{\hat{a}^2 + \frac{2}{\gamma+1}u_1^2 - u_1v_1}. \tag{3.13}$$

Or in terms of the normalised velocity:

$$\xi_2^2 = \frac{(\xi_1\lambda - 1)(\xi_1-\lambda)^2}{1 + \frac{2}{\gamma+1}\lambda^2 - \lambda\xi_1}, \tag{3.14}$$

where λ is the normalised velocity before the shock, namely,

$$\lambda = \frac{u_1}{\hat{a}} \tag{3.15}$$

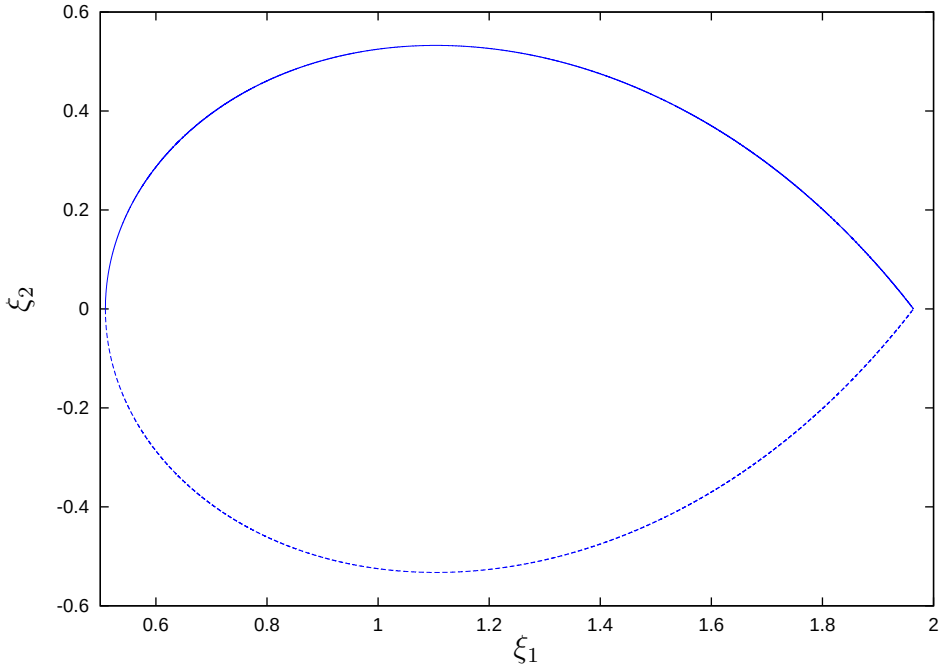

Figure 3.2: Shock Polar, $M = 3$, $\lambda = 1.96$

The limits of the graph are:

$$\frac{1}{\lambda} \leq \xi_1 \leq \lambda. \tag{3.16}$$

It is possible to plot additional information on the shock polar, that of the flow deflection angle. The flow deflection angle can be given as a *constant* ratio of vertical to horizontal velocities after the shock, so the flow deflection angle will be a straight line from the origin. As the shock polar is the locus of shock states, the intersection of the flow deflection line and the shock polar will correspond shocked states corresponding to the given flow deflection angle.

The flow deflection line will intersect the shock polar in two points $\alpha_s < \alpha_w$ on the ξ_1 axis. The first point, α_s corresponds to the strong shock solution where the speed *after* the shock is subsonic. The second point α_w corresponds to the weak shock solution which is of interest in shock reflection.

There are three possible types of flow deflection line. The first type has already been discussed, there are three points of intersection between the flow deflection line and the shock polar. The second type, there is only one point of intersection, this is

when the flow deflection line is tangent to the shock polar, a physical solution still exists but there is only one. The third type is when the flow deflection angle is too large and are no intersection points which means that there is no regular reflection solutions.

Returning to the derivation of the shock polar, expanding $u_{1t} = u_{2t}$ in terms of the flow deflection angle and shock angle yields equation (3.10), dividing throughout by $\cos\theta$ and using the hodograph co-ordinates gives for points on the shock polar results in:

$$\tan\theta = \frac{u_1 - v_1}{v_2}. \tag{3.17}$$

Dividing the numerator and denominator by the critical velocity $\hat{a}$ gives:

$$\tan\theta = \frac{\lambda - \xi_1}{\xi_2}, \tag{3.18}$$

where (ξ_1, ξ_2) correspond to the points of intersection of the flow deflection line and the shock polar. Consider a line which passes through the point $(\lambda, 0)$ and the point (ξ_1, ξ_2). The gradient of this line will be:

$$\tan\alpha = \frac{\xi_2}{\xi_1 - \lambda}. \tag{3.19}$$

Note that $\tan\theta\tan\alpha = -1$, so this describes a new method of calculating the shock angle from the flow deflection angle.

For a given Mach number before the shock, plot the shock polar and then plot the flow deflection line. If φ is the flow deflection angle, solve the pair of equations:

$$\begin{aligned} \xi_1^2 \tan^2\alpha &= \frac{(\lambda\xi_1 - 1)(\lambda - \xi_1)^2}{1 + \frac{2}{\gamma+1}\lambda^2 - \lambda\xi_1} \\ \xi_2 &= \tan\varphi\xi_1 \end{aligned}$$

to find the points of intersection of the flow deflection angle and the shock polar. Then calculate the gradient of the line, L from $(\lambda, 0)$ to (ξ_1, ξ_2). The gradient of the line from $(0, 0)$ which is at right angles to L will be equal to $\tan\theta$, where θ is the shock angle.

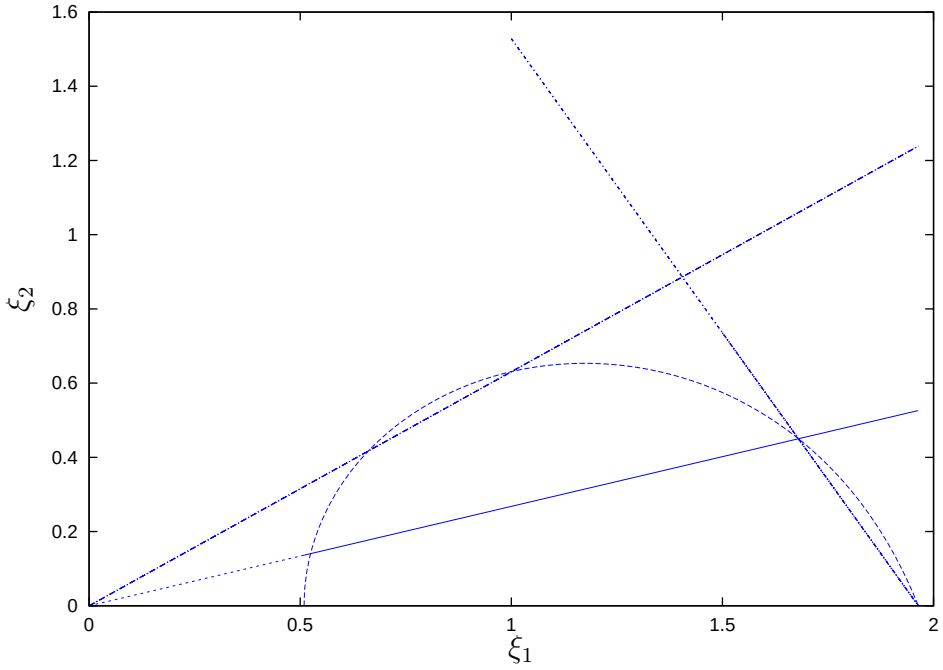

Figure 3.3: Calculating the Shock Angle

3.2 Pressure Deflection Diagrams

3.2.1 Incident Shock

The shock polar represents information about the velocities before and after an oblique shock. The pressure deflection diagram[2] is a graph of pressure ratio across the shock against flow deflection angle. The diagram can be plotted for both strong and weak shocks for left and right going waves (figure 3.4 The relationship between the flow deflection angle and shock angle gives a maximum shock angle for a given Mach number, which in turn gives a maximum possible flow deflection angle. The maximum possible flow deflection angle gives the maximum possible turning angle for there to be an attached shock at the tip of the wedge turning the flow, if the flow deflection angle is any larger than this then the resulting shock is detached from the tip. The maximum flow deflection is where the tangent line to the pressure deflection diagram is vertical (see figure 3.4).

When dealing with other materials, it is more usual to use a pressure deflection

[2]In some texts, a pressure deflection diagram is also called a shock polar

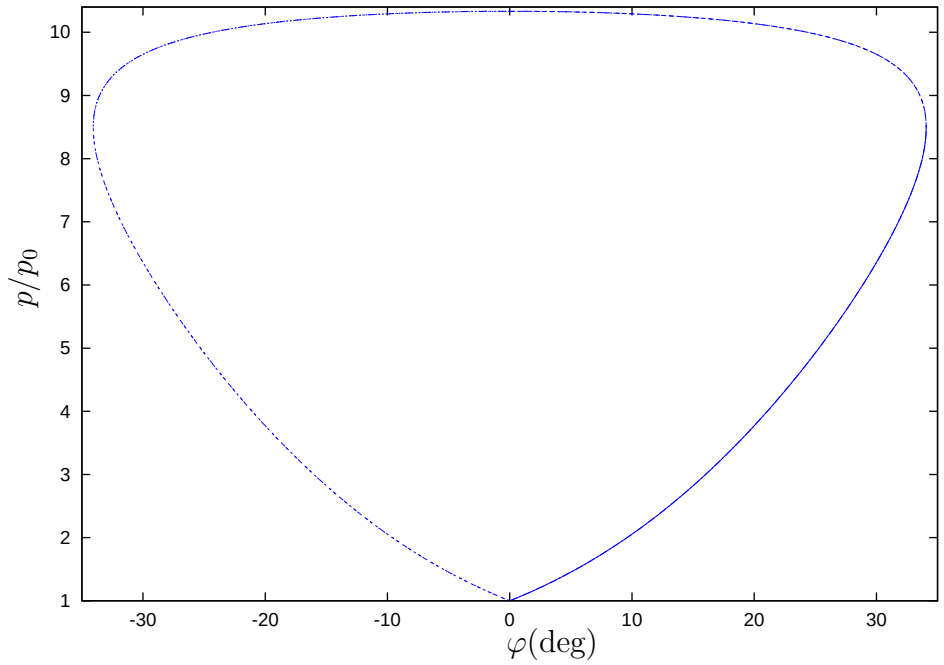

Figure 3.4: Pressure Deflection Diagram for a Perfect Gas

diagram rather than a shock polar. Figure 3.5 shows a pressure deflection diagram for a linear shock equation of state[3]. For solids it is customary to take the initial pressure to be zero.

3.2.2 Reflected Shock

The physical set up is material flows over an impermeable wedge and creates an incident shock at the wedge tip, the incident shock then hits another impermeable wall and creates a reflected shock (figure 2.4). The reflected polar can also be plotted on the same set of axes. The pressure deflection diagram can give information about regular reflections, the "tip" of the reflected polar should lie on the incident shock.

For the case of the regular reflection, if the reflected polar crosses the p-axis then the points at which it crosses will be the pressure after the reflected shock. There are three possibilities for the reflected shock:

- The reflected polar intersects the p-axis in two places, corresponding to both

[3]The linear shock EoS is given by $U_S = a + bu_p$, where a and b are determined by experiment

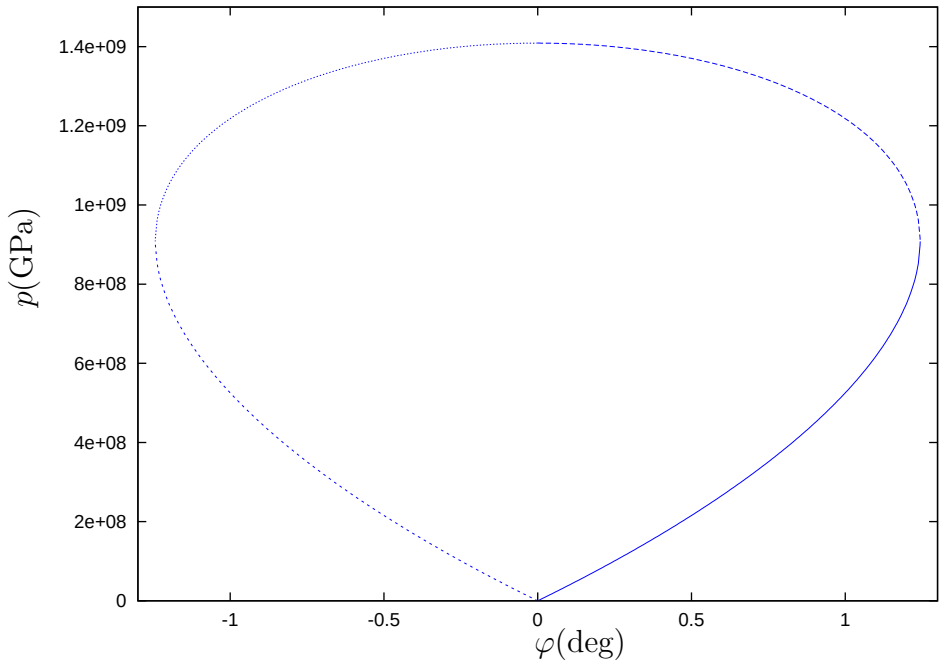

Figure 3.5: Pressure Deflection Diagram Linear Shock EoS

the strong and weak solutions to the Rankine-Hugoniot equations.

- The reflected polar is tangent to the p-axis, so there is only one point of contact of the reflected polar and p-axis. Regular reflection still exists but for only one single shock angle.

- There is no intersection of the reflected polar and the p-axis, there is no possible regular reflection.

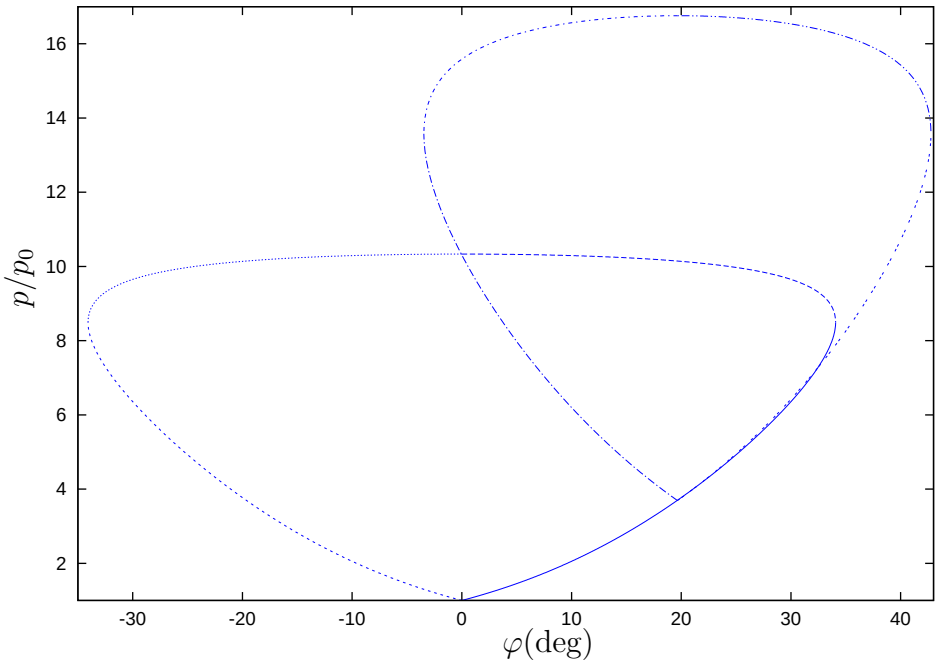

Figure 3.6: Reflected Shock

Chapter 4

Mach Reflection

This chapter investigates when a regular reflection cannot happen and discusses when such phenomenon called *Mach reflection* happen as a function of the initial Mach number and shock/flow deflection angle.

4.1 Mach Reflection Configuration

It has been observed in experiments that for certain shock angles and for certain Mach numbers, the following configuration of shocks exists (see figure 4.1).

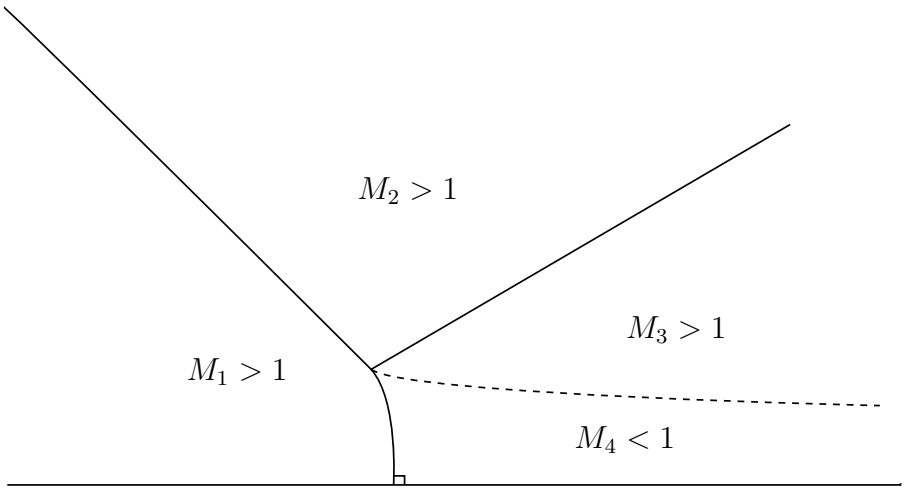

Figure 4.1: Mach Reflection

There are then two questions which follow this observation: 1) Is it possible to model

this phenomenon with a set of equations and 2) When is the transition from regular reflection to Mach reflection. The second of these questions will be answered in the second part of this chapter.

Consider an oblique incident shock in the laboratory frame of reference on a surface, moving horizontally to the surface at a speed u_1 (as shown in figure 4.2). The incident shock gives rise to a reflected shock which moves horizontally to the surface at a speed u_2.

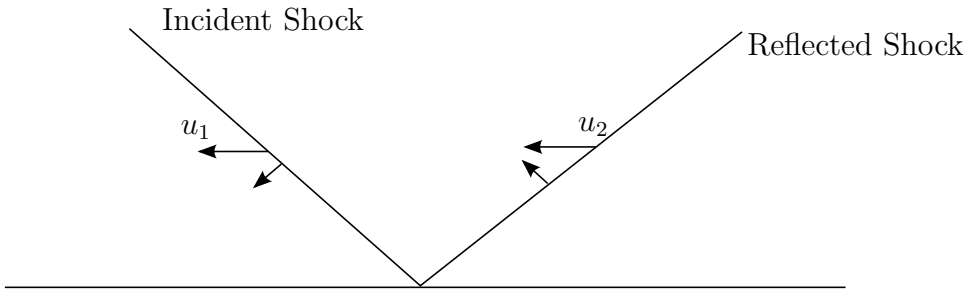

Figure 4.2: Reflected Shocks

If $u_1 = u_2$ then the resulting shock pattern will be a regular reflection. If however $u_1 < u_2$, then this means the reflected shock is moving faster than the incident shock. The reflected shock will begin to merge with the incident shock forming a single strong shock which meets the wall at right angles in order to keep the flow tangential to the wall. The flow behind a strong shock is always subsonic so there will be a dividing contact discontinuity between the subsonic flow and the supersonic flow behind the reflected shock, which is shown as the dashed line in figure 4.1. The pressure is the same on both sides of the contact discontinuity otherwise there would be flow between regions 3 and 4 in figure 4.1 which isn't possible.

Once the reflected shock catches up with the incident shock and merges with it then there are two different types of Mach reflections configurations possible, usually called direct and indirect Mach reflection. The difference between the two configurations is the way the Mach stem bends upstream (figure 4.3), or downstream (figure 4.4). The flow deflection angle for region 4 (figure 4.7) for an indirect Mach reflection

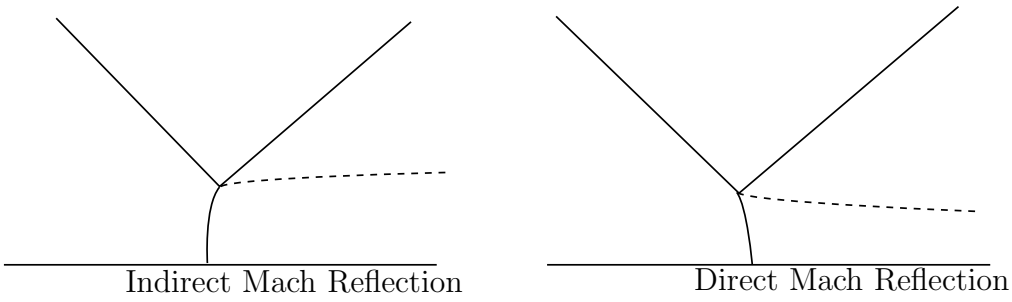

Figure 4.3: Types of Mach Reflection

is given by:

$$\varphi_3 = \varphi_2 + \varphi_1 \tag{4.1}$$

As can be seen by the pressure deflection diagram (figure 4.4), that there are two

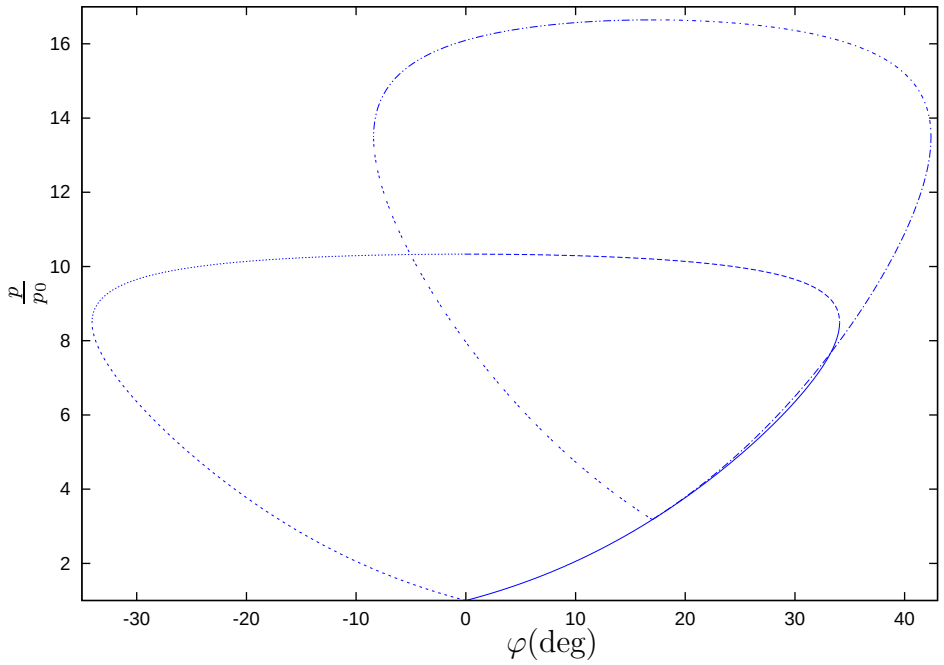

Figure 4.4: Indirect Mach Reflection

possibilities for shock reflection, the first is that of regular reflection as the reflected polar crosses the p-axis, the final pressure is given at the intersection point of the p-axis and the reflected polar. The other possibility is the indirect Mach reflection, the pressure on the stem is calculated from the intersection of the reflected with the strong branch of the shock polar as shown. It is an ongoing area of research to find out

which shock configuration happens. With direct Mach reflection there are still two

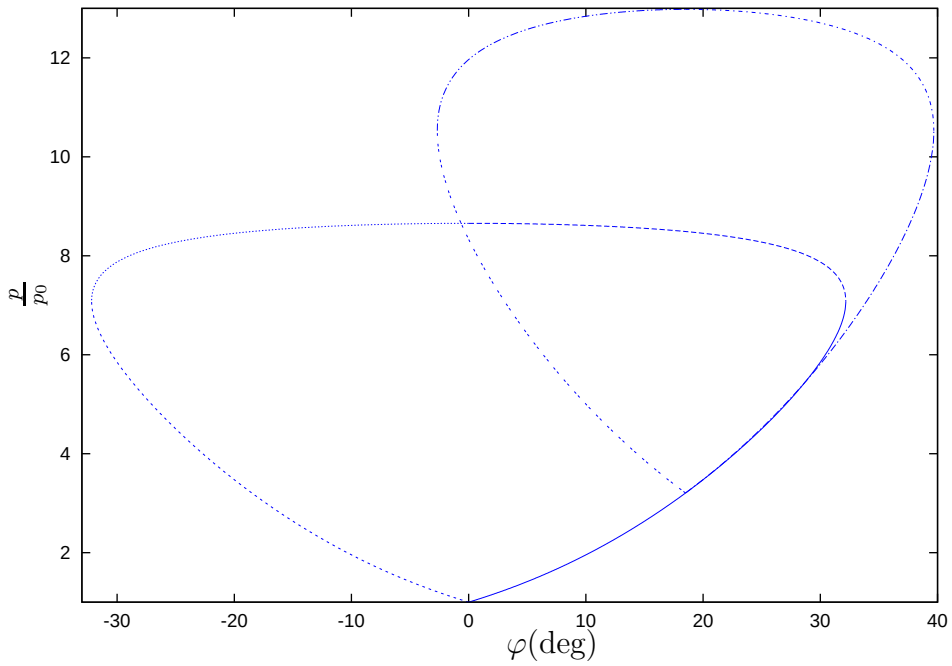

Figure 4.5: Direct Mach Reflection

shock configurations possible (figure 4.5) as the reflected polar crosses the p axis and the portion of the reflected polar which denotes weak shocks intersects the portion of the incident shock polar which denotes strong shocks. The latter scenario is the direct Mach reflection. However if the flow deflection angle of the incident shock is increased then there will be no regular reflection solution and only a direct Mach reflection is possible. Again, the intersection of the reflected polar with the strong branch of the incident shock will give the pressure in the subsonic region. The flow deflection angle in region 4 for a direct Mach reflection (figure 4.7) is given by:

$$\varphi_3 = \varphi_2 - \varphi_1 \tag{4.2}$$

There is also the question of the transition from indirect Mach reflection to direct Mach reflection. In this shock configuration the stem is a straight line, as is the contact discontinuity. In terms of pressure deflection diagrams, the reflection polar intersects the incident polar on the p-axis. The pressures will be equal in regions 3 and 4 (see figure 4.1 for definition of the regions) given by the pressure across the

stem which is a normal shock.

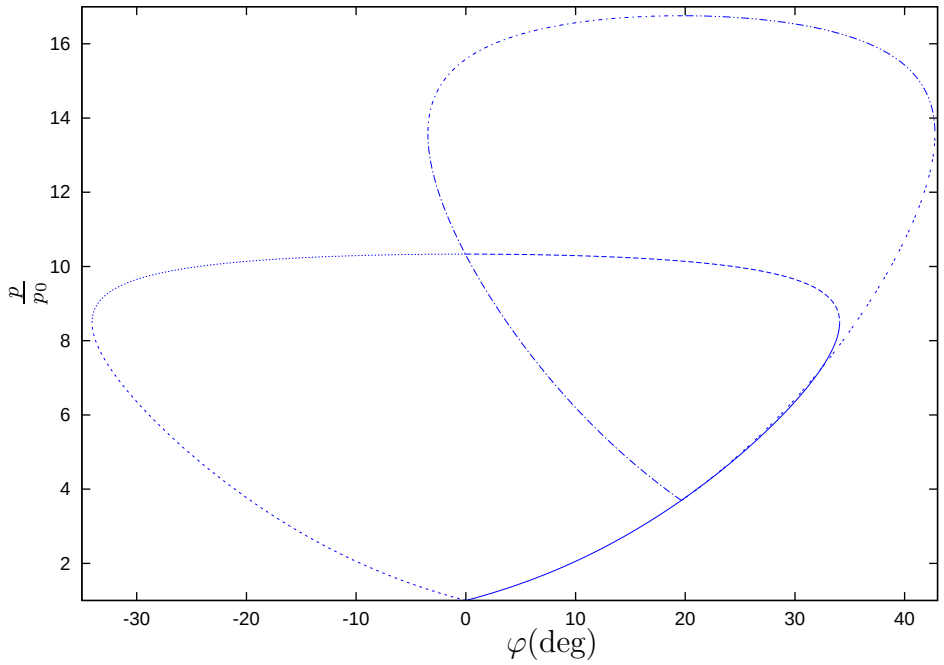

Figure 4.6: Indirect Mach Reflection

The usual method to analyse a Mach reflection is to assume that the contact discontinuity is a straight line at some given angle to be calculated, so this gives a well-defined shock angle to work with. Using this approximation, three shock theory can be applied. Three shock theory applies the Rankine-Hugoniot equations across the incident and reflected shock and the Mach stem.

The key fact to use is that the pressure of either side of the contact discontinuity and so $p_3 = p_4$ and so:

$$\frac{p_4}{p_1} = \frac{p_3}{p_1} = \frac{p_3}{p_2}\frac{p_2}{p_1}. \tag{4.3}$$

The shock angle is a function of the pressure ratio via:

$$\sin^2\theta = \frac{1}{M^2}\left[1 + \frac{\gamma+1}{2\gamma}\left[\frac{p}{p_0} - 1\right]\right]. \tag{4.4}$$

Applying (4.4) and (4.3) to the shock angle on the stem gives:

$$\sin^2\theta_3 = \frac{1}{M_1^2}\left[1 + \frac{\gamma+1}{2\gamma}\left[\frac{p_3}{p_2}\frac{p_2}{p_1} - 1\right]\right]. \tag{4.5}$$

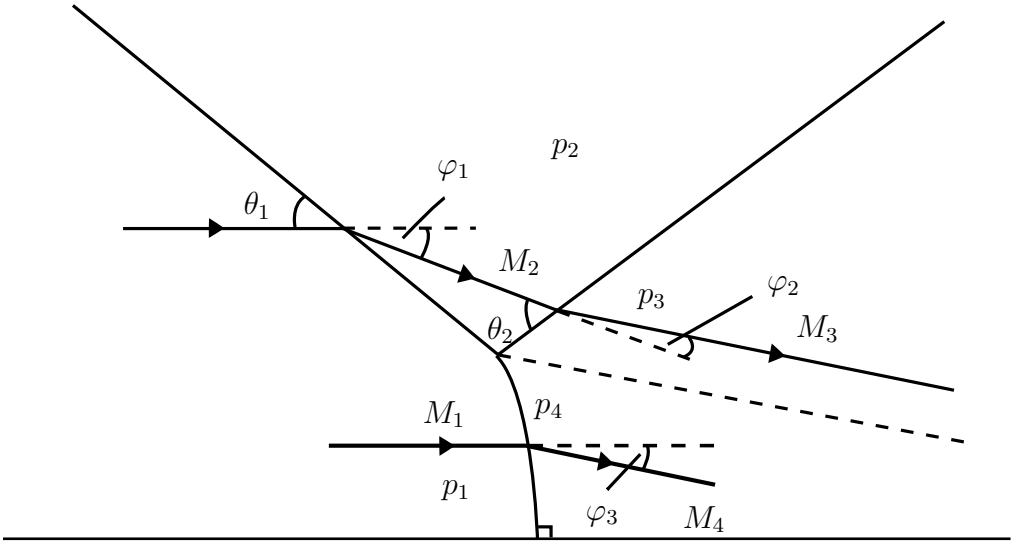

Figure 4.7: Idealisation of Mach Reflection

The ratio of pressures p_2/p_1 can be expressed in terms of θ_1 and M_1. The Mach number in region 2 is given by:

$$M_2^2 = \frac{1}{\sin^2(\theta_1 - \varphi_1)} \frac{2 + (\gamma - 1)M_1^2 \sin^2\theta}{1 - \gamma + 2\gamma M_1^2 \sin^2\theta_1} \tag{4.6}$$

as $M_{1n} = M_1 \sin\theta$ and $M_{2n} = M_2 \sin(\theta - \varphi)$. From (figure 4.7) the flow deflection angles are related by the expression:

$$\varphi_3 = \varphi_1 - \varphi_2. \tag{4.7}$$

The shock and flow deflection angles are related by:

$$\tan\varphi_3 = \cot\theta_3 \frac{M_1^2 \sin^2\theta_3 - 1}{2 + M_1^2(\gamma + \cos 2\theta_3)} \tag{4.8}$$

$$\tan\varphi_2 = \cot\theta_2 \frac{M_2^2 \sin^2\theta_2 - 1}{2 + M_2^2(\gamma + \cos 2\theta_2)} \tag{4.9}$$

$$\tan\varphi_1 = \cot\theta_1 \frac{M_1^2 \sin^2\theta_1 - 1}{2 + M_1^2(\gamma + \cos 2\theta_1)} \tag{4.10}$$

and the pressures across the shocks are given by:

$$\frac{p_2}{p_1} = 1 + \frac{2\gamma}{\gamma + 1}(M_1^2 \sin^2\theta_1 - 1) \tag{4.11}$$

$$\frac{p_3}{p_2} = 1 + \frac{2\gamma}{\gamma + 1}(M_2^2 \sin^2\theta_2 - 1) \tag{4.12}$$

$$\frac{p_4}{p_1} = 1 + \frac{2\gamma}{\gamma + 1}(M_1^2 \sin^2\theta_3 - 1) \tag{4.13}$$

The value for p_3 is calculated as the point of intersection of the strong shock part of the shock polar for the Mach stem (as an incident shock) and the reflected shock. Once this has been done, then the angles θ_2 and θ_3 can be calculated easily.

4.2 Transition from Regular Reflection to Mach Reflection

A number of different criteria have been put forward for the transition from regular reflection to Mach reflection and they will be discussed one by one.

4.2.1 Detachment Criterion

When computing the reflected polar, there are essentially two possible configurations, when the reflected polar does and does not intersect with the p-axis. The limiting case is where the reflected polar is tangent to the p-axis, this is called the *detachment criterion*. (figure 4.8)

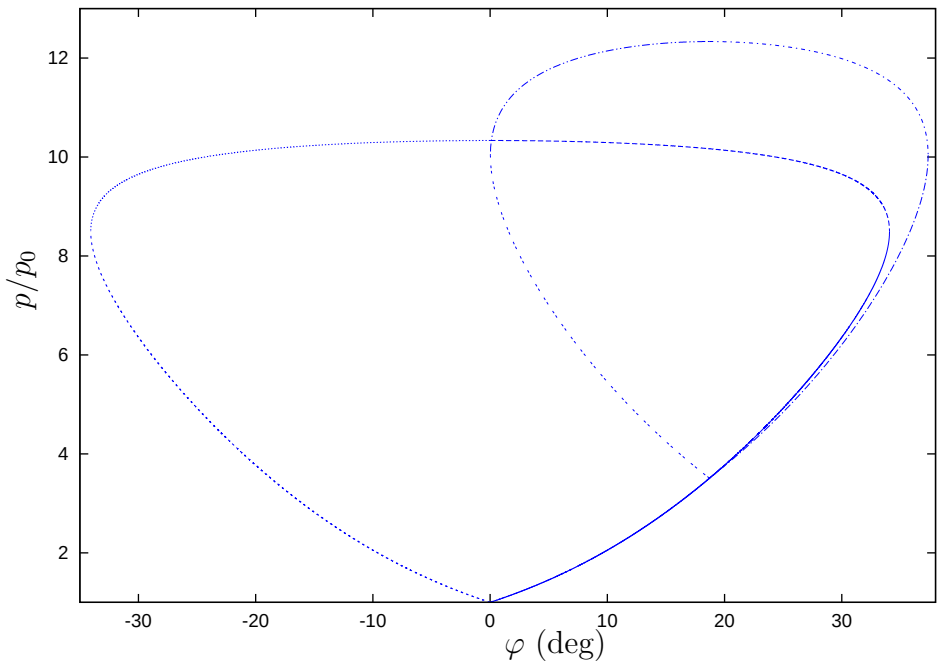

Figure 4.8: Detachment Criterion

There is one other possible shock configuration, that is where there is no reflected shock, this is because the flow after the incident shock is *subsonic*, these criteria are close to each other.

4.2.2 von Neumann Criterion

When the Mach stem forms, the following conditions should be satisfied. Firstly, the pressure immediately above the contact discontinuity (in region 3) should coincide with the pressure immediately below the contact discontinuity (in region 4. This is written as

$$p_3 = p_4. \tag{4.14}$$

Secondly, the velocity vector in regions 3 and 4 should be tangent to the contact discontinuity, which gives:

$$\varphi_3 = \varphi_2 - \varphi_1 = 0. \tag{4.15}$$

The shape of the stem in a von Neumann reflection is a straight line as the von Neumann reflection (figure 4.9) is the transition point between the indirect and direct Mach reflection. The stem will be perpendicular to the wall because the flow has be remain parallel to the wall.

Examining the points at which the reflection polar intersects the p axis (figure 4.9) yields two possible solutions, a Mach reflection and a regular reflection. The point of intersection of the reflected polar and the incident polar gives the reflected pressure equal to a normal shock:

$$\frac{p_{\text{reflected}}}{p_1} = 1 + \frac{2\gamma}{\gamma + 1}(M_1^2 - 1) \tag{4.16}$$

This also indicates that the stem is a straight line parallel to the wall. A graph of shock angle vs initial Mach number can be plotted for both the detachment and von Neumann criteria for $\gamma = 1.4$ (figure 4.11). It should be noted that before Mach number $2.3 - 2.4$ the detachment and von Neumann criteria are the same and they start to diverge after this.

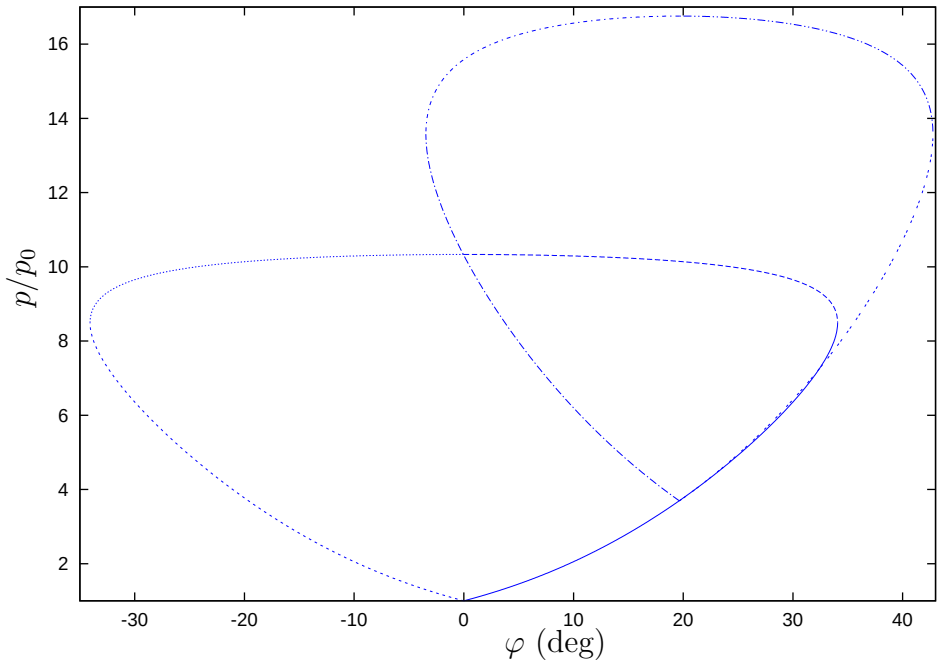

Figure 4.9: Pressure Deflection diagram depicting the von Neumann Criterion

4.2.3 Sonic Criterion

This criterion depends upon signals generated at the tip of the wedge. The transition from regular reflection to Mach reflection depends upon whether the signals at the wedge catch up with the reflected wave. As long as the flow behind the reflected wave is supersonic then the corner generated signals will not affect the reflected shock.

Note from the shock polar for the sonic criterion that the reflected polar crosses the p-axis which indicates that theoretically that regular reflection is possible (figure 4.10). A comparison of the detachment and von Neumann conditions is given by figure 4.11, the sonic criterion is not added because the difference between the detachment and sonic criteria is less than a degree, so it is not included in the graph.

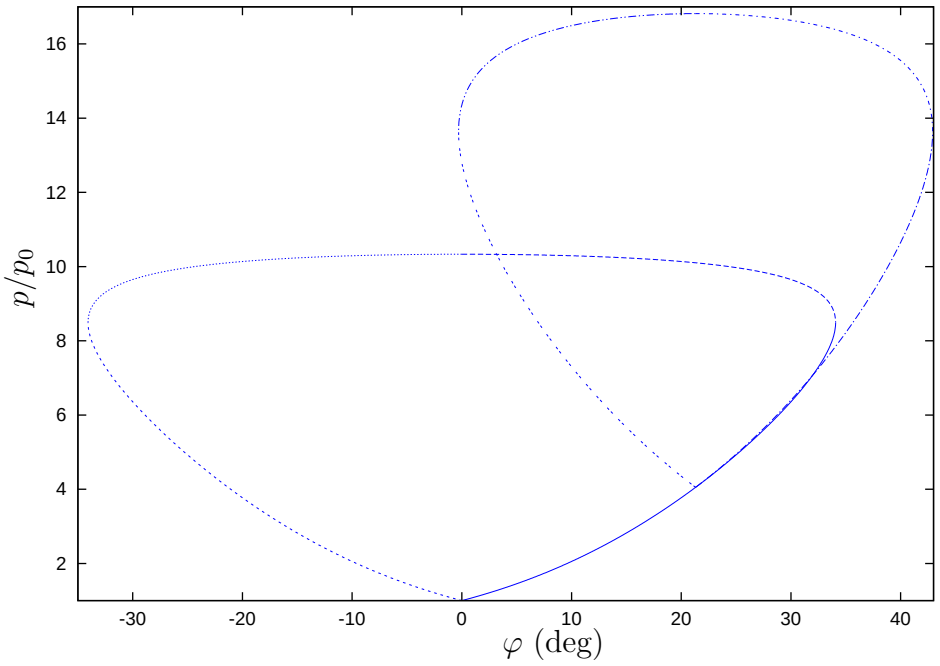

Figure 4.10: Sonic Criterion

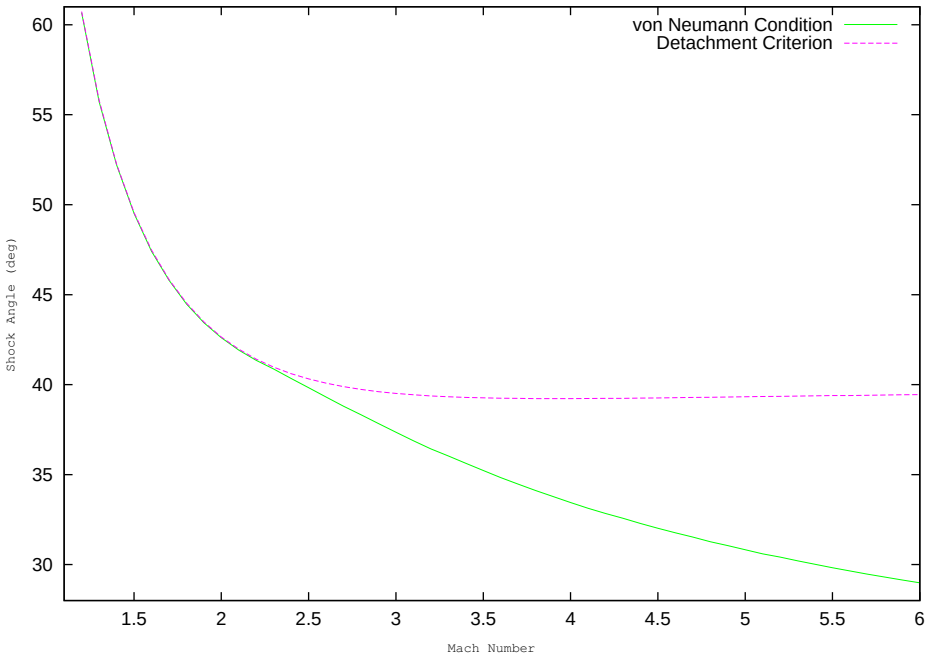

Figure 4.11: Detachment and von Neumann Criterion's

Chapter 5

Numerical Results

In order to test the different criteria mentioned in the previous chapter, the Lax-Wendroff method is applied to the Euler equations. The Lax-Wendroff method uses the conservation form of these equations, i.e. they are written as:

$$\frac{\partial A}{\partial t} + \frac{\partial B}{\partial x} + \frac{\partial C}{\partial y} = 0. \tag{5.1}$$

5.1 Conservation form of the Euler Equations

The Euler equations are:

$$\begin{aligned}
\frac{\partial \rho}{\partial t} + \frac{\partial}{\partial x}(\rho u) + \frac{\partial}{\partial y}(\rho v) &= 0, && (5.2)\\
\rho\frac{\partial u}{\partial t} + \rho u\frac{\partial u}{\partial x} + \rho v\frac{\partial u}{\partial y} &= -\frac{\partial p}{\partial x}, && (5.3)\\
\rho\frac{\partial v}{\partial t} + \rho u\frac{\partial v}{\partial x} + \rho v\frac{\partial v}{\partial y} &= -\frac{\partial p}{\partial y}, && (5.4)\\
\rho\frac{\partial e}{\partial t} + \rho u\frac{\partial e}{\partial x} + \rho v\frac{\partial e}{\partial y} &= \frac{p}{\rho}\left[\frac{\partial \rho}{\partial t} + u\frac{\partial \rho}{\partial x} + v\frac{\partial \rho}{\partial y}\right]. && (5.5)
\end{aligned}$$

The continuity equation (5.2) is already written in conservation form. In order to express the x-momentum equation (5.3) in conservation form multiply (5.2) by u and add to (5.3), resulting in:

$$\frac{\partial}{\partial t}(\rho u) + \frac{\partial}{\partial x}(p + \rho u^2) + \frac{\partial}{\partial y}(\rho uv) = 0. \tag{5.6}$$

Multiplying (5.2) by v and adding to the y-momentum equation (5.4) renders it into the form:

$$\frac{\partial}{\partial t}(\rho v) + \frac{\partial}{\partial x}(\rho uv) + \frac{\partial}{\partial y}(p + \rho v^2) = 0. \tag{5.7}$$

With the help of (5.2), the energy equation (5.5) may be converted into the form:

$$\rho \frac{De}{Dt} = -p\frac{\partial u}{\partial x} - p\frac{\partial v}{\partial x}. \tag{5.8}$$

Or equivalently:

$$\rho \frac{De}{Dt} = -\frac{\partial}{\partial x}(pu) - \frac{\partial}{\partial y}(pv) + u\frac{\partial p}{\partial x} + v\frac{\partial p}{\partial y}. \tag{5.9}$$

Multiplying (5.3) by u and (5.4) by v gives:

$$\rho \frac{D}{Dt}\left(\frac{u^2}{2}\right) = -u\frac{\partial p}{\partial x}, \quad \rho \frac{D}{Dt}\left(\frac{v^2}{2}\right) = -v\frac{\partial p}{\partial y}. \tag{5.10}$$

Introduce the "full energy" function:

$$E = e + \frac{1}{2}(u^2 + v^2). \tag{5.11}$$

Then substituting (5.10) into (5.5) results in:

$$\rho \frac{\partial E}{\partial t} + \frac{\partial}{\partial x}(pu) + \frac{\partial}{\partial y}(pv) = 0. \tag{5.12}$$

It remains to multiply (5.2) by E and add the result to (5.12). This leads to the conservation form of the energy equation:

$$\frac{\partial}{\partial t}(\rho E) + \frac{\partial}{\partial x}(u(p + \rho E)) + \frac{\partial}{\partial y}(v(p + \rho E)) = 0. \tag{5.13}$$

5.2 Non-dimensionalisation and Initial Conditions

When attempting to undertake a numerical solution of the Euler equations, the first task is to non-dimensionalise them. In the free-stream flow there are reference quantities which can be used to define non-dimensional variables. The quantities are:

V_∞ – free-stream flow

ρ_∞ – free-stream density

p_∞ – free-steam pressure

L – reference length scale

The dimensionless quantities are then defined as:

$$t = \tfrac{L}{V_\infty}\bar{t}, \quad x = L\bar{x}, \qquad y = L\bar{y}, \qquad u = V_\infty \bar{u},$$
$$v = V_\infty, \quad \rho = \rho_\infty \bar{\rho}, \quad p = \rho_\infty V_\infty^2, \quad E = V_\infty^2$$

The equations now become (after dropping the bars):

$$\begin{aligned}
\frac{\partial \rho}{\partial t} + \frac{\partial}{\partial x}(\rho u) + \frac{\partial}{\partial y}(\rho v) &= 0, \\
\frac{\partial}{\partial t}(\rho u) + \frac{\partial}{\partial x}(p + \rho u^2) + \frac{\partial}{\partial y}(\rho u v) &= 0, \\
\frac{\partial}{\partial t}(\rho v) + \frac{\partial}{\partial x}(\rho u v) + \frac{\partial}{\partial y}(p + \rho v^2) &= 0, \\
\frac{\partial}{\partial t}(\rho E) + \frac{\partial}{\partial x}(u(p + \rho E)) + \frac{\partial}{\partial y}(v(p + \rho E)) &= 0. \\
E - \frac{1}{\gamma - 1}\frac{p}{\rho} + \frac{1}{2}(u^2 + v^2) &= 0
\end{aligned}$$

5.2.1 Initial Conditions

The previous analysis was based upon the Rankine-Hugoniot equations. The aim of this study is to examine numerically, the transition from regular reflection to Mach reflection. In particular the difference between the two different transition conditions is of interest. The formation of the shocks are important, the Rankine-Hugoniot equations have no information how the shocks are formed, only that they exist and how to calculate their properties.

The computational domain is set up in the following way: The reflected wall is at the upper boundary and the material flows in through the lower boundary. The lower boundary is split up into two parts. On part of the lower boundary, there is free-stream flow and on the rest the Rankine-Hugoniot equations are applied, simulating the transition through an oblique shock. The flow then reaches the upper boundary and the boundary conditions deal with flow after this.

This approach whilst not being a full numerical method (due to the use of the Rankine-Hugoniot equations on the lower boundary) it does solve the Euler equations to give a numerical picture of what happens after the incident shock.

The initial conditions for the problem are the free-steam conditions and the boundary conditions for the shock is the Rankine-Hugoniot equations, the dimensionless

values for the velocities and the densities are $u = 1$, $v = 0$ and $\rho = 1$ respectively. The equation for the pressure is given by $p_\infty = \rho_\infty V_\infty^2 p$ and using the expression for the speed of sound in air gives $p = 1/\gamma M_\infty^2$ where M_∞ is the free-stream Mach number. The initial condition for energy takes (by a similar reasoning used for the pressure) the form:

$$E = \frac{1}{\gamma(\gamma-1)M_\infty^2} + \frac{1}{2} \tag{5.14}$$

Suppose the location of the shock is x_{sh}, for $x < x_{sh}$ the free-stream conditions are used for $x \geq x_{sh}$, the Rankine-Hugoniot equations are used. Suppose there is a unit free-stream velocity parallel to the fixed boundary crossing a shock which is at an angle θ, then:

$$u_{1n} = \sin\theta, \quad u_{1t} = \cos\theta. \tag{5.15}$$

From the Rankine-Hugoniot equations:

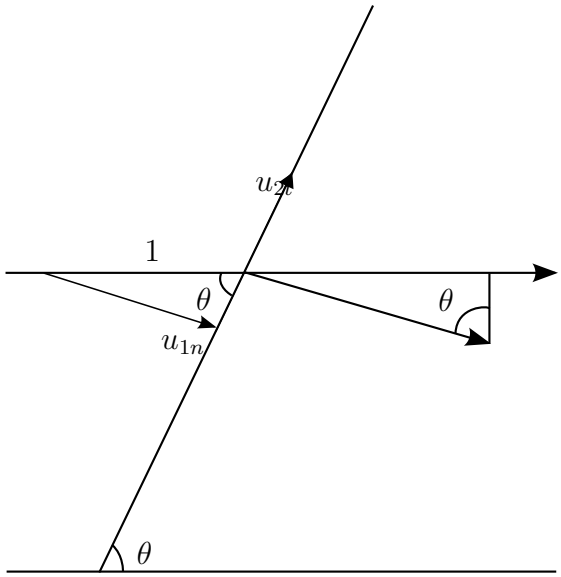

Figure 5.1: Initial Value From the Shock

$$\begin{aligned} u_{2n} &= \left[\frac{\gamma-1}{\gamma+1} + \frac{1}{(\gamma+1)M_\infty^2 \sin^2\theta}\right]\sin\theta \\ u_{2t} &= \cos\theta \end{aligned}$$

To obtain the initial conditions for the shock, apply a rotation of angle $-\theta$ to get u_2

and v_2,

$$u_2 = u_{2n}\sin\theta + v_{2t}\cos\theta \tag{5.16}$$

$$v_2 = u_{2t}\sin\theta - u_{2n}\cos\theta \tag{5.17}$$

For pressure, density and energy the relations (which come from the Rankine-Hugoniot equations) are:

$$\rho_2 = \frac{(\gamma+1)M_\infty^2\sin^2\theta}{2+(\gamma-1)M_\infty^2\sin^2\theta} \tag{5.18}$$

$$p_2 = \frac{1}{\gamma M_\infty^2}\frac{2\gamma M_\infty^2\sin^2\theta-(\gamma-1)}{\gamma+1} \tag{5.19}$$

$$E_2 = \frac{1}{\gamma-1}\frac{p_2}{\rho_2}+\frac{1}{2}(u_2^2+v_2^2) \tag{5.20}$$

5.3 Numerical method

A predictor-corrector method is used, all of the equations have been written in the form:

$$\frac{\partial A}{\partial t}+\frac{\partial B}{\partial x}+\frac{\partial C}{\partial y}=0. \tag{5.21}$$

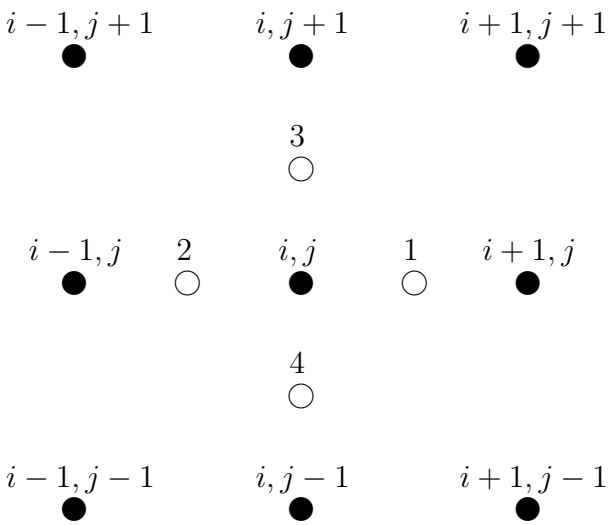

5.3.1 Predictor

At point 1 (5.21) is written as:

$$\frac{A_1^\star - \frac{1}{2}(A_{i,j} + A_{i+1,j})}{\delta t/2} + \left.\frac{\partial B}{\partial x}\right|_1 + \left.\frac{\partial C}{\partial y}\right|_1 = 0. \tag{5.22}$$

Where:

$$\begin{aligned}\left.\frac{\partial B}{\partial x}\right|_1 &= \frac{B_{i+1,j} - B_{i,j}}{\delta x} \\ \left.\frac{\partial C}{\partial y}\right|_1 &= \frac{C_{i+1,j+1} - C_{i+1,j-1} + C_{i,j+1} - C_{i,j-1}}{4\delta y}.\end{aligned}$$

All the quantities without a $\star$ are evaluated at the previous time-step, $t_n = n\delta t$.

Equation (5.21) at point 2 is given by:

$$\frac{A_2^\star - \frac{1}{2}(A_{i,j} + A_{i-1,j})}{\delta t/2} + \left.\frac{\partial B}{\partial x}\right|_2 + \left.\frac{\partial C}{\partial y}\right|_2 = 0, \tag{5.23}$$

where

$$\begin{aligned}\left.\frac{\partial B}{\partial x}\right|_2 &= \frac{B_{i,j} - B_{i-1,j}}{\delta x} \\ \left.\frac{\partial C}{\partial y}\right|_2 &= \frac{C_{i,j+1} - C_{i.j-1} + C_{i-1,j+1} - C_{i-1,j-1}}{4\delta y}.\end{aligned}$$

At point 3, equation (5.21) becomes:

$$\frac{A_3^\star - \frac{1}{2}(A_{i,j+1} + A_{i,j})}{\delta t/2} + \left.\frac{\partial B}{\partial x}\right|_3 + \left.\frac{\partial C}{\partial y}\right|_3 = 0, \tag{5.24}$$

where:

$$\begin{aligned}\left.\frac{\partial B}{\partial x}\right|_3 &= \frac{B_{i+1,j+1} - B_{i-1,j+1} + B_{i+1,j} - B_{i-1,j}}{4\delta x} \\ \left.\frac{\partial C}{\partial y}\right|_3 &= \frac{C_{i,j+1} - C_{i,j}}{\delta y}.\end{aligned}$$

At point 4, equation (5.21) becomes:

$$\frac{A_4^\star - \frac{1}{2}(A_{i,j} + A_{i,j-1})}{\delta t/2} + \left.\frac{\partial B}{\partial x}\right|_4 + \left.\frac{\partial C}{\partial y}\right|_4 = 0, \tag{5.25}$$

where:

$$\begin{aligned}\left.\frac{\partial B}{\partial x}\right|_4 &= \frac{B_{i+1,j} - B_{i-1,j} + B_{i+1,j-1} - B_{i-1,j-1}}{4\delta x} \\ \left.\frac{\partial C}{\partial y}\right|_4 &= \frac{C_{i,j} - C_{i,j-1}}{\delta y}.\end{aligned}$$

5.3.2 Corrector

The second step is the corrector part, equation (5.21) can be written as a finite difference equation:

$$\frac{A_{i,j}^{new} - A_{i,j}}{\delta t} + \frac{B_1 - B_2}{\delta x} + \frac{C_3 - C_4}{\delta y} = 0, \tag{5.26}$$

where $A_{i,j}^{new}$ is the value of the function A at the new time-step $t_{n+1} = (n+1)\delta t$

5.3.3 Artificial Viscosity

The Euler equations have discontinuous solutions, that is, variables have an infinite spatial gradient which isn't possible to model numerically. The way around this problem is to introduce some viscosity, this has the effect of smearing out the shock over a number of cells making the spatial gradients large but manageable.

For any quantity $\{\alpha_{i,j}^{new}\}$, introduce:

$$\begin{aligned} D_1 &= \alpha_{i+1,j}^{new} - \alpha_{i,j}^{new} \\ D_2 &= \alpha_{i,j}^{new} - \alpha_{i-1}^{new}. \end{aligned}$$

Then the correction to $\{\alpha_{i,j}^{new}\}$ is given by:

$$\Omega = \nu(|D_1|D_1 - |D_2|D_2) \tag{5.27}$$

and the proper value is given by:

$$\alpha_{i,j} = \Omega + \alpha_{i,j}^{new} \tag{5.28}$$

5.3.4 Numerical Results

The free-stream Mach number used was 2.75 in order to distinguish the von Neumann (figure 5.3) and detachment criteria (figure 5.2). The calculations were performed for the same length of time to make a fair comparison of the results.

The first thing to note is that the pressure in the reflected shock is not constant, it peaks at the stem and then decreases as the distance from the reflecting boundary is increased. For the incident shock however the pressure is *uniform*, this is due to

the boundary condition imposed on the lower boundary being the Rankine-Hugoniot equations and not an artifact of the real boundary geometry. However, away from the shock the pressure at the rear of the reflected shock seems to be converging to a uniform pressure.

As the difference in the detachment and von Neumann criteria are close at $M_\infty = 2.75$, the size of the Mach stem is approximately the same size as can be seen in figures 5.2 and 5.3. For situations which give a regular reflection, the stem-like shock still appears, this is due to the fact that close to the reflecting boundary the incident shock and the reflected shock are very close and the flow direction changes very rapidly which causes the incident and reflected shocks to merge together close to the boundary. It is possible that the shocks in figures 5.2 and 5.3 are regular reflections as the stems are the same size. Note that moving away from the upper boundary the pressure from the reflected wave appears to be decreasing to a constant pressure as the distance from the incident and reflected shocks increase.

There are two types of "ripples" in the results. The first is located by the incident shock and can be removed by having a longer run-time for the program. The second of these ripples is located at the lower boundary where the material flows in. These are due to the mesh size, decreasing the mesh size will in general increase the accuracy of the results. The ripples are in just one direction which would indicate that only reducing the mesh size in one direction would remove the ripples.

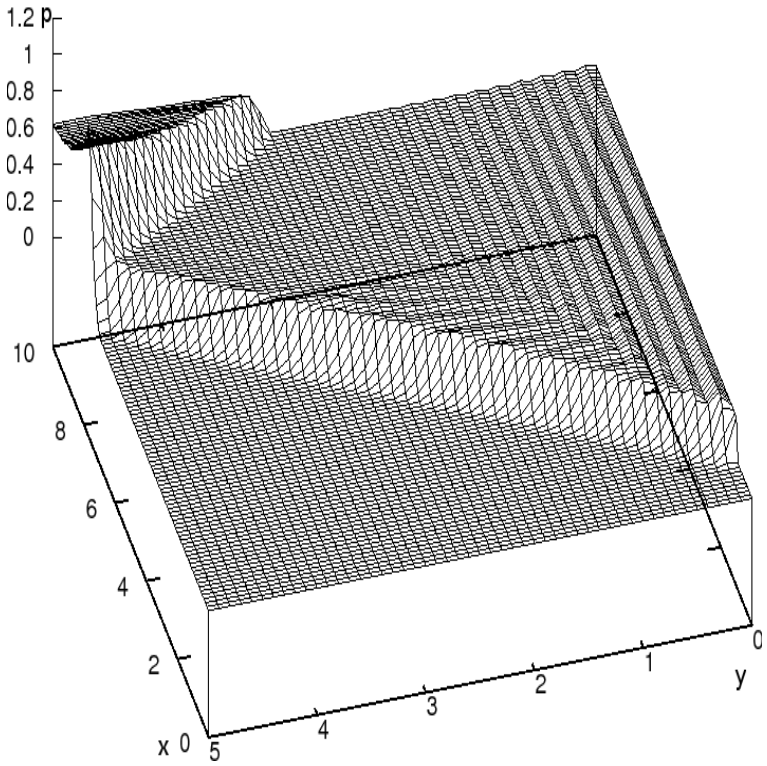

Figure 5.2: Detachment Point

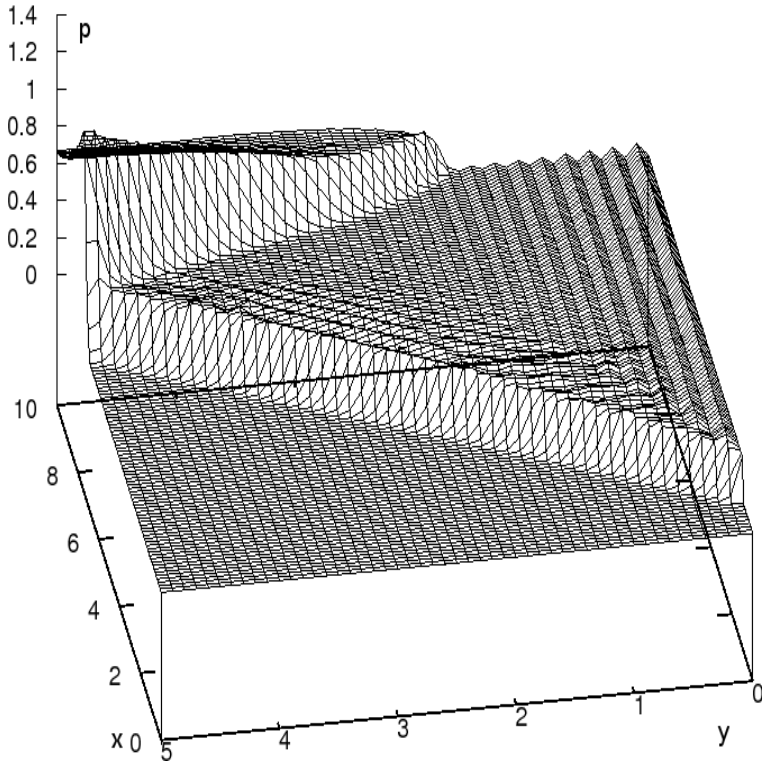

Figure 5.3: von Newmann Point

Chapter 6

The Shape of the Contact Discontinuity; Downstream Asymptote

Much of the analysis of Mach stems has been carried out by approximating the contact discontinuity as a straight line (see ref [7]).

Experimentally however the contact discontinuity is seen to be curved, this is also known about theoretically but has been very difficult to calculate, so the straight line approximation has been used. In this chapter, the shape of the contact discontinuity is computed when the conditions are close to the von Neumann criterion where the Mach stem and contact discontinuity are straight lines and so the method used is perturbation theory.

6.1 von Mises Variables

It is occasionally useful to have a set of co-ordinates which are intrinsic to the problem studied. The von Mises co-ordinate system fit around the body surface by using the stream function in their definition.

6.1.1 Definition

In the analysis of the contact discontinuity the von Mises variables are used. The co-ordinate transformation is given by:

$$(x, y) \mapsto (s, \psi) \tag{6.1}$$

where $s = x$ and ψ is defined by:

$$\frac{\partial \psi}{\partial x} = -\rho v, \quad \frac{\partial \psi}{\partial y} = \rho u. \tag{6.2}$$

6.1.2 Derivatives in von Mises Co-ordinates

The task now is to rewrite the Euler equations using the von Mises variables. From the chain rule:

$$\begin{aligned} \frac{\partial}{\partial x} &= \frac{\partial s}{\partial x}\frac{\partial}{\partial s} + \frac{\partial \psi}{\partial x}\frac{\partial}{\partial \psi} \\ &= \frac{\partial}{\partial s} - \rho v \frac{\partial}{\partial \psi}. \end{aligned}$$

Also

$$\begin{aligned} \frac{\partial}{\partial y} &= \frac{\partial s}{\partial y}\frac{\partial}{\partial s} + \frac{\partial \psi}{\partial y}\frac{\partial}{\partial \psi} \\ &= \rho u \frac{\partial}{\partial \psi}. \end{aligned}$$

From the definition of the material derivative:

$$\begin{aligned} \frac{D}{Dt} &= \frac{\partial}{\partial t} + u\frac{\partial}{\partial x} + v\frac{\partial}{\partial y} \\ &= \frac{\partial}{\partial t} + u\left[\frac{\partial}{\partial s} - \rho v \frac{\partial}{\partial \psi}\right] + v\left[\rho u \frac{\partial}{\partial \psi}\right] \\ &= \frac{\partial}{\partial t} + u\frac{\partial}{\partial s} \end{aligned}$$

6.1.3 The Euler Equations in von Mises Variables

The continuity equation

$$\frac{D\rho}{Dt} + \rho \nabla \cdot \mathbf{u} = 0 \tag{6.3}$$

becomes

$$\begin{aligned}\frac{D\rho}{Dt}+\rho\nabla\cdot\mathbf{u} &= \frac{\partial\rho}{\partial t}+u\frac{\partial\rho}{\partial s}+\rho\left[\frac{\partial u}{\partial s}-\rho v\frac{\partial u}{\partial\psi}+\rho u\frac{\partial v}{\partial\psi}\right]\\ &= \frac{\partial\rho}{\partial t}+\frac{\partial}{\partial s}\rho u+\rho^2\left[u\frac{\partial v}{\partial\psi}-v\frac{\partial u}{\partial\psi}\right]\\ &= \frac{\partial\rho}{\partial t}+\frac{\partial}{\partial s}\rho u+(\rho u)^2\frac{\partial}{\partial\psi}\left(\frac{v}{u}\right)\\ &= (\rho u)^2\left[\frac{1}{(\rho u)^2}\frac{\partial\rho}{\partial t}+\frac{1}{(\rho u)^2}\frac{\partial}{\partial s}(\rho u)+\frac{\partial}{\partial\psi}\left(\frac{v}{u}\right)\right].\end{aligned}$$

Dividing through by $(\rho u)^2$ gives the final form of the continuity equation:

$$\frac{1}{(\rho u)^2}\frac{\partial\rho}{\partial t}-\frac{\partial}{\partial s}\left(\frac{1}{\rho u}\right)+\frac{\partial}{\partial\psi}\left(\frac{v}{u}\right)=0. \tag{6.4}$$

The x-momentum equation has the form

$$\frac{Du}{Dt}=-\frac{1}{\rho}\frac{\partial p}{\partial x}, \tag{6.5}$$

Upon using the von Mises variables:

$$\frac{\partial u}{\partial t}+u\frac{\partial u}{\partial s}=-\frac{1}{\rho}\frac{\partial p}{\partial s}-v\frac{\partial p}{\partial\psi}. \tag{6.6}$$

Similarly, the y-momentum equation:

$$\frac{Dv}{Dt}=-\frac{1}{\rho}\frac{\partial p}{\partial y}, \tag{6.7}$$

becomes

$$\frac{\partial v}{\partial t}+u\frac{\partial v}{\partial s}=-u\frac{\partial p}{\partial\psi}. \tag{6.8}$$

Finally, the conservation of energy:

$$\frac{DS}{Dt}=0 \quad \Rightarrow \frac{D}{Dt}\left[\frac{p}{\rho^\gamma}\right]=0, \tag{6.9}$$

takes the form

$$\frac{\partial S}{\partial t}+u\frac{\partial S}{\partial s}=\left[\frac{\partial}{\partial t}+u\frac{\partial}{\partial s}\right]\frac{p}{\rho^\gamma}=0. \tag{6.10}$$

The flow studied is stationary, in which case the above equations reduce to

$$\frac{\partial}{\partial s}\left(\frac{1}{\rho u}\right) - \frac{\partial}{\partial \psi}\left(\frac{v}{u}\right) = 0 \tag{6.11a}$$

$$u\frac{\partial u}{\partial s} = -\frac{1}{\rho}\frac{\partial p}{\partial s} - v\frac{\partial p}{\partial \psi} \tag{6.11b}$$

$$\frac{\partial v}{\partial s} = -\frac{\partial p}{\partial \psi} \tag{6.11c}$$

$$\frac{\partial}{\partial s}\left[\frac{p}{\rho^\gamma}\right] = 0. \tag{6.11d}$$

From (6.11a), there exists a function $N = N(s, \psi)$ such that

$$\frac{\partial N}{\partial s} = \frac{v}{u}, \quad \frac{\partial N}{\partial \psi} = \frac{1}{\rho u}. \tag{6.12}$$

The physical meaning of N may be revealed as follows. Consider the identities:

$$x \equiv x(s(x,y), \psi(x,y)), \quad y \equiv y(s(x,y), \psi(x,y)), \tag{6.13}$$

Differentiating the second of (6.13) with respect to y:

$$\frac{\partial y}{\partial y} = 1 = \frac{\partial s}{\partial y}\frac{\partial y}{\partial s} + \frac{\partial \psi}{\partial y}\frac{\partial y}{\partial \psi} = \rho u \frac{\partial y}{\partial \psi}.$$

Shows that:

$$\frac{\partial y}{\partial \psi} = \frac{1}{\rho u}. \tag{6.14}$$

Differentiating the second of (6.11b) with respect to x:

$$\frac{\partial y}{\partial x} = 0 = \frac{\partial y}{\partial s}\frac{\partial s}{\partial x} + \frac{\partial y}{\partial \psi}\frac{\partial \psi}{\partial x} = \frac{\partial y}{\partial s} - \frac{v}{u}.$$

which gives:

$$\frac{\partial y}{\partial s} = \frac{v}{u}. \tag{6.15}$$

These calculations show that the physical meaning of N is the distance from the body surface to a particular streamline.

6.2 Linearised Equations

The idea of this section is to examine the shape of the contact discontinuity around the von Neumann criterion. The way to study this is via a perturbation expansion in region 4[1].

[1]The subscripts of the Mach numbers in figure 6.1 denote the region number

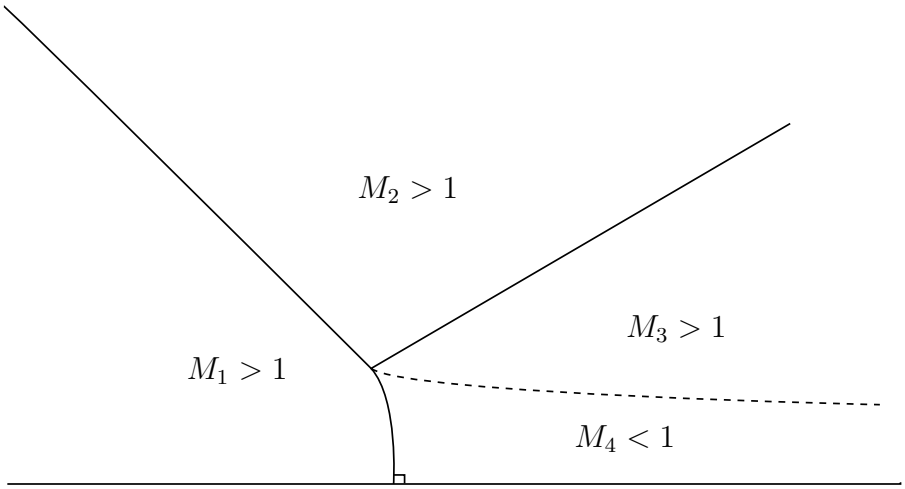

Figure 6.1: Mach Reflection

In order to do this, seek a solution in the form:

$$p(s,\psi) = p_0(s,\psi) + \varepsilon p_1(s,\psi) + O(\varepsilon^2), \tag{6.16}$$

$$\rho(s,\psi) = \rho_0(s,\psi) + \varepsilon \rho_1(s,\psi) + O(\varepsilon^2), \tag{6.17}$$

$$u(s,\psi) = u_0(s,\psi) + \varepsilon u_1(s,\psi) + O(\varepsilon^2), \tag{6.18}$$

$$v(s,\psi) = \varepsilon v_1(s,\psi) + O(\varepsilon^2) \tag{6.19}$$

Inserting these expansions into the continuity equation (6.11a) yields:

$$\begin{aligned} \frac{\partial}{\partial s}\left[\frac{1}{\rho u}\right] - \frac{\partial}{\partial \psi}\left[\frac{v}{u}\right] &= \frac{\partial}{\partial s}\left[\frac{1}{\rho_0 u_0 + (\rho_1 u_0 + \rho_0 u_1)\varepsilon}\right] - \frac{\partial}{\partial \psi}\left[\frac{\varepsilon v_1}{u_0 + \varepsilon u_1}\right] \\ &= \frac{\partial}{\partial s}\left[\frac{1}{\rho_0 u_0}\left[1 - \left[\frac{\rho_1}{\rho_0} + \frac{u_1}{u_0}\right]\varepsilon\right]\right] + \varepsilon \frac{\partial}{\partial \psi}\left[\frac{v_1}{u_0}\right]. \end{aligned}$$

To leading order the equation becomes:

$$\frac{\partial}{\partial s}\left[\frac{1}{\rho_0 u_0}\right] = 0. \tag{6.20}$$

By the principle of least degeneracy this cannot happen, so define $X = \varepsilon s$ as a new variable. This rescaling means that the analysis presented here is valid for large distances downstream of the Mach stem. The rescaling makes the continuity equation become:

$$\frac{\partial}{\partial X}\left[\frac{1}{\rho_0 u_0}\right] - \frac{\partial}{\partial \psi}\left[\frac{v_1}{u_0}\right] = 0. \tag{6.21}$$

with (6.16)-(6.19) the x-momentum equation (6.11b) takes the form:

$$\varepsilon(u_0+\varepsilon u_1)\frac{\partial}{\partial X}(u_0+\varepsilon u_1)=\varepsilon v_1\frac{\partial}{\partial \psi}(p_0+\varepsilon p_1)-\frac{\varepsilon}{\rho_0+\varepsilon\rho_1}\frac{\partial}{\partial X}(p_0+\varepsilon p_1) \tag{6.22}$$

which to $O(\varepsilon)$ is:

$$u_0\frac{\partial u_0}{\partial X}=v_1\frac{\partial p_0}{\partial \psi}-\frac{1}{\rho_0}\frac{\partial p_0}{\partial X}. \tag{6.23}$$

Substituting (6.16)-(6.19) into the y-momentum equation (6.11b) yields:

$$\varepsilon\frac{\partial}{\partial X}(\varepsilon v_1)=-\frac{\partial}{\partial \psi}(p_0+\varepsilon p_1). \tag{6.24}$$

The leading order term shows that $\partial_\psi p_0=0$ which makes the x-momentum equation (6.23) become:

$$u_0\frac{\partial u_0}{\partial X}=-\frac{1}{\rho_0}\frac{\partial p_0}{\partial X}. \tag{6.25}$$

Finally the conservation of energy (6.11d) shows that:

$$\frac{\partial}{\partial X}\left[\frac{p_0+\varepsilon p_1}{(\rho_0+\varepsilon\rho_1)^\gamma}\right]=0. \tag{6.26}$$

Which to the leading order reduces to:

$$\frac{\partial}{\partial X}\left[\frac{p_0}{\rho_0^\gamma}\right]=0. \tag{6.27}$$

Equation (6.27) can be re-arranged to:

$$\frac{1}{\gamma p_0}\frac{\partial p_0}{\partial X}=\frac{1}{\rho_0}\frac{\partial \rho_0}{\partial X} \tag{6.28}$$

Integrating (6.27) w.r.t X yields $p_0=b(\psi)\rho^\gamma$. Inserting this into (6.25) gives:

$$\frac{\partial}{\partial X}\left[\frac{\gamma}{\gamma-1}\frac{p_0}{\rho_0}+\frac{1}{2}u_0^2\right]=0. \tag{6.29}$$

This yields two equations:

$$\frac{\gamma}{\gamma-1}\frac{p_0}{\rho_0}+\frac{1}{2}u_0^2 = a \tag{6.30}$$

$$\frac{p}{\rho^\gamma} = b \tag{6.31}$$

Where a and b are functions of ψ, they can be calculated via the Rankine-Hugoniot equations on the stem. Write quantities in region 1 as $\bar{\rho}, \bar{u}, \bar{p}$, then from the Rankine-Hugoniot equations:

$$\frac{p_0}{\bar{p}} = 1 + \frac{2\gamma}{\gamma+1}(M^2-1) \tag{6.32}$$

$$\frac{\rho_0}{\bar{\rho}} = \frac{(\gamma+1)M^2}{2+(\gamma-1)M^2} \tag{6.33}$$

$$\frac{u_0}{\bar{u}} = \frac{\gamma-1}{\gamma+1} + \frac{2}{(\gamma+1)M^2} \tag{6.34}$$

Inserting these equations into (6.30) and (6.31) gives:

$$a = \frac{\gamma\bar{p}}{\bar{\rho}}\left[\frac{\gamma-1}{\gamma+1} + \frac{2}{(\gamma+1)M^2}\right]\left[\frac{2}{\gamma+1} + \frac{1}{\gamma-1} - \frac{2\gamma}{\gamma+1} + \frac{\gamma+1}{\gamma-1}M^2\right] \tag{6.35}$$

$$b = \frac{\bar{p}}{\bar{\rho}^\gamma}\left[1 + \frac{2\gamma}{\gamma+1}(M^2-1)\right]\left[\frac{\gamma-1}{\gamma+1} + \frac{2}{(\gamma+1)M^2}\right]^\gamma \tag{6.36}$$

6.3 Calculating the Shape of the Contact Discontinuity

The pressures at each side of the contact discontinuity are equal, so the idea in calculating the shape of the contact discontinuity is to obtain expressions for the pressure at both sides and equate them. As the contact discontinuity is expected to vary only via a small amount from the von Neumann condition and hence the gradient of the contact discontinuity will be very small.

The conservation of mass is:

$$\frac{\partial}{\partial X}\left[\frac{1}{\rho_0 u_0}\right] = \frac{\partial}{\partial \psi}\left[\frac{v_1}{u_0}\right]. \tag{6.37}$$

Integrating (6.37) w.r.t ψ from 0 to ψ gives:

$$\frac{\partial}{\partial X}\left[\frac{\psi}{\rho_0 u_0}\right] = \frac{v_1}{u_0} = \frac{dy}{dX} \tag{6.38}$$

Integrating (6.38) w.r.t. X gives:

$$y = \frac{\psi}{\rho_0 u_0}. \tag{6.39}$$

At $\psi = \psi_S$ is where is the contact discontinuity is, and writing the equation of the contact discontinuity as $y = f(X)$ gives:

$$f(X) = \frac{\psi_S}{\rho_0 u_0} \tag{6.40}$$

The next task to to write (6.40) in terms of pressure. Using equations (6.30) and (6.31) to give:

$$\rho_0 = \left(\frac{p_0}{b}\right)^{\frac{1}{\gamma}} \tag{6.41}$$

$$u_0 = \left[2a - \frac{2\gamma}{\gamma - 1} p_0^{\frac{\gamma-1}{\gamma}} b^{\frac{1}{\gamma}}\right]^{\frac{1}{2}}. \tag{6.42}$$

So for region 4:

$$f(X) = \psi_S \left(\frac{p_0}{b}\right)^{-\frac{1}{\gamma}} \left[2a - \frac{2\gamma}{\gamma - 1} p_0^{\frac{\gamma-1}{\gamma}} b^{\frac{1}{\gamma}}\right]^{-\frac{1}{2}}. \tag{6.43}$$

This ends the analysis for region 4. Use the Ackeret formula for region 3, which is:

$$p = p_3 + \rho_3 V_3^2 \frac{\theta}{\sqrt{M_3^2 - 1}}. \tag{6.44}$$

Now $\theta = f'(X)$ and so, for brevity write:

$$p = \alpha + \beta f'(X), \tag{6.45}$$

where $\alpha = p_3$ and $\beta = \rho_3 V_3^2 (M_3^2 - 1)^{-1/2}$. As the pressures are equal on either side of the contact discontinuity $p = p_0$, insert (6.45) into (6.43) and obtain a differential equation for $f(X)$. By expanding the LHS of (6.43) to first order in $f'(X)$. Inserting (6.45) into (6.43) gives:

$$f(X) = \psi_S \left(\frac{\alpha + \beta f'}{b}\right)^{-\frac{1}{\gamma}} \left[2a - \frac{2\gamma}{\gamma - 1} (\alpha + \beta f')^{\frac{\gamma-1}{\gamma}} b^{\frac{1}{\gamma}}\right]^{-\frac{1}{2}}. \tag{6.46}$$

The result of doing this is:

$$\begin{aligned} f(X) = {} & \left(\frac{\alpha}{b}\right)^{-1/\gamma} \sqrt{2a - \frac{2b^{\frac{1}{\gamma}} \alpha^{1-\frac{1}{\gamma}} \gamma}{\gamma - 1}} \psi_S - \left[\frac{\beta \sqrt{2a - \frac{2b^{\frac{1}{\gamma}} \alpha^{1-\frac{1}{\gamma}} \gamma}{\gamma-1}} \psi \left(\frac{\alpha}{b}\right)^{-1/\gamma}}{\alpha\gamma} + \right. \\ & \left. + \frac{b^{\frac{1}{\gamma}} \alpha^{-1/\gamma} \beta \psi_S \left(\frac{\alpha}{b}\right)^{-1/\gamma}}{\sqrt{2a - \frac{2b^{\frac{1}{\gamma}} \alpha^{1-\frac{1}{\gamma}} \gamma}{\gamma-1}}}\right] f'(X). \end{aligned} \tag{6.47}$$

This differential equation is in the form:

$$f(X) = A - Bf'(X). \tag{6.48}$$

Where $A, B > 0$. The solution of this equation is:

$$f(X) = A - f(0)e^{-\frac{X}{B}} \tag{6.49}$$

Which is the equation of the contact discontinuity. Note that this is not a straight line as most of the theoretical analysis uses.

Chapter 7

The Shape of the Mach Stem

This chapter investigates the shape the Mach stem makes and also the shape of the contact discontinuity at finite distance from the Mach stem. In order to do this, a PDE for the pressure will be derived for the subsonic region (region 4) and then solved and examining the boundary value for this will give the shape of the Mach stem. This chapter will be split into three sections:

- Derive the PDE for pressure
- Obtain the boundary conditions for the PDE
- Solve the PDE and relate the solution to the shape of the Mach stem

7.1 Deriving the Pressure Equation

To model the Mach stem, the steady 2D Euler equations are used:

$$\frac{\partial}{\partial x}(\rho u) + \frac{\partial}{\partial y}(\rho v) = 0, \tag{7.1}$$

$$u\frac{\partial u}{\partial x} + v\frac{\partial u}{\partial v} = -\frac{\partial p}{\partial x}, \tag{7.2}$$

$$u\frac{\partial v}{\partial x} + v\frac{\partial v}{\partial v} = -\frac{\partial p}{\partial y}, \tag{7.3}$$

$$\left[u\frac{\partial}{\partial x} + v\frac{\partial}{\partial y}\right]\frac{p}{\rho^\gamma} = 0. \tag{7.4}$$

The idea is to examine the perturbations about the flow satisfying the von Neumann criterion. The first task is to non-dimensionalise the Euler equations, for this use the values in region 4. Let the quantities U_4,ρ_4 and p_4 be the values obtained at the von Neumann condition. Also let the height of the triple point be d (see figure 7.1). Define the following:

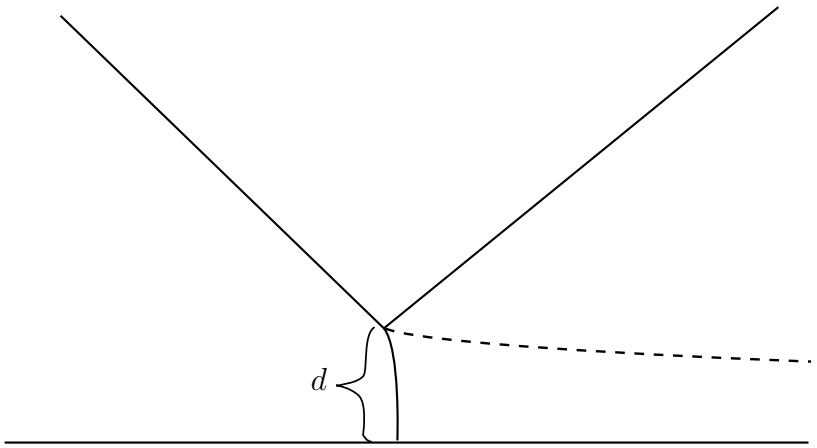

Figure 7.1: Scaling of x and y

$$\begin{aligned} p = p_4 + \rho_4 U_4^2 \varepsilon \bar{p}(x,y), \qquad & u = U_4(1 + \varepsilon \bar{u}(x,y)), \\ \rho = \rho_4(1 + \varepsilon \bar{\rho}(x,y)), \qquad & v = U_4 \varepsilon \bar{v}(x,y), \\ x = d\bar{x}, \qquad & y = d\bar{y}. \end{aligned}$$

The Euler equations reduce to (dropping the bars) at $O(\varepsilon)$:

$$\frac{\partial u}{\partial x} + \frac{\partial \rho}{\partial x} + \frac{\partial v}{\partial y} = 0, \tag{7.5}$$

$$\frac{\partial u}{\partial x} = -\frac{\partial p}{\partial x}, \tag{7.6}$$

$$\frac{\partial v}{\partial x} = -\frac{\partial p}{\partial y}, \tag{7.7}$$

$$\frac{\partial p}{\partial x} = \frac{1}{M_4^2}\frac{\partial \rho}{\partial x}. \tag{7.8}$$

In order to obtain the equation for pressure, differentiate (7.5) w.r.t. x to get:

$$\frac{\partial^2 u}{\partial x^2} + \frac{\partial^2 \rho}{\partial x^2} + \frac{\partial^2 v}{\partial x \partial y} = 0. \tag{7.9}$$

Differentiating (7.6) and (7.8) w.r.t. x to get:

$$\frac{\partial^2 u}{\partial x^2} = -\frac{\partial^2 p}{\partial x^2}, \quad M_4^2 \frac{\partial^2 p}{\partial x^2} = \frac{\partial^2 \rho}{\partial x^2}. \tag{7.10}$$

Substituting equations (7.10) into (7.5) giving:

$$-\frac{\partial^2 p}{\partial x^2} + M_4^2 \frac{\partial^2 p}{\partial x^2} + \frac{\partial^2 v}{\partial x \partial y} = 0. \tag{7.11}$$

Differentiate (7.7) w.r.t. y which yields:

$$\frac{\partial^2 v}{\partial x \partial y} = -\frac{\partial^2 p}{\partial y^2}. \tag{7.12}$$

Inserting this into (7.11) gives:

$$(1 - M_4^2)\frac{\partial^2 p}{\partial x^2} + \frac{\partial^2 p}{\partial y^2} = 0. \tag{7.13}$$

As (7.13) applies to the subsonic region the term $(1 - M_1^2)$ is positive and so (7.13) is an elliptic equation. Another useful equation is obtained by substituting (7.6) and (7.8) into (7.5) which yields:

$$(1 - M_4^2)\frac{\partial p}{\partial x} = \frac{\partial v}{\partial y} \tag{7.14}$$

7.2 Boundary Conditions

In order to obtain a unique solution for (7.13), it is necessary to specify the boundary conditions for all four sides[1].

7.2.1 Fixed Boundary ($y = 0$)

Along the body surface the impermeability condition holds:

$$v\big|_{y=0} = 0. \tag{7.15}$$

Inserting this into (7.7) gives:

$$\left.\frac{\partial p}{\partial y}\right|_{y=0} = 0. \tag{7.16}$$

[1] One of the boundary conditions is at infinity

7.2.2 The Mach Stem ($x = 0$)

As the Mach stem deviates only slightly from a straight line normal to the wall, it's equation may be written as $x = \varepsilon f(y)$, where ε is a small parameter.

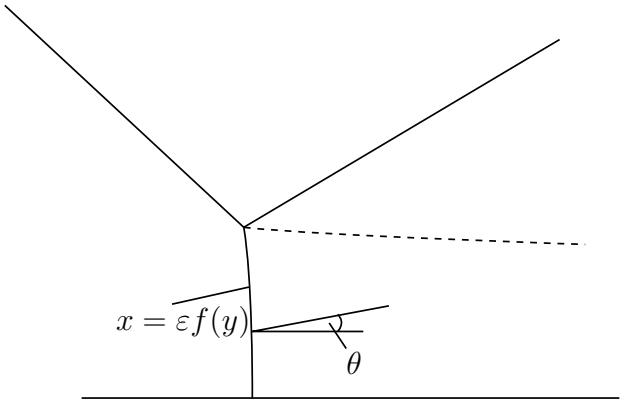

Figure 7.2: Mach Stem

Let the normal to the Mach stem be denoted by $\mathbf{n}$ and the angle between the normal and the horizontal be dentoted by θ (figure 7.2). Write $\varphi = x - \varepsilon f(y)$, then $\mathbf{n} = \nabla\varphi$, so

$$\mathbf{n} = \mathbf{i} - \varepsilon f'(y)\mathbf{j}. \tag{7.17}$$

Then θ is related to $f(y)$ by:

$$\tan\theta = -\varepsilon f'(y). \tag{7.18}$$

The angle that the stem makes with the wall is:

$$\phi = \frac{\pi}{2} - \theta \tag{7.19}$$

The way to obtain the boundary condition is to insert (7.19) into the Rankine-Hugoniot equations and expand to $O(\varepsilon)$. As θ is small then $\tan\theta \approx \theta$ and:

$$\phi = \frac{\pi}{2} + \varepsilon f'(y) \tag{7.20}$$

Now:

$$\begin{aligned}
\sin\phi &= \sin\left(\frac{\pi}{2}+\varepsilon f'(y)\right) \\
&= \sin\left(\frac{\pi}{2}\right)\cos(\varepsilon f'(y)) + \cos\left(\frac{\pi}{2}\right)\sin(\varepsilon f'(y)) \\
&= \cos(\varepsilon f'(y)) \\
&= 1-\frac{1}{2}\varepsilon^2 f'^2 + o(\varepsilon^2) \qquad (7.21)
\end{aligned}$$

Inserting (7.21) into the Rankine-Hugoniot equations will give the boundary condition for the stem. For completeness all the variables are calculated:

Pressure

The approximation (7.21) in (2.29) gives:[2]

$$\begin{aligned}
\frac{p}{p_1} &= 1+\frac{2\gamma}{\gamma-1}(M_1^2\sin^2\phi-1) \\
&= 1+\frac{2\gamma}{\gamma-1}(M_1^2(1-\varepsilon^2 f'^2/2)^2-1+o(\varepsilon^2) \\
&= 1-\frac{2\gamma}{\gamma-1}+\frac{2\gamma}{\gamma-1}(M_1^2(1-\varepsilon^2 f'^2))+o(\varepsilon^2) \\
&= 1+\frac{2\gamma}{\gamma-1}(M_1^2-1)-\frac{2\gamma}{\gamma-1}M_1^2\varepsilon^2 f'^2+o(\varepsilon^2) \\
&= \left.\frac{p}{p_1}\right|_{\text{normal}} - \frac{2\gamma}{\gamma-1}M_1^2\varepsilon^2 f'^2+o(\varepsilon^2)
\end{aligned}$$

So the approximation is:

$$\frac{p}{p_1} = \left.\frac{p}{p_1}\right|_{\text{normal}} - \frac{2\gamma}{\gamma-1}M_1^2\varepsilon^2 f'^2+o(\varepsilon^2) \qquad (7.22)$$

Density

The density ratio is given by:

$$\frac{\rho}{\rho_1} = \frac{(\gamma+1)M_1^2\sin^2\phi}{2+(\gamma-1)M_1^2\sin^2\phi}$$

[2]The notation $X|_{\text{normal}}$ denotes evaluation at $\phi=\pi/2$

Examining the denominator initially:

$$\begin{aligned}\frac{1}{2+(\gamma-1)M_1^2\sin^2\phi} &= (2+\gamma-1)M_1^2(1-\varepsilon f'^2/2)^2)^{-1} \\ &= (2+(\gamma-1)M_1^2-(\gamma-1)M_1^2\varepsilon^2 f'^2)^{-1} \\ &= (2+(\gamma-1)M_1^2)^{-1}\left[1-\frac{(\gamma-1)M_1^2\varepsilon^2 f'^2}{2+(\gamma-1)M_1^2}\right]^{-1} \\ &= (2+(\gamma-1)M_1^2)^{-1}\left[1+\frac{(\gamma-1)M_1^2\varepsilon^2 f'^2}{2+(\gamma-1)M_1^2}\right]+o(\varepsilon^2)\end{aligned}$$

The numerator is:

$$\begin{aligned}(\gamma+1)M_1^2\sin^2\phi &= (\gamma+1)M_1^2(1-\varepsilon^2 f'^2/2)^2 \\ &= (\gamma+1)M_1^2(1-\varepsilon^2 f'^2)+o(\varepsilon^2) \\ &= (\gamma+1)M_1^2-(\gamma+1)M_1^2\varepsilon^2 f'^2+o(\varepsilon^2)\end{aligned}$$

With the numerator:

$$\begin{aligned}\frac{\rho}{\rho_1} &= \left[(\gamma+1)M_1^2-(\gamma+1)M^2\varepsilon^2 f'^2\right]\left[(2+(\gamma-1)M_1^2)^{-1}\left[1+\frac{(\gamma-1)M_1^2\varepsilon^2 f'^2}{2+(\gamma-1)M_1^2}\right]\right] \\ &= \frac{(\gamma+1)M_1^2}{2+(\gamma-1)M_1^2}-\frac{(\gamma+1)M_1^2\varepsilon^2 f'^2}{2+(\gamma-1)M_1^2}+\frac{(\gamma-1)(\gamma+1)M_1^4\varepsilon^2 f'^2}{(2+(\gamma-1)M_1^2)^2}+o(\varepsilon^2) \\ &= \frac{(\gamma+1)M_1^2}{2+(\gamma-1)M_1^2}-\frac{2(\gamma+1)M_1^2\varepsilon^2 f'^2}{(2+(\gamma-1)M_1^2)^2}+o(\varepsilon^2) \\ &= \left.\frac{\rho}{\rho_1}\right|_{\text{normal}}-\frac{2(\gamma+1)M_1^2\varepsilon^2 f'^2}{(2+(\gamma-1)M_1^2)^2}+o(\varepsilon^2)\end{aligned}$$

Hence

$$\frac{\rho}{\rho_1}=\left.\frac{\rho}{\rho_1}\right|_{\text{normal}}-\frac{2(\gamma+1)M_1^2\varepsilon^2 f'^2}{(2+(\gamma-1)M_1^2)^2}+o(\varepsilon^2) \tag{7.23}$$

Mach Number

The normal component of the Mach number across a shock is given by:

$$M_{2n}^2=\frac{2+(\gamma-1)M_1^2\sin^2\phi}{1-\gamma+2\gamma M_1^2\sin^2\phi}$$

Examining the numerator and denominator separately for ease. The numerator is:

$$\begin{aligned}2+(\gamma-1)M_1^2\sin^2\phi &= 2+(\gamma-1)M_1^2(1-\varepsilon^2 f'^2/2)^2 \\ &= 2+(\gamma-1)M_1^2(1-\varepsilon^2 f'^2)+o(\varepsilon^2) \\ &= 2+(\gamma-1)M_1^2-(\gamma-1)M_1^2\varepsilon^2 f'^2+o(\varepsilon^2)\end{aligned}$$

The denominator is:

$$\begin{aligned}
\frac{1}{(1-\gamma+2\gamma M_1^2\sin^2\phi)} &= (1-\gamma+2\gamma M_1^2(1-\varepsilon^2 f'^2/2)^2)^{-1} \\
&= (1-\gamma+2\gamma M_1^2-2\gamma M_1^2\varepsilon^2 f'^2)^{-1} \\
&= (1-\gamma+2\gamma M_1^2)^{-1}\left[1-\frac{2\gamma M_1^2 f'^2\varepsilon^2}{1-\gamma+2\gamma M_1^2}\right]^{-1} \\
&= (1-\gamma+2\gamma M_1^2)^{-1}\left[1+\frac{2\gamma M_1^2 f'^2\varepsilon^2}{1-\gamma+2\gamma M_1^2}\right]+o(\varepsilon^2)
\end{aligned}$$

Putting these expressions together gives

$$\begin{aligned}
M_{2n}^2 &= \left[2+(\gamma-1)M_1^2-(\gamma-1)M_1^2\varepsilon^2 f'^2\right]\left[(1-\gamma+2\gamma M_1^2)^{-1}\times\right. \\
&\quad \left.\times\left[1+\frac{2\gamma M_1^2 f'^2\varepsilon^2}{1-\gamma+2\gamma M_1^2}\right]\right]+o(\varepsilon^2) \\
&= \frac{2+(\gamma-1)M_1^2}{1-\gamma+2\gamma M_1^2}+\frac{(2+(\gamma-1)M_1^2)(2\gamma M_1^2 f'^2\varepsilon^2)}{(1-\gamma+2\gamma M_1^2)^2}-\frac{(\gamma-1)M_1^2 f'^2\varepsilon^2}{1-\gamma+2\gamma M_1^2}+o(\varepsilon^2) \\
&= M_2^2\big|_{\text{normal}}+\left[\frac{(2+(\gamma-1)M_1^2)(2\gamma M_1^2 f'^2)}{(1-\gamma+2\gamma M_1^2)^2}-\frac{(\gamma-1)M_1^2 f'^2}{1-\gamma+2\gamma M_1^2}\right]\varepsilon^2+o(\varepsilon^2) \\
&= M_2^2\big|_{\text{normal}}+\frac{M_1^2 f'^2\varepsilon^2}{(1-\gamma+2\gamma M_1^2)^2}\left[2\gamma(2+(\gamma-1)M_1^2)-\right. \\
&\quad \left.-(\gamma-1)(1-\gamma+2\gamma M_1^2)\right]+o(\varepsilon^2) \\
&= M_2^2\big|_{\text{normal}}+\frac{M_1^2 f'^2\varepsilon^2}{(1-\gamma+2\gamma M_1^2)^2}\left[2(\gamma-1)^2M_1^2+(\gamma+1)^2\right]+o(\varepsilon^2)
\end{aligned}$$

So:

$$M_{2n}^2 = M_2^2\big|_{\text{normal}}+\frac{M_1^2 f'^2\varepsilon^2}{(1-\gamma+2\gamma M_1^2)^2}\left[2(\gamma-1)^2M_1^2+(\gamma+1)^2\right]+o(\varepsilon^2) \qquad (7.24)$$

Velocity Components

The Rankine-Hugoniot equations currently give the velocity components tangential and normal to the stem, in order to get the boundary values for u and v, a rotation by an angle θ in the clockwise direction has to be made. The ratio of normal velocities is given by:

$$\frac{u_{2n}}{u_{1n}} = \frac{\gamma+1}{\gamma-1}+\frac{2}{(\gamma+1)M_1^2\sin^2\phi} \qquad (7.25)$$

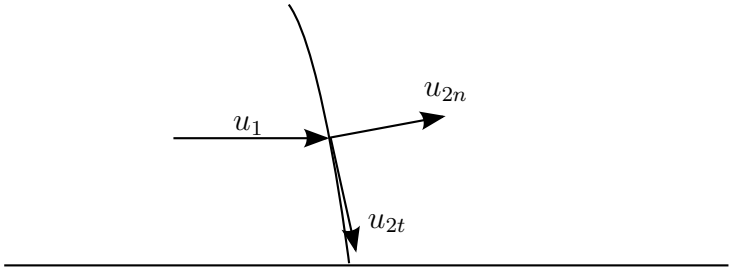

Figure 7.3: Velocity Components

Using (7.21) gives:

$$\begin{aligned}\frac{u_{2n}}{u_{1n}} &= \frac{\gamma-1}{\gamma+1}+\frac{2}{(\gamma+1)M_1^2(1+\varepsilon^2 f'^2)} \\ &= \frac{\gamma+1}{\gamma-1}+\frac{2}{(\gamma+1)M_1^2}(1-\varepsilon^2 f'^2)\end{aligned}$$

As the tangential components are equal, $u_{2t} = u_1 \cos\phi$, and so the boundary conditions become:

$$\begin{pmatrix} u \\ -v \end{pmatrix} = \begin{pmatrix} \cos\theta & \sin\theta \\ -\sin\theta & \cos\theta \end{pmatrix} \begin{pmatrix} u_{2n} \\ u_{2t} \end{pmatrix}$$

Which expanding gives:

$$\begin{aligned} u &= u_{2n}\cos\theta + u_{2t}\sin\theta \\ v &= u_{2n}\sin\theta - u_{2t}\cos\theta \end{aligned}$$

In particular, for u

$$\begin{aligned} u &= \left[\frac{\gamma-1}{\gamma+1}+\frac{2}{(\gamma+1)M_1^2}(1-\varepsilon^2 f'^2)\right]\sin\phi\cos\theta+\cos\phi\sin\theta \\ &= \left[\frac{\gamma-1}{\gamma+1}+\frac{2}{(\gamma+1)M_1^2}(1-\varepsilon^2 f'^2)\right](1+\varepsilon^2 f'^2)+\varepsilon^2 f'^2 \\ &= \frac{\gamma-1}{\gamma+1}+\frac{2}{(\gamma+1)M_1^2}+\left[\frac{\gamma-1}{\gamma+1}f'^2+f'^2\right]\varepsilon^2 \\ &= \frac{\gamma-1}{\gamma+1}+\frac{2}{(\gamma+1)M_1^2}+\frac{2\gamma}{\gamma+1}f'^2\varepsilon^2 \end{aligned}$$

Calculating v gives:

$$\begin{aligned} v &= \left[\frac{\gamma-1}{\gamma+1}+\frac{2}{(\gamma+1)M_1^2}(1-\varepsilon^2 f'^2)\right]\sin\phi\sin\theta-\cos\phi\cos\theta \\ &= \left[\frac{\gamma-1}{\gamma+1}+\frac{2}{(\gamma+1)M_1^2}(1-\varepsilon^2 f'^2)\right]\cos\theta\sin\theta+\sin\theta\cos\theta \\ &= \left[\frac{\gamma-1}{\gamma+1}+\frac{2}{(\gamma+1)M_1^2}(1-\varepsilon^2 f'^2)\right]\left(1-\frac{1}{2}\varepsilon^2 f'^2\right)(-\varepsilon f')+(-\varepsilon f')\left(1-\frac{1}{2}\varepsilon^2 f'^2\right) \\ &= \left[-\frac{2\gamma}{\gamma+1}-\frac{2}{(\gamma+1)M_1^2}\right]\varepsilon f'+O(\varepsilon^2). \end{aligned}$$

So:

$$v(0,y)=\left[-\frac{2\gamma}{\gamma+1}-\frac{2}{(\gamma+1)M_1^2}\right]\varepsilon f'. \tag{7.26}$$

Comparing (7.22) with the asymptotic expansion for pressure (7.22), yields the boundary condition for the Mach stem:

$$p(0,y)=0. \tag{7.27}$$

Contact Discontinuity ($y=1$)

Integrating (7.14) w.r.t. y from 0 to 1 gives:

$$v(x,1)=(1-M_4^2)\int_0^1\frac{\partial p}{\partial x}dy, \tag{7.28}$$

using the condition $v(x,0)=0$ on the lower boundary. Let ϑ be the angle which is made by the contact discontinuity. Then as ϑ is small $\tan\vartheta\approx\vartheta$ and so

$$\vartheta=\frac{v}{u}=\varepsilon v_1=\varepsilon(1-M_4^2)\int_0^1\frac{\partial p}{\partial x}dy. \tag{7.29}$$

Inserting this into (1.83) gives:

$$p=p_3+\varepsilon\frac{\rho_3 V_3^2}{\sqrt{M_3^2-1}}(1-M_4^2)\int_0^1\frac{\partial p_1}{\partial x}dy. \tag{7.30}$$

Writing $p_3=p_4+\varepsilon\rho_1 U_1^2$, which in turn defines ε. This reduces the boundary condition to be:

$$p=1+\varepsilon\kappa\int_0^1\frac{\partial p_1}{\partial x}dy, \tag{7.31}$$

where

$$\kappa=\frac{\rho_3 U_3^2}{\rho_1 U_1^3\sqrt{M_3^2-1}}(1-M_4^2) \tag{7.32}$$

Long Distance Behavior ($x \to \infty$)

As $x \to \infty$, it is expected that $\partial p/\partial x \to 0$. Inserting this into (7.13) gives:

$$\frac{\partial^2 p}{\partial y^2} = 0. \tag{7.33}$$

Integrating (7.33) twice gives:

$$p(\infty, y) = a + by. \tag{7.34}$$

The boundary condition for p at $y = 0$ ($\partial_y p(x, 0) = 0$) shows that $b = 0$ and taking the limit as $x \to \infty$ of (7.31) shows that $a = 1$, so the boundary condition as $x \to \infty$ is $p(\infty, y) = 1$.

7.3 The Numerical Solution of Equation (7.13)

7.3.1 The Numerical Method

The method for discretising the Laplace equation is done via central differences:

$$\frac{\partial^2 p}{\partial x^2} = \frac{p_{i+1,j} - 2p_{i,j} + p_{i-1,j}}{\delta x^2}, \quad \frac{\partial^2 p}{\partial y^2} = \frac{p_{i,j+1} - 2p_{i,j} + p_{i,j-1}}{\delta y^2}. \tag{7.35}$$

So upon using (7.35), the numerical scheme is given by:

$$\beta^2 \frac{p_{i+1,j} - 2p_{i,j} + p_{i-1,j}}{\delta x^2} + \frac{p_{i,j+1} - 2p_{i,j} + p_{i,j-1}}{\delta y^2} = 0, \tag{7.36}$$

where $\beta^2 = 1 - M_4^2$. Equation (7.36) can be written in the form:

$$a_i p_{i+1,j} + b_i p_{i,j} + c_i p_{i-1,j} + d_i = 0, \tag{7.37}$$

where

$$a_i = \frac{\beta^2}{\delta x^2}, \quad b_i = -\frac{2\beta^2}{\delta x^2} - \frac{2}{\delta y^2}, \quad c_i = a_i, \quad d_i = \frac{p_{i,j+1} + p_{i,j-1}}{\delta y^2} \tag{7.38}$$

To obtain a method for solving (7.36) write,

$$p_{i,j} = r_i p_{i-1,k} + q_i \tag{7.39}$$

Using the boundary condition $p(\infty, y) = 1$ in conjunction with (7.39) gives:

$$p_{N,j} = r_N p_{N-1,j} + q_N = 1, \tag{7.40}$$

which shows that $r_N = 0$ and $q_N = 1$. Applying (7.39) to $i+1$ results in:

$$\begin{aligned} p_{i+1,j} &= r_{i+1}p_{i,j} + q_{i+1} \\ &= r_{i+1}(r_i p_{i-1,k} + q_i) + q_{i+1} \\ &= r_{i+1}r_i p_{i-1,j} + r_{i+1}q_i + q_{i+1}. \end{aligned} \tag{7.41}$$

Inserting (7.41) and (7.39) into (7.36) yields $Ap_{i-1,j} + B = 0$, where

$$A = a_i r_{i+1} r_i + b_i r_i + c_i \tag{7.42}$$

$$B = a_i r_{i+1} q_i + b_i q_i + a_i q_{i+1} + d_i \tag{7.43}$$

Compairing coefficients gives $A = 0$ and $B = 0$, which means:

$$r_i = -\frac{c_i}{a_i r_{i+1} + b_i}, \quad q_i = -\frac{a_i q_{i+1} + d_i}{a_i r_{i+1} + b_i}. \tag{7.44}$$

This completes the method for solving the main equation. The next step in the solutions is to update the pressure along the lower wall, the boundary condition is given by $\partial_y p(x, 0) = 0$. Note:

$$\left.\frac{\partial p}{\partial y}\right|_{j=1/2} = \frac{p_{i,1} - p_{i,0}}{\delta y} \tag{7.45}$$

$$\left.\frac{\partial p}{\partial y}\right|_{j=1} = \frac{p_{i,2} - p_{i,0}}{2\delta y} \tag{7.46}$$

$$\tag{7.47}$$

However:

$$\left.\frac{\partial p}{\partial y}\right|_{j=1/2} = \frac{1}{2}\left[\left.\frac{\partial p}{\partial y}\right|_{j=1} + \left.\frac{\partial p}{\partial y}\right|_{j=0}\right]. \tag{7.48}$$

Hence:

$$\left.\frac{\partial p}{\partial y}\right|_{j=0} = 2\left.\frac{\partial p}{\partial y}\right|_{j=1/2} - \left.\frac{\partial p}{\partial y}\right|_{j=1} = 0. \tag{7.49}$$

Inserting (7.45) and (7.45) into (7.49) yields:

$$p_{i,0} = \frac{4p_{i,1} - p_{i,2}}{3} \tag{7.50}$$

In order to obtain the pressure on the contact discontinuity use the trapezium rule for evaluating integrals:

$$\int_0^1 f(x)dx = \frac{\delta x}{2} f_M + \frac{\delta x}{2} f_0 + \sum_{k=1}^{M-1} f_k \delta y. \tag{7.51}$$

Which means that:

$$\begin{aligned}\int_0^1 \frac{\partial p}{\partial x} dy &= \frac{p_{i+1,M} - p_{i-1,M}}{2\delta x}\frac{\delta y}{2} + \\ &+ \left(\frac{p_{i+1,0} - p_{i-1,0}}{2\delta x}\frac{\delta y}{2} + \sum_{k=1}^{M-1} \frac{p_{i+1,k} - p_{i-1,k}}{2\delta x}\delta y \right) \end{aligned} \tag{7.52}$$

The boundary condition on the contact discontinuity (7.31) can be written as:

$$\begin{aligned} p_{i,M} &= \kappa(p_{i+1,M} - p_{i-1,M})\frac{\delta y}{4\delta x} + 1 + \kappa(p_{i+1,0} - p_{i-1,0})\frac{\delta y}{4\delta x} + \\ &+ \kappa \sum_{k=1}^{M-1} (p_{i+1,k} - p_{i-1,k})\frac{\delta y}{2\delta x}. \end{aligned} \tag{7.53}$$

which is equivalent to:

$$a_i p_{i+1,M} + b_i p_{i,M} + c_i p_{i-1,M} + d_i = 0, \tag{7.54}$$

where:

$$\begin{aligned} a_i &= \kappa\frac{\delta y}{4\delta x} \\ b_i &= -1 \\ c_i &= -a_i \\ d_j &= 1 + \kappa(p_{i+1,0} - p_{i-1,0})\frac{\delta y}{4\delta x} + \kappa \sum_{k=1}^{M-1} (p_{i+1,k} - p_{i-1,k})\frac{\delta y}{2\delta x}. \end{aligned}$$

Exactly the same method can be applied to (7.54) as was used to solve (7.36). This completes the numerical solution of (7.36).

7.3.2 Numerical Results

In the numerical solution, the triple point is located in the upper left hand corner of the computational domain. The pressure gradient at $x = 0$ for the solution is given by figure 7.4.

From figure 7.4, it can be seen that there is a singularity is the pressure field at the triple point, it is then possible to attach a polar co-ordinate system at this point.

In order to calculate the shape of the Mach stem, use equation (7.14):

$$\frac{\partial v}{\partial y} = (1 - M_4)^2 \frac{\partial p}{\partial x} \tag{7.55}$$

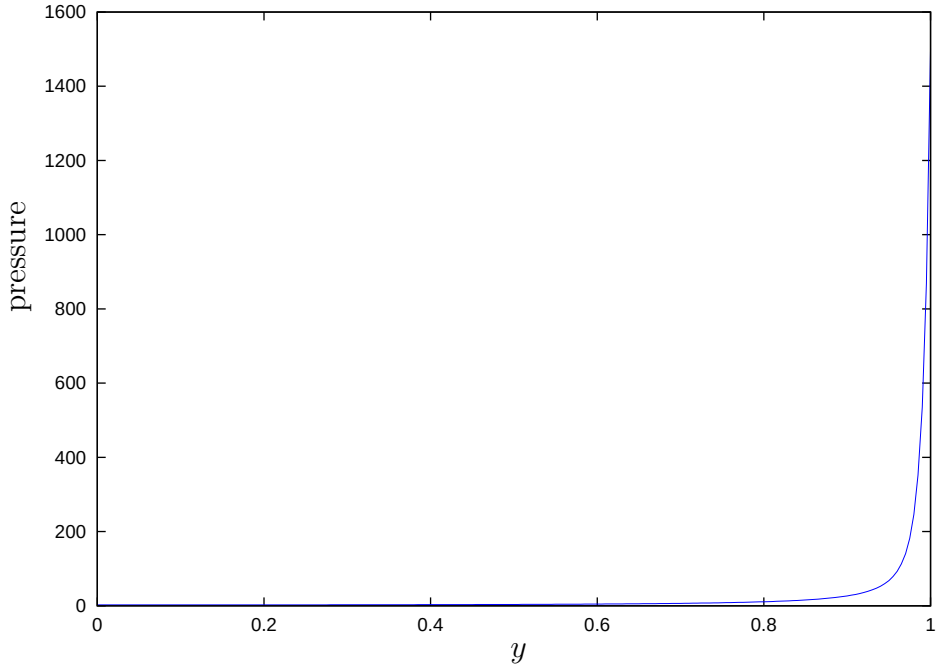

Figure 7.4: Pressure gradient at $x = 0$

Once (7.13) has been solved to obtain the pressure, integrate (7.14) to obtain v and then set $x = 0$ to get:

$$f'(y) = \left[-\frac{2\gamma}{\gamma+1} - \frac{2}{(\gamma+1)M_4^2} \right]^{-1} v(0,x) \tag{7.56}$$

As $v\|_{y=0} = 0$ then the finite difference scheme is:

$$\frac{v_i - v_{i-1}}{\delta y} = \frac{\beta^2}{2} \left(\frac{4p_{1,i} - 3p_{0,i} - p_{2,i}}{2\delta x} + \frac{4p_{1,i-1} - 3p_{0,i=1} - p_{2,i-1}}{2\delta x} \right) \tag{7.57}$$

which results in the numeric scheme for v:

$$v_i = v_{i-1} + \frac{\beta^2 \delta y}{4\delta x}(4p_{1,i} - 3p_{0,i} - p_{2,i} + 4p_{1,i-1} - 3p_{0,i=1} - p_{2,i-1}) \tag{7.58}$$

It remains to integrate (7.58). Set $f(1) = 0$, the scheme becomes:

$$\frac{f_{i+1} - f_i}{\delta y} = \frac{1}{2} \left[-\frac{2\gamma}{\gamma+1} - \frac{2}{(\gamma+1)M_4^2} \right]^{-1} (v_{i+1} + v_i) \tag{7.59}$$

The shape of the stem is given in figure 7.5.

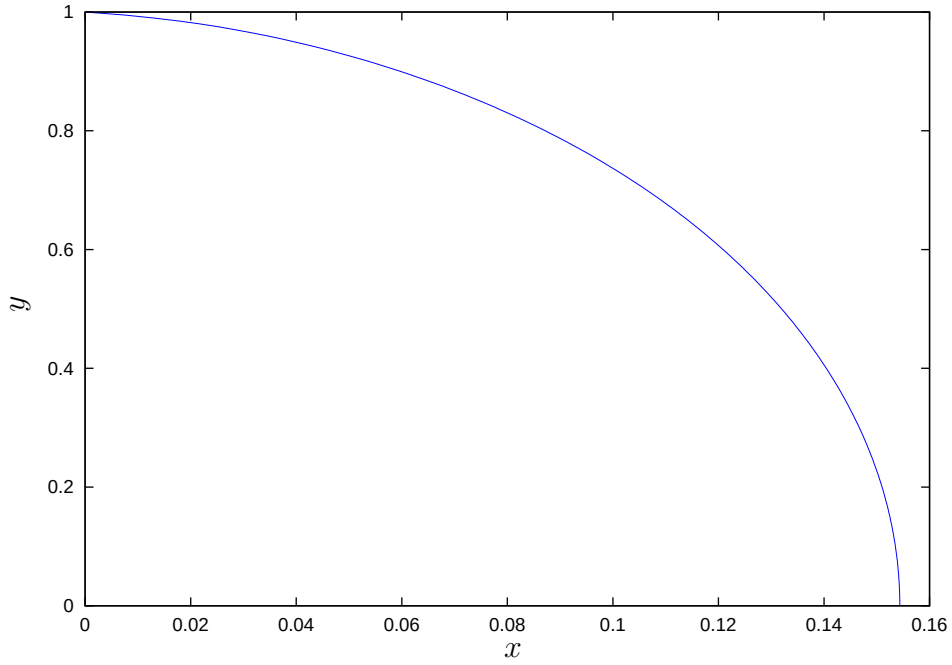

Figure 7.5: Shape of the Mach stem

7.4 The Solution

The Laplace equation is invariant under the transformation $(x, y) \mapsto (sx, sy)$. This shows that pressure is independent of the distance from the triple point. Write $X = x\sqrt{1 - M_4^2}$ and transform to polar co-ordinates to give the Laplace equation as:

$$\frac{\partial^2 p}{\partial r^2} + \frac{1}{r}\frac{\partial p}{\partial r} + \frac{1}{r^2}\frac{\partial p}{\partial \theta^2} = 0. \tag{7.60}$$

Writing the pressure as $p = g(\theta)$ gives:

$$g''(\theta) = 0 \tag{7.61}$$

The boundary conditions for this equation are:

$$g(0) = 0, \quad g\left(\frac{\pi}{2}\right) = p_4. \tag{7.62}$$

The solution of this is:

$$g(\theta) = \frac{2}{\pi} p_4 \theta. \tag{7.63}$$

In terms of the co-ordinates (x, y), the pressure is given by:

$$p(x, y) = \frac{2}{\pi} p_4 \tan^{-1}\left(\frac{y}{x}\right). \tag{7.64}$$

Using (7.14), this gives v to be:

$$v = \frac{2p_4}{\pi\sqrt{1-M_4^2}} \log\left[\frac{x^2}{1-M_4^2} + y^2\right]. \tag{7.65}$$

Using the boundary condition for v gives:

$$\left[-\frac{2\gamma}{\gamma+1} - \frac{2}{(\gamma+1)M_4^2}\right] f'(y) = \frac{4p_4}{\pi\sqrt{1-M_4^2}} \log y \tag{7.66}$$

Integrating (7.66) gives the shape of the stem given by:

$$f(y) = -\frac{2p_4}{\pi\sqrt{1-M_4^2}}\left[\frac{2\gamma}{\gamma+1} + \frac{2}{(\gamma+1)M_4^2}\right]^{-1} (y\log y - y) \tag{7.67}$$

7.5 Stem Shape for Solids

A good experimental result which relates shock speed, U_S to particle velocity, u_p is given by:

$$U_S = a + bu_p. \tag{7.68}$$

Where a and b are values determined by experiment. The value a is identified with the speed of sound in the material. Pressures in shocked materials tend to be of the order of 10^9 Pa, as the initial pressures of the material are essentially atmospheric pressure which is of the order 10^5 Pa, the initial pressure is usually taken to be zero, $p_1 = 0$. So the non-dimensionalisation for solids will take the form:

$$\begin{aligned} p &= \rho_1 U_S^2 \varepsilon \bar{p}(x,y) & u &= U_S(1+\varepsilon\bar{u}(x,y)) \\ \rho &= \rho_1(1+\varepsilon\bar{\rho}(x,y)) & v &= U_S\varepsilon\bar{v}(x,y) \\ x &= d\bar{x} & y &= d\bar{y} \end{aligned}$$

The conservation of energy for a solid is given by:

$$\frac{Dp}{Dt} = a^2\frac{D\rho}{Dt} \tag{7.69}$$

The sound speed can be expressed as $a^2 = a_1^2 + o(1)$, and so the conservation of energy reduces to:

$$\frac{\partial p}{\partial x} = \frac{1}{M_1^2}\frac{\partial \rho}{\partial x} \tag{7.70}$$

The basic equations remain the same and as a result the equation representing the pressure remains the same. The only difference is the boundary condition on the stem. The equation for pressure is given by:

$$p = \rho_1 U_S \sin\phi \left[\frac{U_S \sin\phi - a}{b} \right] \tag{7.71}$$

Expanding this in terms of ε gives:

$$\begin{aligned} p &= \frac{\rho_1 U_S}{b}\left(1+\frac{1}{2}\varepsilon^2 f'^2\right)\left(U_S\left(1+\frac{1}{2}\varepsilon^2 f'^2\right)-a\right) \\ &= \frac{\rho_1 U_S}{b}\left(U_S - a + \left(U_S f'^2 - \frac{a}{2}f'^2\right)\varepsilon^2\right) \end{aligned}$$

There are no terms of order ε, so the boundary condition on the stem remains the same and the result will remain the same. The only difference is the boundary condition of v on the stem. The velocities in the subsonic region are given by (using the scaling):

$$\begin{aligned} u_n &= \frac{a}{bU_S} + \frac{b-1}{b}\cos\theta \\ u_t &= \sin\theta \end{aligned}$$

So this gives v on the stem as:

$$\begin{aligned} v &= u_n \sin\theta - u_t \cos\theta \\ &= \left[\frac{a}{b} + \frac{b-1}{b} U_S \cos\theta\right]\sin\theta - \sin\theta\cos\theta \\ &= -\left[\frac{b+1}{2} + \frac{a}{bU_S}\right] f'(y)\varepsilon + o(\varepsilon) \end{aligned}$$

So the shape of a Mach stem for a solid is given by:

$$f(y) = -\frac{2p_4}{\pi\sqrt{1-M_1^2}}\left[\frac{b+1}{2} + \frac{a}{bU_S}\right]^{-1}(y\log y - y) \tag{7.72}$$

Chapter 8

Conclusions

This chapter is an executive summary of the thesis as well as adding some conclusions to each of the chapters in the case of new material.

8.1 Chapter 1

This chapter introduced the basic concepts of supersonic flow and went on to develop the governing equations used in this thesis: the Euler equations. To close the set of equations, the first law of thermodynamics was used under the assumption of constant entropy. The method of characteristics was introduced and as an example of their use, the Riemann invariants of the steady 2D Euler equations were computed and the characteristics which the Riemann invariants were constant along. The Riemann invariants were applied to Prandtl-Meyer flow and it was shown that the positive characteristics were straight lines around the corner. Prandtl-Meyer flow was examined when the turning angle was small.

8.2 Chapter 2

This chapter introduced the Rankine-Hugoniot equations for an oblique shock in a perfect gas and their solution. Prandtl's relation was derived for an oblique shock. Using the expression for the ratio of densities, two expressions relating shock angle

to flow deflection angle were derived and from these expressions the maximum possible flow deflection angle for shock attachment was derived. The Rankine-Hugoniot equations for solids were examined using the relationship: $U_S = a + bu_p$, two expressions relating shock angle and flow deflection were derived for this relationship. These expressions only assume that the solid is in the hydrodynamic phase and has no strength to talk of, so the author is unsure how accurate the solutions of these equations will be when dealing with real materials, however 1D planar shocks this method seems to agree with experiments relatively well. The modern way of dealing with weak oblique shock reflections is also introduced.

8.3 Chapter 3

Shock polars are a basic tool when dealing with oblique shocks is the shock polar which is dealt with in this chapter. There are two types: shock polars in the hodograph plane and shock polars in the (p, φ) plane which is also called a pressure deflection diagram. Both are examined for perfect gases but only the pressure deflection diagram is extended to solids. For solids it was found that the same basic shape of the pressure deflection diagram was still apparent. Reflected shocks in solids create "off Hugoniot states" and really when dealing with pressure deflection diagrams for reflected shocks the full equation of state should be used. However most experimentalists when dealing with planar shocks ignore this to little effect; it is this approach that is taken here.

8.4 Chapter 4

The concept of a Mach reflection is introduced in this chapter using the pressure deflection diagram. There are many different types of Mach reflection which may be split into two main types: direct and indirect. The pressure deflection diagrams can give more than one possible shock configuration (indirect Mach reflections *always* share the pressure deflection diagram of regular reflection), so it is difficult

to say which configuration will be a regular reflection or Mach reflection. Criteria for transition from regular reflection to Mach reflection was given for von Neumann, sonic and detachment conditions. There are regions where it is possible to say that according to the Rankine-Hugoniot equations the only one shock pattern is possible (this is the case for direct Mach reflections) but for many of the other configurations there are more than just one solution. The detachment criterion gives the condition necessary for a unique Mach reflection solution. It is thought by the author that extra conditions on the flow are required to fully say when a Mach reflection will occur. For solids this is technically the same question but the notion of strength will change things considerably and it is possible that the Rankine-Hugioniot equations are possibly not the correct tool as they may be too crude, only experiments can say if this is indeed the case.

8.5 Chapter 5

The numerical method used to solve the Euler equation is a standard one, the predictor-corrector method using the half step leapfrog method as the predictor. Numerical viscosity was used for stability in the region with shocks and the standard outflow boundary conditions were used. In order to obtain oblique shocks in the calculation, the Rankine-Hugoniot equations were used as inflow boundary conditions.

The object of the numerical study was to examine if the transition from regular reflection to Mach reflection was the same as predicted in the pressure deflection diagram. From the results it appears that the two criteria didn't differ by much which was confirmed by the numerical simulations. When performing a calculation that would result in regular reflection, a small stem was still seen in the results and this is thought to reflect that the assumption of two shocks meeting at a single point is not valid. From the results it can be seen that the pressure falls away after the reflected shock but there is no similar phenomenon with the incident shock, it is thought that this is due to the inflow conditions being the Rankine-Hugoniot equations. It is thought that this would no be the case in a full 2D hydrocode.

8.6 Chapter 6

In previous analysis the contact discontinuity has always been assumed to have been a straight line, either parallel to the reflection surface or at an angle to it, inclined toward the reflecting surface (a direct Mach reflection) or away from the reflecting surface (indirect Mach reflection). This has led (in the case of direct Mach reflection) to incorrect conclusions concerning the physics of such flows.

The results in this chapter are quite general, applying to any equation of state as long as the expression for sound speed can be linearised. The Euler equations are written in terms of von Mises variables and are then linearised and solved. The assumption is that the curvature of the contact discontinuity is small, so higher order terms can be ignored, which in turn leads to a differential equation for the contact discontinuity. The assumption of small curvature indicates that the solution is for the downstream asymptote. The solution of the equation shows that instead of reaching the reflection surface, the contact discontinuity levels off, so there is a finite width to the subsonic corridor. There is an arbitrary constant left in the solution, it is thought that this can be fixed via asymptotic matching to the contact discontinuity in the neighbourhood of the triple point.

8.7 Chapter 7

There has been a great deal of work done on determining the shape of the Mach stem. Old references like [7] refer to it as a simple straight line, and for the von Neumann Mach reflection, this is indeed the case as shown by the pressure deflection diagram. However there have been some more recent work done on the subject ([20], [27] and [28]) where a proof/experiment has shown the Mach stem to be the arc of a circle. The aim of this chapter is to show that this is not the case, at least in the neighbourhood of the triple point.

To find the shape of the Mach stem, an expression for pressure is derived for

the subsonic region, along with boundary conditions which come from the Rankine-Hugoniot equations, the governing equations themselves and the impermeability condition for the reflecting surface. The resulting equation cannot be solved analytically but can be solved numerically using the Thomas technique. The numerical results show two things: a singularity at the triple point in the pressure, and the shape of the Mach stem which isn't a circle. A radial co-ordinate system is then fixed at the triple point and an asymptotic solution for the Mach stem is derived, which again shows that the Mach stem is not an arc of a circle.

Bibliography

[1] H.W. Leipmann and A. Roshko, Elements of gas dynamics. Dover 2001

[2] M van Dyke, Perturbation methods in fluid mechanics. Parabolic press 1978

[3] G.B. Whitham, Linear and nonlinear waves. John Wiley and sons 1999

[4] A.B. Tayler, Mathematical models in appled mechanics. OUP 2006

[5] J. David Logan, Nonlinear partial differential equations. John Wiley and sons 1994

[6] D.J. Acheson, Elementary fluid mechanics. OUP 2005

[7] R. Courant and K.O. Friedrichs, Supersonic flow and shock waves. Interscience publishers inc.

[8] J. Ockendon, S. Howison, A. Lacey and A. Movchan, Applied partial differential equations. OUP 2003

[9] E.J. Hinch, Perturbation methods. CUP 2002

[10] Y.B. Zel'dovich and Y.P. Razier, Physics of shock waves and high temperature hydrodynamic phenomena. Dover 2002

[11] C.J. Chapman, High speed flow. CUP 2000

[12] J.S.E. Lee, The detonation phenomenon. CUP 2008

[13] G. Ben-Dor, Shock-wave Reflection phenomena. Springer 2007

[14] H. Ockendon and J. Ockendon, Waves and compressible flow. Springer 2000

[15] R. Winter, Introduction to shock hydrodynamics. AWE internal lecture notes

[16] B.B. Dunne, Mach reflection of detonation waves in condensed high explosives. Physics of fluids vol 4 number 7, 1961

[17] B.B. Dunne, Mach reflection of detonation waves in condensed high explosives II. Physics of fluids vol 7, number 16, 1964

[18] L.F. Henderson and R. Menikoff, Triple-shock entropy theorem and its consequences. J.Fluid. Mech (1998) vol 366 pp 179-210

[19] I.C. Skidmore, An introduction to shock waves in solids. Applied materials research July 1965

[20] L. Tan, Y. Ren and Z. Wu, Analytical and numerical study of the near flow field and shape of the Mach stem in steady flows. J. Fluid. Mech vol 546, pp 341-362, 2006

[21] W. Bleakney and A.H. Taub, Interaction of shock waves. Reviews of modern physics vol 21 number 4 1949

[22] H.M. Sternberg and D. Placesi, Interaction of oblique detonation waves with iron. Physics of fluids vol 9, number 7, 1966

[23] A.V. Trotsyuk, A.N. Kudryavtsev and M.S. Ivanov, Mach reflection of shock and detonation waves in steady supersonic chemically reacting flows. Recent Advances in Space Technologies, 2003. RAST '03. Page(s): 495 - 503

[24] H. Li and G. Ben-Dor, A parametric study of Mach reflection in steady flows. J. Fluid Mech. (1997), vol. 341, pp. 101-125

[25] H. Hornung, Regular and Mach reflection of shock waves. Ann. Rev. Fluid Mech. 1986. 18: 33-58

[26] B. D. Lambourn. and P. W. Wright, Mach Interaction of Two Plane Detonation Waves. 4th detonation symposium

[27] J.M. Dewey and D.J. McMillin, Observation and Analysis of the Mach Reflection of Weak Uniform Plane Shock Waves, Part 1. Observations, J. Fluid Mech., Vol. 152, pp 49-66, 1985

[28] J.M. Dewey and D.J. McMillin, Observation and Analysis of the Mach Reflection of Weak Uniform Plane Shock Waves. Part 2. Analysis, J. Fluid Mech., Vol. 152, pp 67-81, 1985

Appendix A

Calculation of the von Neumann and Detachment Criterion

This appendix contains the octave/matlab program to calculate the von Neumann criterion for a given initial Mach number.

A.1 von Neumann Criterion

```
function y=vN(M)
g=1.4;
M_1=M;
p_max=1+((2*g)/(g+1))*(M^2-1);
%Shock angles vary from the mach angle to pi/2

theta_i=asin(1/M):0.0001:0.5*pi;

%Calculate corresponding flow deflection angles

A=2*cot(theta_i);
B=(M^2)*sin(theta_i).^2-1;
C=2+M^2*(g+cos(2*theta_i));
```

```
phi=atan(A.*B./C);
phi_max=max(phi);

%Convert the flow deflection angles into shock angles
phi=0:0.0005:phi_max;
X=[phi phi_max]; %This is a test
n=length(X);
a_1=(1+0.5*(g-1)*M^2)*tan(X); %phi is replaced by X
a_2=-(M^2-1)*ones(1,n);
a_3=(1+0.5*(g+1)*M^2)*tan(X); %phi is replaced by X
a_4=ones(1,n);

Q=[a_1' a_2' a_3' a_4'];

Z=zeros(n-1,2);

for i=2:n
     sol=sort(roots(Q(i,:)));
     Z(i-1,:)=[real(atan(sol(2))) real(atan(sol(3)))];
end

weak=Z(:,1);
p_w=1+((2*g)/(g+1))*(M^2*sin(weak).^2-1);
p_weak=[1 p_w'];

%Calculate ALL the mach numbers for the second region

M_new_n=sqrt((2+(g-1)*M^2*sin(weak).^2)./(2*g*M^2*sin(weak).^2+1-g));
M_new=M_new_n./(sin(weak-phi'));
```

```
%Calculate the maximum flow deflection angle for these

n=length(M_new);
phi_max=zeros(1,n);
for i=1:n
   theta_i=asin(1/M_new(i)):0.0001:0.5*pi;
   A=2*cot(theta_i);
   B=(M_new(i)^2)*sin(theta_i).^2-1;
   C=2+M_new(i)^2*(g+cos(2*theta_i));
   x=atan(A.*B./C);
   phi_max(i)=max(x);
end

%See if the corresponding reflected shocks go past the p axis.
c=0;
diff=phi'-phi_max';
for i=1:n
    if(diff(i)<0)
       c=c+1;
    end
end

%For those values of diff<0 indicates a crossing of the p axis. The next
%task is to find out when this happens.
%For the value phi, find the pressure at thet point.

%Turn flow deflection angles into shock angles

X=phi(1:c);
M=M_new(1:c)';
```

```
a_1=(1+0.5*(g-1)*M.^2).*tan(X); %phi is replaced by X
a_2=-(M.^2-1).*ones(1,c);
a_3=(1+0.5*(g+1)*M.^2).*tan(X); %phi is replaced by X
a_4=ones(1,c);

Q=[a_1' a_2' a_3' a_4'];
 Z=zeros(c,2);
for i=2:c
     sol=sort(roots(Q(i,:)));
     Z(i-1,:)=[real(atan(sol(2))) real(atan(sol(3)))];
end

weak=Z(:,1);

%Calculate the pressures
mu=M';
p_old=p_weak(1:c)';
p=(1+((2*g)/(g+1))*(mu.^2.*sin(weak).^2-1)).*p_old;

%Then look to see when this reaches the von Neumann point.

d=0;
for i=1:c
    if (p(i)<p_max)
        d=d+1;
    end
end

%The correct value to take will be phi at point d, use this to plot the
%reflected polar.
```

```
phi_vN=X(d);

a_1=(1+0.5*(g-1)*M_1^2)*tan(phi_vN); %phi is replaced by X
a_2=-(M_1^2-1);
a_3=(1+0.5*(g+1)*M_1^2)*tan(phi_vN); %phi is replaced by X
a_4=1;

X=[a_1 a_2 a_3 a_4];
sol=sort(roots(X));
y=atan(sol(2))*180/pi;
end
```

A.2 Detachment Criterion

```
function y=d(M)

g=1.4;

%Shock angles vary from the mach angle to pi/2

theta_i=asin(1/M):0.0001:0.5*pi;

%Calculate corresponding flow deflection angles

A=2*cot(theta_i);
B=(M^2)*sin(theta_i).^2-1;
C=2+M^2*(g+cos(2*theta_i));
phi=atan(A.*B./C);
phi_max=max(phi);
```

```
%Convert the flow deflection angles into shock angles
phi=0:0.0001:phi_max;
X=[phi phi_max]; %This is a test
phi_deg=X*180/pi; %phi is changed to X
%n=length(phi);
n=length(X);
a_1=(1+0.5*(g-1)*M^2)*tan(X); %phi is replaced by X
a_2=-(M^2-1)*ones(1,n);
a_3=(1+0.5*(g+1)*M^2)*tan(X); %phi is replaced by X
a_4=ones(1,n);

Q=[a_1' a_2' a_3' a_4'];

Z=zeros(n-1,2);

for i=2:n
     sol=sort(roots(Q(i,:)));
     Z(i-1,:)=[atan(sol(2)) atan(sol(3))];
end

weak=Z(:,1);

%Calculate the right angle for the detachment criterion.
%calculate the new Mach numbers in the shocked region.
M_new_n=sqrt((2+(g-1)*M^2*sin(weak).^2)./(2*g*M^2*sin(weak).^2+1-g));
M_new=M_new_n./(sin(weak-phi'));

%Calculate the maximum flow deflection angle for these
```

```
n=length(M_new);
phi_max=zeros(1,n);
for i=1:n
   theta_i=asin(1/M_new(i)):0.0001:0.5*pi;
   A=2*cot(theta_i);
   B=(M_new(i)^2)*sin(theta_i).^2-1;
   C=2+M_new(i)^2*(g+cos(2*theta_i));
   x=atan(A.*B./C);
   phi_max(i)=max(x);
end

%See if the corresponding reflected shocks go past the p axis.
c=0;
diff=phi'-phi_max';
for i=1:n
    if(diff(i)<0)
       c=c+1;
    end
end

y=weak(c)*180/pi;
```

Appendix B

Fortran Programs

In the course of the work, two fortran programs were used: one to solve the Euler equations and the other to solve the elliptic PDE for pressure in region 4.

B.1 Solution of the Euler Equations

```
PROGRAM wake
implicit none
integer :: i,j,k,L,LL,a,b
integer,parameter :: n=500,m=250,m1=251,NS=50
real :: gamma,dx,dy,dum1,dum2,dum3,dum4,pi
real,parameter :: M_infty=3.0, UMIN=1.0, YD=1.0
real,parameter :: YM=5.0, XM=10.0
real,parameter :: dt=0.001
real,parameter :: VIS=1.0
real,parameter :: ST=3.588
real,dimension(0:n,0:m1) :: rho, rho_new
real,dimension(0:n,0:m1) :: u, u_new
real,dimension(0:n,0:m1) :: v, v_new
real,dimension(0:n,0:m1) :: p, p_new
real,dimension(0:n,0:m1) :: e, e_new
```

```
real :: cos_alpha,sin_alpha,v_n_2,v_t_2,EPS,SM,SHCH,D1,D2,OM,T,X,Y,UC,HN
real :: H1,H2,H3,H4
real :: R1,R2,R3,R4
real :: U1,U2,U3,U4
real :: V1,V2,V3,V4
real :: E1,E2,E3,E4
real :: P1,P2,P3,P4
real :: df_dx,dg_dy
pi=4.0*atan(1.0)
open (21, FILE='u.dat', FORM='FORMATTED', STATUS='NEW')
open (22, FILE='p.dat', FORM='FORMATTED', STATUS='NEW')
25 format(2F11.6)
26 format(3F11.6)
      write(22,*) 'VARIABLES = "x", "y", "p"'
      write(22,*) 'ZONE i=', n+1, ', j=', m+1, ', F=POINT'
      gamma=1.4
      dx=XM/n
      dy=YM/m



do i=0,n
   do j=0,m+1
      rho(i,j)=1.0
      u(i,j)=1.0
      v(i,j)=0.0
      p(i,j)=1.0/(gamma*M_infty**2.0)
      e(i,j)=1.0/(gamma*(gamma-1.0)*M_infty**2.0)+0.5
   end do
 end do
```

```
(sqrt(1.0+(gamma+1.0)*ST/(2.0*gamma)))/M_infty
cos_alpha=sqrt(1-sin_alpha**2)
SM=(M_infty*sin_alpha)**2.0

do i=NS,n
   rho(i,m+1)=(gamma+1.0)*SM/(2.0+(gamma-1.0)*SM)
   v_n_2=sin_alpha*((gamma-1.0)/(gamma+1.)+2.0/((gamma+1.0)*SM))
   v_t_2=cos_alpha
   u(i,m+1)=v_n_2*sin_alpha+v_t_2*cos_alpha
   v(i,m+1)=v_t_2*sin_alpha-v_n_2*cos_alpha
   p(i,m+1)=(2.0*gamma*SM-gamma+1.0)/(gamma*(gamma+1.0)*M_infty**2.0)
   e(i,m+1)=p(i,m+1)/((gamma-1.0)*rho(i,m+1))+(u(i,m+1)**2.0
            +v(i,m+1)**2.0)/2.0
 end do
write(*,*) 'alpha= ',sin_alpha*180/pi
do L=1,30000
   EPS=0.0

   do i=1,n-1
   do j=1,m
!C--POINT 1
      df_dx=(rho(i+1,j)*u(i+1,j)-rho(i,j)*u(i,j))/dx
      dg_dy=(rho(i+1,j+1)*v(i+1,j+1)-rho(i+1,j-1)*v(i+1,j-1)
            +rho(i,j+1)*v(i,j+1)-rho(i,j-1)*v(i,j-1))/(4.*dy)
      R1=0.5*(rho(i,j)+rho(i+1,j))-0.5*dt*(df_dx+dg_dy)
      df_dx=(rho(i+1,j)*u(i+1,j)**2+p(i+1,j)-rho(i,j)*u(i,j)**2-p(i,j))/dx
      dum1=rho(i+1,j+1)*u(i+1,j+1)*v(i+1,j+1)
      dum2=rho(i+1,j-1)*u(i+1,j-1)*v(i+1,j-1)
      dum3=rho(i,j+1)*u(i,j+1)*v(i,j+1)
      dum4=rho(i,j-1)*u(i,j-1)*v(i,j-1)
```

```
      dg_dy=(dum1-dum2+dum3-dum4)/(4.0*dy)
      H1=(rho(i,j)*u(i,j)+rho(i+1,j)*u(i+1,j))/2.0-dt*(df_dx+dg_dy)/2.0
      U1=H1/R1
      df_dx=(rho(i+1,j)*u(i+1,j)*v(i+1,j)-rho(i,j)*u(i,j)*v(i,j))/dx
      dum1=rho(i+1,j+1)*v(i+1,j+1)**2+p(i+1,j+1)
           -rho(i+1,j-1)*v(i+1,j-1)**2-p(i+1,j-1)
      dum2=rho(i,j+1)*v(i,j+1)**2+p(i,j+1)-rho(i,j-1)*v(i,j-1)**2-p(i,j-1)
      dg_dy=(dum1+dum2)/(4.0*dy)
      H1=(rho(i,j)*v(i,j)+rho(i+1,j)*v(i+1,j))/2.0-dt*(df_dx+dg_dy)/2.0
      V1=H1/R1
      df_dx=(u(i+1,j)*(p(i+1,j)+rho(i+1,j)*e(i+1,j))-u(i,j)*(p(i,j)
            +rho(i,j)*e(i,j)))/dx
      dum1=v(i+1,j+1)*(p(i+1,j+1)+rho(i+1,j+1)*e(i+1,j+1))
      dum2=v(i+1,j-1)*(p(i+1,j-1)+rho(i+1,j-1)*e(i+1,j-1))
      dum3=v(i,j+1)*(p(i,j+1)+rho(i,j+1)*e(i,j+1))
      dum4=v(i,j-1)*(p(i,j-1)+rho(i,j-1)*e(i,j-1))
      dg_dy=(dum1-dum2+dum3-dum4)/(4.0*dy)
      H1=(rho(i,j)*e(i,j)+rho(i+1,j)*e(i+1,j))/2.0-dt*(df_dx+dg_dy)/2.0
      E1=H1/R1
      P1=(gamma-1.0)*R1*(E1-(U1*U1+V1*V1)/2.0)
!C--POINT 2
      df_dx=(rho(i,j)*u(i,j)-rho(i-1,j)*u(i-1,j))/dx
      dg_dy=(rho(i,j+1)*v(i,j+1)-rho(i,j-1)*v(i,j-1)+rho(i-1,j+1)*v(i-1,j+1)
            -rho(i-1,j-1)*v(i-1,j-1))/(4.*dy)
      R2=(rho(i-1,j)+rho(i,j))/2.-dt*(df_dx+dg_dy)/2.
      df_dx=(rho(i,j)*u(i,j)**2+p(i,j)-rho(i-1,j)*u(i-1,j)**2-p(i-1,j))/dx
      dum1=rho(i,j+1)*u(i,j+1)*v(i,j+1)-rho(i,j-1)*u(i,j-1)*v(i,j-1)
           +rho(i-1,j+1)*u(i-1,j+1)*v(i-1,j+1)
      dum2=rho(i-1,j-1)*u(i-1,j-1)*v(i-1,j-1)
      dg_dy=(dum1+dum2)/(4.0*dy)
```

```
      H2=(rho(i-1,j)*u(i-1,j)+rho(i,j)*u(i,j))/2.0-dt*(df_dx+dg_dy)/2.0
      U2=H2/R2
      df_dx=(rho(i,j)*u(i,j)*v(i,j)-rho(i-1,j)*u(i-1,j)*v(i-1,j))/dx
      dum1=rho(i,j+1)*v(i,j+1)**2+p(i,j+1)-rho(i,j-1)*v(i,j-1)**2-p(i,j-1)
      dum2=rho(i-1,j+1)*v(i-1,j+1)**2+p(i-1,j+1)-rho(i-1,j-1)*v(i-1,j-1)**2
           -p(i-1,j-1)
      dg_dy=(dum1+dum2)/(4.0*dy)
      H2=(rho(i-1,j)*v(i-1,j)+rho(i,j)*v(i,j))/2.0-dt*(df_dx+dg_dy)/2.0
      V2=H2/R2
      df_dx=(u(i,j)*(p(i,j)+rho(i,j)*e(i,j))-u(i-1,j)*(p(i-1,j)
            +rho(i-1,j)*e(i-1,j)))/dx
      dum1=v(i,j+1)*(p(i,j+1)+rho(i,j+1)*e(i,j+1))-v(i,j-1)*(p(i,j-1)
           +rho(i,j-1)*e(i,j-1))
      dum2=v(i-1,j+1)*(p(i-1,j+1)+rho(i-1,j+1)*e(i-1,j+1))
           -v(i-1,j-1)*(p(i-1,j-1)+rho(i-1,j-1)*e(i-1,j-1))
      dg_dy=(dum1+dum2)/(4.0*dy)
      H2=(rho(i-1,j)*e(i-1,j)+rho(i,j)*e(i,j))/2.0-dt*(df_dx+dg_dy)/2.0
      E2=H2/R2
      P2=(gamma-1.)*R2*(E2-(U2*U2+V2*V2)/2.0)
!C--POINT 3
      df_dx=(rho(i+1,j+1)*u(i+1,j+1)-rho(i-1,j+1)*u(i-1,j+1)
            +rho(i+1,j)*u(i+1,j)-rho(i-1,j)*u(i-1,j))/(4.0*dx)
      dg_dy=(rho(i,j+1)*v(i,j+1)-rho(i,j)*v(i,j))/dy
      R3=(rho(i,j+1)+rho(i,j))/2.-dt*(df_dx+dg_dy)/2.0
      dum1=rho(i+1,j+1)*u(i+1,j+1)**2+p(i+1,j+1)-rho(i-1,j+1)*u(i-1,j+1)**2
           -p(i-1,j+1)
      dum2=rho(i+1,j)*u(i+1,j)**2+p(i+1,j)-rho(i-1,j)*u(i-1,j)**2-p(i-1,j)
      df_dx=(dum1+dum2)/(4.0*dx)
      dg_dy=(rho(i,j+1)*u(i,j+1)*v(i,j+1)-rho(i,j)*u(i,j)*v(i,j))/dy
      H3=(rho(i,j+1)*u(i,j+1)+rho(i,j)*u(i,j))/2.-dt*(df_dx+dg_dy)/2.0
```

```
      U3=H3/R3
      dum1=rho(i+1,j+1)*u(i+1,j+1)*v(i+1,j+1)-rho(i-1,j+1)*u(i-1,j+1)*v(i-1,j+
      dum2=rho(i+1,j)*u(i+1,j)*v(i+1,j)-rho(i-1,j)*u(i-1,j)*v(i-1,j)
      df_dx=(dum1+dum2)/(4.0*dx)
      dg_dy=(rho(i,j+1)*v(i,j+1)**2+p(i,j+1)-rho(i,j)*v(i,j)**2-p(i,j))/dy
      H3=(rho(i,j+1)*v(i,j+1)+rho(i,j)*v(i,j))/2.-dt*(df_dx+dg_dy)/2.0
      V3=H3/R3
      dum1=u(i+1,j+1)*(p(i+1,j+1)+rho(i+1,j+1)*e(i+1,j+1))
           -u(i-1,j+1)*(p(i-1,j+1)+rho(i-1,j+1)*e(i-1,j+1))
      dum2=u(i+1,j)*(p(i+1,j)+rho(i+1,j)*e(i+1,j))-u(i-1,j)*(p(i-1,j)
           +rho(i-1,j)*e(i-1,j))
      df_dx=(dum1+dum2)/(4.0*dx)
      dg_dy=(v(i,j+1)*(p(i,j+1)+rho(i,j+1)*e(i,j+1))-v(i,j)*(p(i,j)
            +rho(i,j)*e(i,j)))/dy
      H3=(rho(i,j+1)*e(i,j+1)+rho(i,j)*e(i,j))/2.0-dt*(df_dx+dg_dy)/2.0
      E3=H3/R3
      P3=(gamma-1.0)*R3*(E3-(U3*U3+V3*V3)/2.0)
!C--POINT 4
      df_dx=(rho(i+1,j)*u(i+1,j)-rho(i-1,j)*u(i-1,j)+rho(i+1,j-1)*u(i+1,j-1)
            -rho(i-1,j-1)*u(i-1,j-1))/(4.0*dx)
      dg_dy=(rho(i,j)*v(i,j)-rho(i,j-1)*v(i,j-1))/dy
      R4=(rho(i,j)+rho(i,j-1))/2.0-dt*(df_dx+dg_dy)/2.0
      dum1=rho(i+1,j)*u(i+1,j)**2+p(i+1,j)-rho(i-1,j)*u(i-1,j)**2-p(i-1,j)
      dum2=rho(i+1,j-1)*u(i+1,j-1)**2+p(i+1,j-1)-rho(i-1,j-1)*u(i-1,j-1)**2
           -p(i-1,j-1)
      df_dx=(dum1+dum2)/(4.0*dx)
      dg_dy=(rho(i,j)*u(i,j)*v(i,j)-rho(i,j-1)*u(i,j-1)*v(i,j-1))/dy
      H4=(rho(i,j)*u(i,j)+rho(i,j-1)*u(i,j-1))/2.0-dt*(df_dx+dg_dy)/2.0
      U4=H4/R4
      dum1=rho(i+1,j)*u(i+1,j)*v(i+1,j)-rho(i-1,j)*u(i-1,j)*v(i-1,j)
```

```
      dum2=rho(i+1,j-1)*u(i+1,j-1)*v(i+1,j-1)
           -rho(i-1,j-1)*u(i-1,j-1)*v(i-1,j-1)
      df_dx=(dum1+dum2)/(4.0*dx)
      dg_dy=(rho(i,j)*v(i,j)**2+p(i,j)-rho(i,j-1)*v(i,j-1)**2-p(i,j-1))/dy
      H4=(rho(i,j)*v(i,j)+rho(i,j-1)*v(i,j-1))/2.0-dt*(df_dx+dg_dy)/2.0
      V4=H4/R4
      dum1=u(i+1,j)*(p(i+1,j)+rho(i+1,j)*e(i+1,j))-u(i-1,j)*(p(i-1,j)
           +rho(i-1,j)*e(i-1,j))
      dum2=u(i+1,j-1)*(p(i+1,j-1)+rho(i+1,j-1)*e(i+1,j-1))
           -u(i-1,j-1)*(p(i-1,j-1)+rho(i-1,j-1)*e(i-1,j-1))
      df_dx=(dum1+dum2)/(4.0*dx)
      dg_dy=(v(i,j)*(p(i,j)+rho(i,j)*e(i,j))-v(i,j-1)*(p(i,j-1)
            +rho(i,j-1)*e(i,j-1)))/dy
      H4=(rho(i,j)*e(i,j)+rho(i,j-1)*e(i,j-1))/2.0-dt*(df_dx+dg_dy)/2.0
      E4=H4/R4
      P4=(gamma-1.0)*R4*(E4-(U4*U4+V4*V4)/2.0)
!C--CORRECTOR
      rho_new(i,j)=rho(i,j)-dt*((R1*U1-R2*U2)/dx+(R3*V3-R4*V4)/dy)
      HN=rho(i,j)*u(i,j)-dt*((R1*U1**2+P1-R2*U2**2-P2)/dx
         +(R3*U3*V3-R4*U4*V4)/dy)
      u_new(i,j)=HN/rho_new(i,j)
      HN=rho(i,j)*v(i,j)-dt*((R1*U1*V1-R2*U2*V2)/dx
         +(R3*V3**2+P3-R4*V4**2-P4)/dy)
      v_new(i,j)=HN/rho_new(i,j)
      HN=rho(i,j)*e(i,j)-dt*((U1*(P1+R1*E1)-U2*(P2+R2*E2))/dx
         +(V3*(P3+R3*E3)-V4*(P4+R4*E4))/dy)
      e_new(i,j)=HN/rho_new(i,j)
      p_new(i,j)=(gamma-1.0)*rho_new(i,j)*(e_new(i,j)-(u_new(i,j)**2
                 +v_new(i,j)**2)/2.0)
 end do
```

```
 end do
do k=1,m
      rho_new(0,k)=rho(0,k)
      u_new(0,k)=u(0,k)
      v_new(0,k)=v(0,k)
      e_new(0,k)=e(0,k)
      p_new(0,k)=p(0,k)
      rho_new(n,k)=4.0*rho_new(n-1,k)/3.0-rho_new(n-2,k)/3.0
      u_new(n,k)=4.0*u_new(n-1,k)/3.0-u_new(n-2,k)/3.0
      v_new(n,k)=4.0*v_new(n-1,k)/3.0-v_new(n-2,k)/3.0
      e_new(n,k)=4.0*e_new(n-1,k)/3.0-e_new(n-2,k)/3.0
      p_new(n,k)=4.0*p_new(n-1,k)/3.0-p_new(n-2,k)/3.0
 end do
!C--ART VISCOSITY
do a=1,n-1
do b=1,m
      SHCH=p_new(a+1,b)-p_new(a,b)
      D1=rho_new(a+1,b)-rho_new(a,b)
      D2=rho_new(a,b)-rho_new(a-1,b)
      OM=VIS*(ABS(D1)*D1-ABS(D2)*D2)
      IF(SHCH<0.0)OM=0.0
      rho(a,b)=OM+rho_new(a,b)
      D1=u_new(a+1,b)-u_new(a,b)
      D2=u_new(a,b)-u_new(a-1,b)
      OM=VIS*(ABS(D1)*D1-ABS(D2)*D2)
      IF(SHCH<0.0)OM=0.0
      UC=OM+u_new(a,b)
      IF(ABS(UC-u(a,b))>EPS)EPS=ABS(UC-u(a,b))
      u(a,b)=UC
      D1=v_new(a+1,b)-v_new(a,b)
```

```
      D2=v_new(a,b)-v_new(a-1,b)
      OM=VIS*(ABS(D1)*D1-ABS(D2)*D2)
      IF(SHCH<0.0)OM=0.0
      v(a,b)=OM+v_new(a,b)
      D1=e_new(a+1,b)-e_new(a,b)
      D2=e_new(a,b)-e_new(a-1,b)
      OM=VIS*(ABS(D1)*D1-ABS(D2)*D2)
      IF(SHCH<0.0)OM=0.0
      e(a,b)=OM+e_new(a,b)
      D1=p_new(a+1,b)-p_new(a,b)
      D2=p_new(a,b)-p_new(a-1,b)
      OM=VIS*(ABS(D1)*D1-ABS(D2)*D2)
      IF(SHCH<0.0)OM=0.0
      p(a,b)=OM+p_new(a,b)
 end do
 end do
      LL=L/30
      T=dt*L
      IF(L==30*LL)PRINT*,'TIME=',T,'  EPS=',EPS
!C--BOUNDARY CONDIONS

do i=1,NS-1
      rho(i,m+1)=rho(i,m-1)
      u(i,m+1)=u(i,m-1)
      v(i,m+1)=-v(i,m-1)
      e(i,m+1)=e(i,m-1)
      p(i,m+1)=p(i,m-1)
 end do

do j=0,m+1
```

```
      rho(n,j)=rho(n-1,j)
      u(n,j)=u(n-1,j)
      v(n,j)=v(n-1,j)
      e(n,j)=e(n-1,j)
      p(n,j)=p(n-1,j)
end do
end do
do i=0,n
      X=dx*i
do j=0,m
      Y=dy*j
      WRITE(UNIT=22,FMT=26) X, Y, p(i,j)
end do
      WRITE(22,*)
end do
do i=0,n
      X=dx*i
      WRITE(UNIT=21,FMT=25) X, u(i,m)
end do

end program
```

B.2 Solving the Equation for Pressure

```
      PROGRAM STEM
      IMPLICIT DOUBLE PRECISION(A-H, O-Z)
      PARAMETER (S=-1.) !This is the switch from indirect (S=-1)
      !to direct (S=+1) Mach reflection.
      PARAMETER (AK=.25, BET=.5)
      PARAMETER (M=200, N=800, XN=4.)
```

```
      PARAMETER (DEL=.0000001)
      PARAMETER (GAM=1.4, AMINF=4.)
      DIMENSION P(0:N,0:M), PN(0:N,0:M), R(N), Q(N)
      DIMENSION V1(0:M), F(0:M)
      OPEN (21, FILE='dp_dx.dat', FORM='FORMATTED', STATUS='NEW')
      OPEN (22, FILE='p0_x.dat', FORM='FORMATTED', STATUS='NEW')
      OPEN (23, FILE='f_y.dat', FORM='FORMATTED', STATUS='NEW')
      OPEN (24, FILE='p1_x.dat', FORM='FORMATTED', STATUS='NEW')
 25   FORMAT(2F11.6)
      DX=XN/N
      DY=1./M
C -- INITIALIZATION OF THE PRESSURE FIELD
      DO 1 K=0,M
      DO 1 J=0,N
      X=DX*J
 1    P(J,K)=X*S/XN
C -- ITERATION PROCESS
      DO 9 I=1,200000
      EPS=0.
      DO 3 K=1,M-1
      R(N)=0.
      Q(N)=S
      DO 2 L=1,N-1
      J=N-L
      AJ=BET**2/DX**2
      BJ=-2.*BET**2/DX**2-2./DY**2
      CJ=AJ
      DJ=(P(J,K+1)+P(J,K-1))/DY**2
      R(J)=-CJ/(AJ*R(J+1)+BJ)
 2    Q(J)=-(AJ*Q(J+1)+DJ)/(AJ*R(J+1)+BJ)
```

```
      PN(0,K)=0.
      DO 3 J=1,N
 3    PN(J,K)=R(J)*PN(J-1,K)+Q(J)
      DO 4 J=0,N
 4    PN(J,0)=(4.*PN(J,1)-PN(J,2))/3.
      R(N)=0.
      Q(N)=S
      DO 6 L=1,N-1
      J=N-L
      AJ=AK*DY/(4.*DX)
      BJ=-1.
      CJ=-AJ
      DJ=S+AK*(PN(J+1,0)-PN(J-1,0))*DY/(4.*DX)
      DO 5 K=1,M-1
 5    DJ=DJ+AK*(PN(J+1,K)-PN(J-1,K))*DY/(2.*DX)
      R(J)=-CJ/(AJ*R(J+1)+BJ)
 6    Q(J)=-(AJ*Q(J+1)+DJ)/(AJ*R(J+1)+BJ)
      PN(0,M)=0.
      DO 7 J=1,N
 7    PN(J,M)=R(J)*PN(J-1,M)+Q(J)
      DO 8 J=0,N
      DO 8 K=0,M
      IF(ABS(P(J,K)-PN(J,K)).GT.EPS)EPS=ABS(P(J,K)-PN(J,K))
 8    P(J,K)=PN(J,K)
      II=I/20
      IF(I.EQ.20*II)PRINT*,'I=',I,'  EPS=',EPS
      IF(EPS.LT.DEL)GO TO 10
 9    CONTINUE
 10   X=0.
C -- CALCULATION OF V1 ON THE STEM
```

```
      V1(0)=0.
      DO 15 K=1,M
 15   V1(K)=V1(K-1)+BET**2*DY*(4.*P(1,K)-3.*P(0,K)-P(2,K)+
     *4.*P(1,K-1)-3.*P(0,K-1)-P(2,K-1))/(4.*DX)
C -- CALCULATION OF F(Y)
      G=(1.+(GAM-1.)*AMINF**2/2.)/(AMINF**2-1.)
      F(M)=0.
      DO 16 L=1,M
      K=M-L
 16   F(K)=F(K+1)-G*DY*(V1(K+1)+V1(K))/2.
C -- RECORDING THE RESULTS
      DO 11 J=0,N
      X=DX*J
      WRITE(UNIT=22,FMT=25) X, P(J,0)
 11   CONTINUE
      DO 17 J=0,N
      X=DX*J
      WRITE(UNIT=24,FMT=25) X, P(J,M)
 17   CONTINUE
      DO 12 K=0,M
      Y=DY*K
      DPDX=(4.*P(1,K)-3.*P(0,K)-P(2,K))/(2.*DX)
      WRITE(UNIT=21,FMT=25) Y, DPDX
 12   CONTINUE
      DO 18 K=0,M
      Y=DY*K
      WRITE(UNIT=23,FMT=25) Y, F(K)
 18   CONTINUE
      END
```